Power Quality State Estimation

Ali Farzanehrafat

A thesis submitted in partial fulfilment
of the requirements for the degree of
Doctor of Philosophy
in
Electrical and Computer Engineering
at the
University of Canterbury,
Christchurch, New Zealand.

October 2014

ABSTRACT

Traditional state estimation whereby the state of the system is assessed based on a limited number of measurements is a well established tool for steady-state situations where the frequency of the system is 50 Hz. Previous contributions have looked at extending this concept to the power quality area. This area of research is called Power Quality State Estimation (PQSE) and represents a class of techniques. Under the umbrella of PQSE, the main contribution of this work is taking Transient State Estimation (TSE) on step further. A new three-phase formulation for TSE using the Numerical Integrator Substitution (NIS) will be detailed. NIS approach, also known as Dommel's method, gives a numerical solution to describe the transient behaviour of a dynamic system at discrete time points. The new transient state estimator is implemented and verified by applying the proposed algorithm to a real distribution test system. It's performance and accuracy are investigated in presence of measurement noise, background harmonics, multiple faults, etc. The conducted study has shown this technique has a great potential.

LIST OF PUBLICATIONS

The following is a list of papers that have been submitted for publication during the research presented in this thesis.

JOURNAL PAPERS

Farzanehrafat, A., Watson, N.R., 'Power Quality State Estimator for Smart Distribution Grids.', *IEEE Transactions on Power Systems*, Vol.28, Issue:3, pp.2183-2191, Aug.2013.

Watson, N.R., Farzanehrafat, A., 'A Three-phase Transient State Estimation Algorithm for Distribution Systems', Submitted to *IET Proceedings on Generation, Transmission & Distribution* , Vol.8, Issue:10, pp.1656-1666, 2014.

CONFERENCE PAPERS(ACCEPTED & PRESENTED)

Farzanehrafat, A., Watson, N.R., 'Review of Power Quality State Estimation', In *Australasian Universities Power Engineering Conference. (AUPEC2010)*, Christchurch, New Zealand, December 2010.

Farzanehrafat, A., Watson, N.R., 'The Use of Transient State Estimation for Voltage Dip/Sag Assessment', In *POWERCON 2012*, Auckland, New Zealand, 30 Oct.-2 Nov. 2012

Watson, N.R., Farzanehrafat, A., Perera, S., 'Power Quality State Estimation: A New Concept', In *Electricity Engineers' Association Conference 2012 (EEA2012 Conference)*, Auckland, New Zealand, 20-22 Jun 2012.

Watson, N.R., Farzanehrafat, A., 'Identification of the Sources of Transient Disturbances', In *International Conference on Power Systems Transients (IPST2013)*, Vancouver, Canada, 18-20 July 2013.

OTHER PRESENTATIONS

A 20 minutes oral presentation titled 'Review of Power Quality State Estimation' was presented at the *Electricity Engineers' Association (EEA) Annual Power Engineering Exchange (APEX 2010) Southern Summit*, Christchurch, New Zealand, 19 August 2010.

A 30 minutes oral presentation at the *Endeavour Energy/University of Wollongong Joint Technical Meeting*, Wollongong, Australia, January 2013.

ACKNOWLEDGEMENTS

I would like to express my sincere gratitude to my supervisor Professor Neville R. Watson for his generous support in each step of my journey. His advice on both research and my career have been priceless.

I would also gratefully acknowledge the help of Associate Professor Sarath Perera (University of Wollongong, Australia), for hosting me in order to enable me to escape the considerable upheavals due to the Christchurch earthquakes and continue my research work.

I would also wish to thank the EPECentre which this work would not have been possible without their financial support.

I am grateful to my fellow lab mates with whom I have had the pleasure to work and discuss my project during these years. A special thanks to Lance Frater, Bhaba Das, Andrew Lapthorn, James Omrod, Micheal Howang, Kalyan Malla, Jordan Orillaza, Shreejan Pandy, Rowan Sinton, Ryan van Herl, Tahira seyed Jalal and Parash Acharya.

Last but not least, I would like to thank my family and wife who provided me with support and encouragement.

CONTENTS

LIST OF FIGURES

LIST OF TABLES

Chapter 1

MOTIVATION

1.1 RESEARCH TOPIC

1.1.1 Power quality monitoring

Due to the cost of monitoring and telecommunication equipment, it is not feasible to monitor the entire system state of modern power grids. For this reason, state estimation whereby the state of the system is assessed based on a limited number of measurements is used. State estimation is now a well established and crucial part of Energy Management System (EMS) in conjunction with power flow at the fundamental frequency [Abur and Exposito 2004]. An introduction to traditional state estimation will be given later in section 2.1.

Recently the importance of power quality issues due to the significant losses for poor power quality, has resulted in research being focused on extending the concept of state estimation techniques into power quality issues. This area of research is called Power Quality State Estimation (PQSE) [Watson 2010] and represents a class of techniques as will be discussed in Chapter 2. Harmonic state estimation (HSE) and identification of harmonic sources, transient state estimation (TSE) and voltage sag state estimation (VSSE) are all types of PQSE. Therefore, PQSE is not one particular type of analysis but covers many different types in the power quality area. Despite the different formulation and quantities they use, the common feature is that they are applying state estimation techniques to power quality problems.

It should be noted a better and more comprehensive monitoring system which includes harmonics information as well as transient variations in voltages and currents of the system will enable the system operators to run the power system more efficiently.

1.1.2 PQSE in Smart Grids

The need to modernize the grid to enable it to meet the needs of the future is well accepted. This has led to the Smart Grid concept as a pathway of increasing the smartness of the electrical grid

so as to meet the demands of the future. Part of this involves advances in metering infrastructure which will make a large amount of data available in the future. Since advances in metering and deployment of Advanced Metering Infrastructure (AMI) enables access to a wealth of data, the issue is to turn the massive amount of data available into useful information that will help Smart Grids to evolve and achieve the desired functionalities. Smart algorithms are needed for the control of both generation and demand to improve management of the distribution system so as to maximize the efficiency, utilization, reliability and resilience of the infrastructure.

There is already a high level of smart algorithms deployed in some electrical power systems, but these are specially schemes designed as one-off to overcome specifically identified problems. These are based on studying numerous contingencies and determining the best course of action. For example in New Zealand there are "run-back schemes". If a certain contingency occurs then generation at certain locations (or HVDC link) are backed-off to ensure remaining circuits are not overloaded, causing tripping. Run-back schemes are seen as a way of allowing new generation to connect while limiting or avoiding the need for asset upgrades [Transpower New Zealand, Ltd June 2007, David Strong & Associates June 2009].

In the area of condition-based maintenance, if the voltages and currents are monitored, when a circuit breaker has to interrupt a fault (or used for switching) then the duty (stress) on the circuit breaker can be calculated. This information is fed into an algorithm to inform when maintenance is required for the circuit breaker. With sufficient measurements and suitable instrumentation, on-line estimation of the electrical parameters of overhead lines and cables as well as their temperature can be performed. This information allows better utilization of assets through dynamic line ratings. It could also allow signatures of equipment to be determined. This would aid detection of incipient problems in equipment such as bushings, CTs, windings, cables, metal oxide surge arresters and circuit breakers, allowing remedial action to be taken promptly [Transpower New Zealand, Ltd July 2010, Transpower New Zealand, Ltd December 2008]

The need for PQSE is more pronounced with the emergence of smart grids and relevant advances in metering and deployment of Advanced Metering Infrastructure (AMI) which enables access to a wealth of data. This necessitates smart algorithms (such as PQSE) to turn the massive amount of data available into useful information that will help Smart Grids to evolve and achieve the desired functionalities.

Despite the important role played by PQSE, there are not many contributions to this area, with most of them focusing on HSE. Under the umbrella of PQSE the aim of the present work is to take the Transient State Estimation (TSE) a step further by formulating a new three-phase transient state estimator.

1.1.3 TSE for diagnostic purposes

In the past, electromagnetic transient programs (such as EMTP, EMTDC, ATP or similar programs) have been used to simulate a transient disturbance in the system and then match the results with available measurements to determine the probable cause. However, this procedure is time consuming and sometimes doubtful [Yu and Watson 2005].

A better solution would be to extend estimation techniques to transient phenomena to identify the source of disturbances from partial measurements in the system. In essence, TSE is a reverse function of transient simulation. In other words, while transient simulation is used to analyse the consequences of a disturbance on power system quantities (voltage, current, etc.), TSE is exploited to identify the cause of transient change in system parameters. Therefore TSE has the potential to be a valuable tool to identify the cause of transient disturbances in the power system.

1.1.4 TSE prospect

In different types of PQSE, as will be discussed later in section 2.2, estimation techniques are deployed to estimate the power quality related quantities such as harmonic levels, frequency or magnitude of the voltage sags occurred in the network, etc. Regardless of the selected type, the estimated quantity is limited to one of the power quality aspects at a time. For example, HSE could not provide any information regarding the number of voltage sags happening within the network. Similarly, VSSE studies would not be able to add any extra information on harmonic knowledge of the system under investigation. From this point of view TSE has a major advantage over other types of PQSE. This advantage is due to the nature of the estimated quantity in TSE and that is the transient waveform of the voltages and/or currents. In TSE, unlike the other types of PQSE, the information of interest regarding the power quality issues can be simply extracted from the estimated time domain voltage and/or current waveform.

In other words, TSE could provide a time domain waveform of the voltage/current where no local monitoring is available and then opening the doors for many other applications. An example of this would be "Electrical Signature Analysis (ESA)" for residential and industrial purposes. ([Bellini *et al.* 2001, Laughman *et al.* 2003, Shaw *et al.* 2000]).

1.2 THESIS OUTLINE

The thesis is presented in five chapters as follows:

Chapter 2, first gives an introduction to the traditional state estimation techniques. Then briefly reviews the previous work on different types of PQSE including HSE, VSSE and TSE. This chapter also reviews the material being used to formulate the new TSE.

Chapter 3, describes how a new transient state estimator is formulated and gives an overview of the implemented algorithm. For this purpose this chapter explains how the dynamic model of system components are derived using NIS formulation. Then describes how these models must be employed to construct a transient state estimation equation and eventually, how the constructed equation must be solved.

Chapter 4, the implemented algorithm is applied to a distribution test system to verify its performance. Its ability to estimate busbar voltages and thereby location of the source of a voltage dip/sag is used as the test. In addition, to make the test more realistic 5% normally distributed measurement noise and background harmonics are added and the process is repeated.

Chapter 5, draws a conclusion and some of the areas worth studying as future work.

Chapter 2

LITERATURE REVIEW

2.1 INTRODUCTION TO STATE ESTIMATION

The operating conditions of a power system at a given point in time can be specified by a set of bus voltage magnitudes and phase angles which is referred to as the static state of the system. Different states (operation conditions) of the power system can be defined owing to the overload of assets, over/under voltage in the system, transmission line outage, etc. Figure 2.1 shows different states defined in [Abur and Exposito 2004]. The state of the system may move into one of three possible states namely normal state, emergency state and restorative state as the operation conditions change. Once the state of the system is estimated, an appropriate course of action must be taken by the power system operator to maintain the system in a normal state.

In the 1970s, the application of state estimation to power systems was addressed [Schweppe and Wildes 1970, Schweppe and Rom 1970, Schweppe 1970]. Since then, state estimation techniques for the fundamental frequency have been widely utilized to monitor the state of the power system

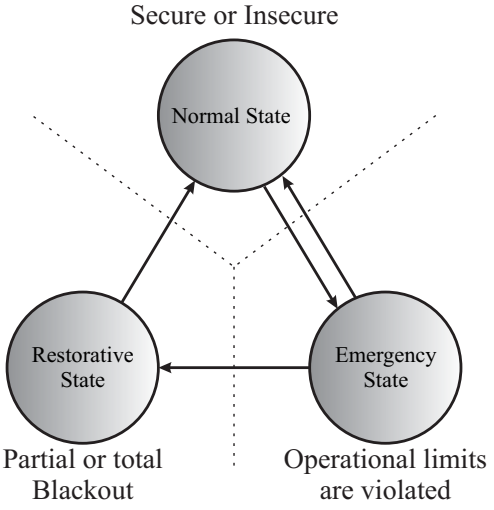

Figure 2.1: Power system states and their relation.

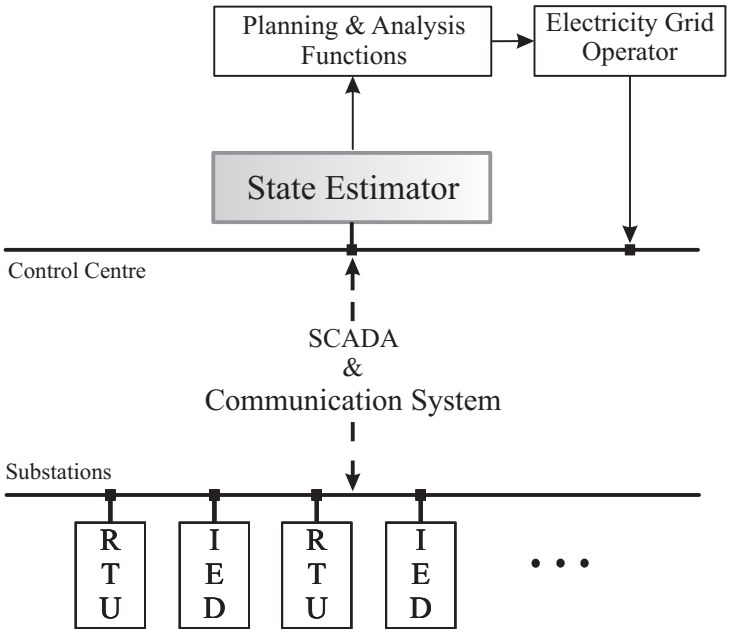

Figure 2.2: Position of state estimation in power systems.

based on the limited number of measurements throughout the network in time intervals from a couple of cycles to seconds. State estimation is now a well established and crucial part of an Energy Management System (EMS) in conjunction with power flow at fundamental frequency, Figure 2.2 depicts this position. The collected data by means of Remote Terminal Units (RTUs) and Intelligent Electronic Devices (IEDs) from all over the network is transmitted to the Control Centre via a SCADA system. However, the raw data may not always be reliable due to the measurement noise and gross errors. Furthermore, the transmitted set of measurements may not be enough to determine the operating state of the system. Besides, even though it is technically feasible but it is not cost effective to transfer all measurements even if they are available. For this reason, State estimator solution provides an optimal estimate of the system state based on the available measurements and the assumed model of the system. In other words, state estimation is indeed a systematic procedure (mathematical procedure) to process the set of telemetered measurements to come up with the best estimation of the current state of the system.

The output of state estimator will be used by the EMS application functions such as contingency analysis, automatic generation control, load forecasting and optimal power flow, etc. In fact, the power system state estimator acts like a filter between the raw measurements collected from the network and the application functions which require a reliable data base representing the existing state of the power system.

The relation between the measurements and state variables forms the mathematical model of the state estimation problem. The general form of the state estimation problem can be expressed

as a system of equations:

$$\underbrace{\begin{bmatrix} z_1 \\ z_2 \\ \vdots \\ z_m \end{bmatrix}}_{Z} = \underbrace{\begin{bmatrix} h_{1,1} & h_{1,2} & \cdots & h_{1,n} \\ h_{2,1} & h_{2,2} & \cdots & h_{2,n} \\ \vdots & \vdots & \ddots & \vdots \\ u_{m,1} & u_{m,2} & \cdots & h_{m,n} \end{bmatrix}}_{H} \cdot \underbrace{\begin{bmatrix} x_1 \\ x_2 \\ \vdots \\ x_m \end{bmatrix}}_{X} + \underbrace{\begin{bmatrix} \varepsilon_1 \\ \varepsilon_2 \\ \vdots \\ \varepsilon_m \end{bmatrix}}_{\varepsilon} \tag{2.1}$$

where z is a (m×1) vector of measured (known) quantities and x is a (n×1) vector of state variables (unknown quantities) for which the equation must be solved. $[H]$ is a (m×n) measurement function relating the known quantities to state variables and ε is the vector of measurement errors.

2.1.1 Non-linear system of equations

In most commercial applications of the state estimators, in order to construct the state estimation problem (equation 2.1), the vector of measurements mostly consists of active (z_P) and reactive power flows (z_Q). These values are widely collected by revenue meters throughout the network. On the other hand, the vector of state variables are a set of busbar voltage magnitudes (V) and voltage phase angles (δ).

Therefore, ignoring the measurement error, equation (2.1) can be rewritten in the form of non-linear system of equations:

$$\begin{bmatrix} z_P \\ z_Q \end{bmatrix} = \begin{bmatrix} H_{P\delta} & H_{PV} \\ H_{Q\delta} & H_{QV} \end{bmatrix} \cdot \begin{bmatrix} \delta \\ V \end{bmatrix} \tag{2.2}$$

2.1.2 Over-determined system of equations and Weighted Least Square (WLS) approach

It should be noted that the state of the system can be estimated only if the system is fully observable. In other words, matrix H must have a full rank. This could be achieved by taking more measurements than state variables (this will be explained in more details in section 3.4). Observability in state estimation is reviewed in [Clements 1990].

Once the state estimation problem is formed, different iterative algorithms using weighted least square techniques are used to estimate (x). [Wu 1990] reviews the formulation and the different solutions for the state estimation problem.

2.1.3 Bad data and state estimation

The collected measurements throughout the system are not usually reliable enough to be directly processed by the state estimator. These erroneous measurement values are called bad data and decrease the accuracy of the estimation.

Among the reasons for bad data are finite accuracy of the measurement devices, telecommunication system failures and incorrect topology information. These effects are inevitable and therefore the extent of their effectiveness on estimation accuracy must be taken into account.

Bad data (measurement error) is traditionally classified as either "extreme errors", "gross errors" or normal "measurement noise". The ability to treat the bad data depends on the number of measurements and the number of unknowns in equation 2.1. Bad data could be detected, identified and corrected effectively in over-determined systems as there are redundant measurements. Extensive research has been performed in the past in order to improve the accuracy of the state estimation [Abur 1990, Lo *et al.* 1992, Wu *et al.* 1988, El Hawary 2002]. For this purpose, the residual in Equation 2.1 ($\varepsilon = z - [H].x$) is calculated and then will be used to detect, identify and remove bad data from the set of measurements.

2.1.4 Phasor Measurements Units (PMU) and state estimation:

PMUs are capable of producing synchronized phasor measurements widely across the network by means of sampling clocks being synchronized through a common timing signal, normally from GPS. This approach initiated the idea of replacing traditional communication system shown in figure 2.2 (using RTUs and collecting data through SCADA) with PMUs.

With the emerge of PMUs in power systems, the possibility of directly measuring the busbar voltage phasors is provided. This approach is different compared to solve a non-linear system of equation 3.38 as described previously in section 2.1.1. In other words, the measured quantities are no longer active and reactive power. So, the the equation 3.38 should be changed accordingly:

$$\begin{bmatrix} z_V \\ z_I \end{bmatrix} = \begin{bmatrix} 1 \\ H_{IV} \end{bmatrix} \cdot V \tag{2.3}$$

where V is the voltage phasor vector which truly represents the state of the power system at a given instant because of the precise time synchronization of the measurements. I is the branch measured current and would provide redundancy in the measurement set.

Recent developments in state estimation with PMUs can be found in [Phadke *et al.* 2009].

2.1.5 Dynamic State Estimation:

Since the load is changing, the state of the system should be recalculated at short intervals of time. This makes the entire system dynamic. To capture dynamic behaviour of the power system based on load variations, another set of algorithms was developed. Dynamic state estimation (DSE) uses the present (and sometimes previous) state of the power system along with the knowledge of the system's physical model, to predict the state vector for the next time instant (predicted state). [Shivakumar and Jain 2008] reviews the developments in this field of research.

In this approach, the power system is assumed to be quasi-static state and hence changes slowly but steadily. An example of changes in which the DSE is deployed is the demand variation and hence the generation level. Therefore, this type of study could neither capture the very fast transients of the system components (such as switching, voltage dips, etc) nor the harmonics levels. Besides, regardless of the selected method for state prediction , it is still uncertain and because of the nature of forecasting methods a high level of risk is involved.

2.2 POWER QUALITY STATE ESTIMATION

State estimation (hereafter called traditional or conventional type) assumes the power system is in a steady-state (or equivalently quasi-static state) situation and all the current and voltage waveforms are purely sinusoidal with constant magnitude and frequency (50Hz) [Monticelli 1999]. For this reason, it is not feasible to track the harmonics load-flow or the transient behaviour of system quantities (such as voltage and current) within the network.

Recently the importance of power quality issues and the reduction in price of meters capable of measuring power quality indices has resulted in research being focused on extending the concept of state estimation techniques into power quality issues. This area of research is called Power Quality State Estimation (PQSE) [Watson 2010].

Figure 2.3 shows an overview of the PQSE based on the estimated quantities and the state estimation techniques which have been investigated in previous contributions. The common feature is that different types of PQSE are applying state estimation techniques to power quality problems. In fact, traditional state estimation for fundamental frequency also fits in the above classification as steady-state under/over-voltage can be considered as a power quality issue.

Although traditional state estimation and PQSE look similar at first glance, there are significant disparities that must be taken into account: With an appropriate choice of state variables and type of measurements in PQSE, $[H]$ becomes linear. Moreover, due to the number of revenue meters in the power systems, the number of measurements is more than the state variables and it leads the system to become over-determined. Unlike traditional state estimation, the

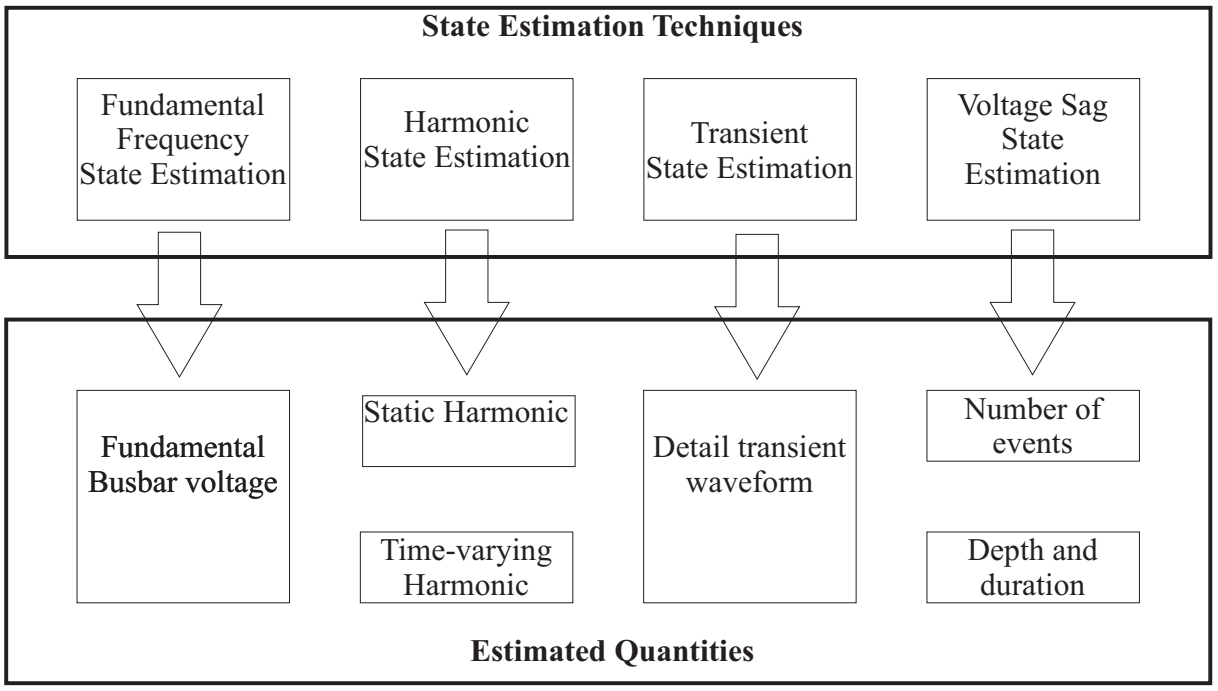

Figure 2.3: Different types of PQSE.

cost of power quality monitoring devices capable of measuring these values results in an underdetermined system for PQSE. These differences necessitate different approaches to solve the estimation problem (equation 2.1).

In the following sections, each type of PQSE and the corresponding contributions in that area will be discussed:

2.3 HARMONIC STATE ESTIMATION

The growing usage of non-linear electrical equipment results in a higher level of harmonic currents being injected into the power system. The problem of harmonic pollution in the power system has been widely recognized. Standards for limiting this pollution have been set in many countries. Harmonic pollution causes a wide range of issues such as additional heating in motors, transformers and cables, accelerating the degradation of their insulation and malfunction of capacitors, etc. On the other hand, knowledge of the source and location of the harmonics is a prerequisite for any remedial action to maintain the desired power quality levels. For this reason, state estimation has been extended to harmonics study.

The task of HSE [Heydt 1989, Meliopoulos *et al.* 1994] is to generate the 'best' estimate of the harmonic levels from limited measured harmonics data, corrupted with measurement noise. This is the reverse of harmonic penetration in that the harmonic sources are unknown and

the harmonic levels throughout the system are determined from a limited number of harmonic measurements.

For HSE, having equation 2.1 in mind, harmonic voltages and harmonic currents are usually measured quantities (z) and the busbar harmonic voltage phasors are chosen as state variables (x). This requires a three-phase multi frequency system model to correspond with each measurement of the relevant state variable for each harmonic order. This is achieved by building a nodal admittance matrix based on the network topology. So, unlike the traditional state estimation, a linear system of equations is derived to be solved.

A great deal of work has been done on HSE from different points of view. Here are some aspects which have been brought up in the previous contributions:

2.3.1 Solution of HSE

Once the HSE problem is formed, there are two main ways of solving the equation for the states variables. The first one is using the normal equation approach [Du *et al.* 1996]. This approach can only be used if the system is fully observable and hence more measurements than state variables (over-determined system) is required. For this reason a prior observability analysis procedure to determine solvability of the measurement equation is needed [Watson *et al.* 2000]. However, due to the cost of devices capable of measuring PQ indices and different ownership of different parts of the network HSE is usually an under-determined problem. The second and more robust approach is to use singular value decomposition (SVD) to develop a pseudo-inverse and use this to solve the estimation problem [Madtharad *et al.* 2003, Matair *et al.* 2000, Yu and Watson 2004]. This approach can also give information about observability. This area will be discussed further in section 3.4.

2.3.2 Optimal number of measurements and the best location

The number of harmonic instruments available is always limited due to cost and the quality of the estimates is a function of the number and location of the measurement points. [Madtharad *et al.* 2005] focus on a new technique for optimal measurement placement for HSE in terms of the optimal number of measurements and the best locations to place them in the network. The proposed measurement system is then used to identify the location and magnitude of harmonic sources.

2.3.3 Bad data analysis and HSE

Bad data was introduced in section 2.1. Unlike traditional state estimation, PQSE is an under-determined system. A statistical approach utilizing a cumulative probability density function resulting from Monte Carlo simulation is used to assess the effect of bad data in [Yu *et al.* 2005]. This paper indicates that the effect of random measurement noise is less significant in comparison to gross errors. The presence of gross errors, has a large impact on the estimations which cannot be easily mitigated in an under-determined system.

2.3.4 Time-varying harmonic levels:

The dynamic nature of the load over a period of time requires the capability of tracking harmonic content versus time in a power system. A Kalman filter is used to investigate the effect of load variation over a one day cycle on estimation of the power system harmonic content and was presented in [Beides and Heydt 1991].

2.3.5 Estimating location and type of loads generating harmonics

The ability of HSE to identify the location, and even the types of harmonic sources has been discussed in [Du *et al.* 1999]. In this approach, the power system is partitioned into two parts: an AC backbone containing no harmonic sources and a set of suspicious harmonic sources. Based on partial harmonic measurement values, HSE provides the harmonic voltages at the suspicious buses and harmonic current injected from the suspicious sources to the backbone. Having the suspicious harmonic source as a Norton equivalent circuit representing the load nonlinearity, the task of load identification is to determine how much of the loads harmonic current is due to the voltage distortion at the load terminals (hence flowing in the Norton admittance) and the magnitude of active harmonic current injection (Norton current source) at each of the harmonic frequencies. Then the types of load(s) generating harmonics can be estimated by looking at the results across a number of harmonic frequencies.

2.3.6 HSE implementation

HSE applicability was verified in 2005 by [Kanao *et al.* 2005] for Japanese field data synchronized with a GPS clock. The paper also shows the estimation of transmission line parameters from measured fundamental frequency data values and uses bad data removal to improve HSE precision.

2.4 VOLTAGE SAG STATE ESTIMATION

Voltage dip/sag is one of the most concerned power quality issues and as defined by [IEEE Recommended Practice for Monitoring Electric Power Quality 1995], is a sudden decrease in RMS voltage at the power frequency for durations from 0.5 cycles to 1 minute, reported as the remaining voltage. With the growing number of hi-tech but sensitive devices, this reduction may result in an unexpected stoppage when such sensitive equipment is located in a process-controlled device within an industrial plant.

The stochastic prediction approach is a well known method for voltage dip evaluation in a network. [C4.102 Feb. 2009] reviews the techniques proposed from different perspectives. These techniques combine mathematical models and statistical data such as historical fault statistic (which are usually known for an existing system) to predict the number and the characteristics of voltage dips experienced by a customer fed from a certain feeder in a network. However, due to the probabilistic nature of stochastic methods, the assessment still remains uncertain. In addition, in some cases historic data is not available when analyzing a part of the system recently introduced or modified.

In recent years a different approach has been introduced for voltage sag assessment. Voltage Sag State Estimation (VSSE) is the extension of the state estimation concept to another power quality issue. Based on the the estimated quantities of interest, this field of research is generally classified in two main areas in the previous contributions:

- *Depth and duration:* The introduced methods employ estimation techniques to measure the sag level (magnitude) at every node of a distribution feeder using a limited number of voltage metering points.
- *Frequency of events:* Refers to estimating the number of voltage sags arising at unmonitored buses from the number (frequency) of sags obtained at a limited number of monitored buses.

Reference [Bin *et al.* 2005] makes use of radial connection characteristic for a distribution feeder and assumes that voltage sags and interruptions within that feeder are generally associated with short circuit faults. Then, it employs a least-square method to estimate the voltage profile (and hence sag levels) along the feeder using a limited number of voltage metering. Finally, this can be used to calculate the feeder power quality indices such as the system Average RMS Frequency Index (SARFIx). Case study results showed good performance of the proposed method. However, this method assumes the system has reached its steady state situation and does not reflect the voltage sags in transient situations (or the one lasting less than two or three cycles). Moreover, the voltage sags caused by transformer energisation, motor starting and sudden load changes are not considered in this approach.

To overcome the bad data influence on the aforementioned VSSE, [Wang *et al.* 2011] introduces an algorithm to identify and replace the bad data owing to the associated noise at PQ meters.

In [Espinosa Juarez and Hernandez 2007] a voltage sag state estimation method which estimates the sag frequency at unmonitored buses is proposed. Considering equation 2.1, the vector of measured quantities indicates the number of defined voltage sags registered by the monitors. The state variables indicate the number of faults occurring at certain segments of the system lines. Then, a binary matrix corresponds a bus of the system based on the fault positions method [Juarez and Hernandez 2006] to a segment of a transmission line. Once the state estimation equation is derived, an integer linear optimization method solves the state estimation equation for the number of faults occurring at certain segments of the system lines. Finally, this is used to calculate the expected number of voltage sags at the bus of interest. The same authors later applied neural networks to solve the same problem in [Espinosa Juarez *et al.* 2009].

The next contribution in this area, optimizes the number and location of the meters for monitoring a large transmission network looking for voltage sags, then this data is deployed for estimating the system voltage sag indices [Olguin *et al.* 2006].

2.5 TRANSIENT STATE ESTIMATION

Some of the power quality issues are transient in nature therefore extending the estimation techniques from quasi-steady state situation to transient situation is desirable. This has initiated a new concept in power quality state estimation and is called Transient State Estimation (TSE). TSE obtains partial synchronized measurements at a certain time point and provides estimations for system quantities such as voltage and current at unmonitored busbars or branches for the same time point.

As discussed in the previous papers in this area, TSE can alternatively be used as a forensic tool in transient studies (instead of using EMTP type or similar programs) to identify the probable cause of a disturbance within the network. In the traditional approach, several cases were considered and simulated, then the results were analysed and compared to the existing system transient response to find the disturbance origin [Long *et al.* 1990]. This approach is time consuming and sometimes indecisive. TSE on the contrary, can obtain the transient waveform at a limited number of measurement points and estimate the waveforms at other locations for the same period of interest to investigate the cause of a transient event.

2.5.1 The Use of TSE for Voltage Dip/Sag Assessment

Voltage dip/sag is one of the most concerned power quality issues and as defined by [IEEE Recommended Practice for Monitoring Electric Power Quality 1995] is a sudden decrease in RMS voltage at the power frequency for durations from 0.5 cycles to 1 minute, reported as the remaining voltage. With the growing number of hi-tech but sensitive devices this reduction may result in an unexpected stoppage when such sensitive equipment is located in a process-controlled device within an industrial plant. As mitigation plans must be carried out, locating the source of disturbance has to be done as a first step. For these reasons, many techniques have further been developed to identify the source of voltage dip/sag in power systems.

Stochastic prediction techniques [Conrad *et al.* 1991, Bollen 1996, Conrad and Bollen 1997, Bollen 1998, Qader *et al.* 1999, Faried and Aboreshaid 2003, Heine and Lehtonen 2003, Faried *et al.* 2005, Wang *et al.* 2005, Juarez and Hernandez 2006] combine mathematical models and statistical data to predict the number and characteristics of voltage dips experienced by a customer fed from a certain feeder in a network. However, due to the fact that assessment of voltage dips/sags requires prior knowledge of the system and is based on stochastic evaluation, the problem of locating voltage sag origins remains uncertain.

Many contributions also used different methods to identify the location of voltage sag origins [Hart *et al.* 2000, Parsons *et al.* 2000, Li *et al.* 2003, Hamzah *et al.* 2004, Seon Ju *et al.* 2004, Gomez *et al.* 2005, Pradhan and Routray 2005, Tayjasanant *et al.* 2005, Leborgne *et al.* 2006, Bollen *et al.* 2007]. Apart from advantages and disadvantages associated with each method, the common feature of these methods are to determine if the disturbance origin is located upstream or downstream in relation to the measuring point. This approach renders useful information particularly for industrial customers who are keen to identify the responsible party for the voltage sag occurring within their plant. However, it still remains as a disadvantage from the network operator point of view.

TSE as an alternative approach, could provide a platform in which particular information of interest about power quality issues including voltage dips/sags can be easily extracted via a limited number of measurement points throughout the network.

2.5.2 TSE formulation

Transient variations in TSE necessitate a time domain solution for the system as well as a dynamic formulation to represent the system components. Differential equations are exploited as a mathematical representation for the dynamic behaviour of a system. On the other hand, digital computation by computers is a discrete time process by it's nature and can only provide solutions for the differential and algebraic equations at discrete points in time.

There are two broad classes of methods used in the digital representation of the differential equations representing continuous systems. The first one is the numerical solution of differential equations using state variable formulation and the second one is the use of Numerical Integrator Substitution (NIS) to derive difference equations. A famous example of the second approach is the Dommel's EMTP method which uses the trapezoidal rule. State variable formulation is discussed here and NIS will be discussed in the next section:

2.5.3 TSE using state variable formulation

State variable formulation describes an n^{th} order linear dynamic system by an n^{th} order linear differential equation which can be rewritten as n first order linear differential equations as well as outputs which are obtained from the state and input quantities in a well known format of:

$$\begin{aligned} \dot{\mathbf{x}}(t) &= [A]\ \mathbf{x}(t) + [B]\ \mathbf{u}(t) \\ \mathbf{y}(t) &= [C]\ \mathbf{x}(t) + [D]\ \mathbf{u}(t) \end{aligned} \tag{2.4}$$

where $\dot{x}$ is the vector of state variable derivatives, y the vector of output variables and u the vector of inputs. Then numerical integration methods (such as Euler method) are employed to approximate the derivative operator equation (2.5). This transformation makes the system ready to be solved, simulated and analysed at discrete time points by an iterative procedure.

$$\dot{\mathbf{x}}(t) \approx \frac{\mathbf{x}(t) - \mathbf{x}(t - \Delta t)}{\Delta t} \tag{2.5}$$

Once the measurement matrix $[H]$ is constructed it can be solved for the state variables using available techniques for other types of PQSE. When the state variables are known, the dependent variables such as branch currents can be calculated and the complete knowledge of the system can be determined.

Extension of HSE into transient phenomena was first introduced by Kent Yu at the University of Canterbury, New Zealand [Yu 2005]. He made a good contribution in this area by introducing the concept and the task of TSE. He used state variable formulation for modelling the system components such as transformers, transmission lines, generators, loads, etc. Then made use of them to develop the measurement matrix to establish equation 2.1. Different options for measurements have been summarized in table 2.1.

It should be noted that to supply extra information to the measurement system, the derivative of voltage and current measurements are also utilized. These can be estimated using present and previous values. This extra information which is used to increase the number of measure-

Table 2.1: Measurements in relation to state variables

Measured	System Variable	Definition
x	x	State variable
dx/dt	[A]x+[B]u	State variable derivitive
y	[C]x+[D]u	Output variable
dy/dt	[C][A]x+[C][B]u+[D]u	Output variable derivative

ments and hence improve the observability of the system and can be classified under pseudo-measurements and virtual measurements.

Pseudo-measurements are estimated based on historical data such as load forecasts, generation dispatch or simply by employing derivatives of the state variables (table 2.1). On the other hand, virtual measurements are type of information that does not need metering. Examples for this are the busbars with no generation or load, hence having zero active and reactive power injection in traditional state estimation. Another example is dividing busbars into suspicious (those that possibly have nonlinear loads connected) and non-suspicious busbars (those busbars known not to have nonlinear loads connected) in HSE.

[Yu and Watson 2005] modelled the system components using state variable formulation and put them together to make the measurement equation. Then demonstrated the use of TSE for determining the fault position, fault type and the magnitude of the fault currents.

The Lower South Island test system was formulated in [Yu and Watson 2007] to investigate the cause of a transient change in voltages and currents of the system by partial measurements. PSCAD/EMTDC simulation was used as actual measurements for the selected points and fed to a TSE algorithm. Noise at 5% which is assumed to be normally distributed, was added to all of the measurements and the same scenario was resimulated. Inspecting the errors showed the algorithm capability even in the presence of measurement noise.

The other contribution [Watson and Yu 2008] proposed a diakoptic formulation to allow a realistic power system to be modelled and showed how to build the measurement equation. The data for the measurements is obtained from a TCS based state-variable simulation written in MATLAB. It then demonstrated its ability to identify the location of the fault using a current mismatch method.

State variable analysis was the dominant technique in transient simulation prior to the appearance of the numerical integration substitution method. The main disadvantages for state variable formulation are greater solution time, extra code complexity and greater difficulty to model distributed parameters [Watson and Arrillaga 2002].

2.6 NUMERICAL INTEGRATOR SUBSTITUTION (NIS)

Another numerical solution of system equations at discrete time points is Numerical Integrator Substitution. As the name implies, Numerical Integrator Substitution involves substituting a numerical integration formula into the differential equation and rearranging it to the form of a difference equation.

Numerical integration in essence, is required to calculate the solution x at time point t from knowledge of the present and previous time points. Appendix C from [Watson and Arrillaga 2002] gives an overview about different classical methods for numerical integration and their relevant error and stability criteria . An example of interest here is the trapezoidal rule.

To summarize the principal concept of the trapezoidal rule as an example of NIS, let us assume that the transient behaviour of a system parameter such as current or voltage represented by function $x(t)$, is described by the following differential equation:

$$\frac{dx(t)}{dt} = f(t) \tag{2.6}$$

Alternatively, this equation can be written as:

$$x(t) = x(0) + \int_0^t f(z)dz \tag{2.7}$$

Figure 2.4 shows the principle of the trapezoidal rule application. Assuming the primitive function as being linear in such a small time interval, the corresponding area can be considered as a trapezoid illustrated in the figure. The area of this trapezoid can be simply approximated by:

$$\frac{\Delta t}{2} \cdot (f(t - \Delta t) + f(t)) \tag{2.8}$$

Therefore, if the value of x is known at the time $t_0 - \Delta t$, the value of x at the time t_0 could be approximated by means of the following expression:

$$x(t_0) = x(t_0 - \Delta t) + \frac{\Delta t}{2} \cdot (f(t_0 - \Delta t) + f(t_0)) \tag{2.9}$$

In other words, by selecting constant time steps the time domain solution of the equation (2.6) can be achieved as a function of time at discrete instants:

$$x(t) = x(t - \Delta t) + \frac{\Delta t}{2} \cdot (f(t - \Delta t) + f(t)) \tag{2.10}$$

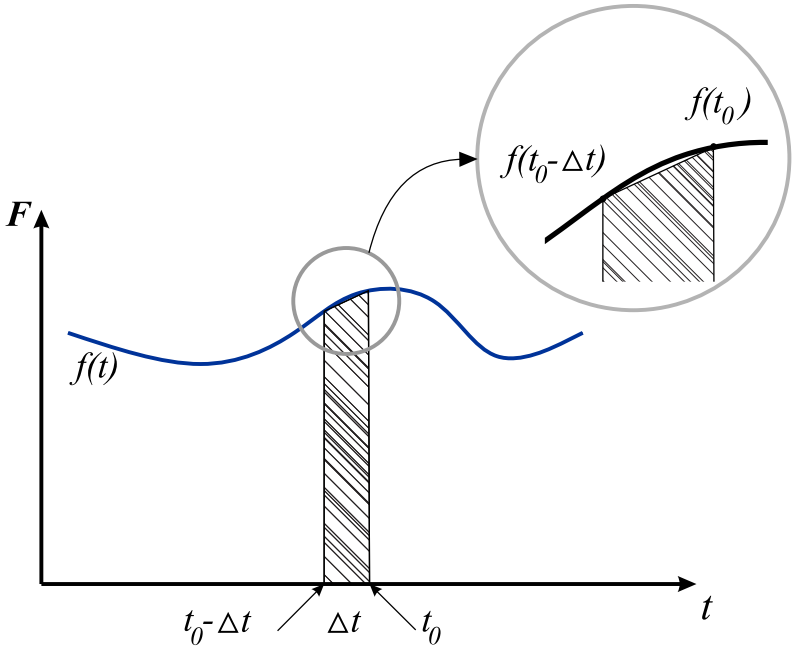

Figure 2.4: Trapezoidal rule application.

or equivalently,

$$x(t) = \underbrace{\frac{\Delta t}{2} \cdot f(t)}_{InstantaneousTerm} + \underbrace{\left[\frac{\Delta t}{2} \cdot f(t-\Delta t) + x(t-\Delta t)\right]}_{HistoryTerm} \tag{2.11}$$

Equations 2.6 - 2.11 describe the way a differential equation can be changed into the form of its difference equation and consequently be solved in a time loop using instantaneous and history terms at each time step. In the next chapter this discretization method will be used to formulate the dynamic behaviour of the system components for TSE.

Hermann W. Dommel in his classical paper [Dommel 1969], proposed a method which is now universally most popular approach for time domain solution of complex power systems. This approach combined method of characteristics for transmission lines [Bergeron 1961] and trapezoidal rule for discretisation of the system elements for finding the time response of electromagnetic transients in arbitrary single or multi-phase networks with lumped and distributed parameters.

The method is generally referred to as Numerical Integration Substitution (NIS) [Arrillaga and Watson 2001]. However this approach sometimes has been referred to by different names in previous contributions. G.T. Heydt referred to Method of Companion Circuit in [Heydt 1991] as the differential equation that can be seen as a Norton equivalent (or companion circuit) for each element in the circuit. The other one, is the Nodal Conductance Approach (NCA) to highlight the use of nodal formulation [Yamamoto *et al.* 1999].

NIS forms the basis of EMTP-type programs such as PSCAD/EMTDC, ATP, etc, [Long *et al.* 1990, Marti and Linares 1994, Lehn *et al.* 1995] that are now widely accepted approaches for electromagnetic transient solutions.

More recently, for transient state estimation one contribution [Watson 2010] showed the possibility of using Numerical Integrator Substitution (NIS) on a simple single-phase system with basic lumped components.

The NIS approach has many advantages over the state variable formulation. Under the umbrella of PQSE, the contribution of the present work is to take the Transient State Estimation (TSE) one step further by using NIS formulation to build up a new three-phase transient state estimator, as outlined in the next chapter.

Chapter 3

TRANSIENT STATE ESTIMATION

During quasi-steady-state operation, the continuous electromechanical and electromagnetic distribution of energy among the system components are not modelled. Under this circumstance, the system behaviour can be represented via voltage and current phasors in the frequency domain. However, the transient events such as switching in/out or fault results are not accounted for in a traditional phasor approach. TSE is the newest extension of well established state estimation techniques to transient phenomena to represent required transient variations in power systems.

TSE could also be referred to as a reverse function of transient simulation (Figure 3.1). In other words, while transient simulation is used to analyse the consequences of a disturbance on a power system voltage, current, etc., TSE is employed to identify the cause of the transient change in system parameters. For this reason, TSE can potentially be used as a valuable tool for diagnostic purposes in power systems.

This chapter is organized as follows: section 3.1 describes how the required information is put together to form the proposed TSE algorithm by explaining TSE framework. Section 3.2 shows how the power system components such as transmission lines, transformers, generators and loads are individually modelled, then combined together to form the dynamic model of the system using NIS formulation. The next section explains how to form a TSE problem in the form of equation 2.1 using a mathematical model of the system based on the measurement type and location. Then, the solution of the derived problem is discussed in section 3.4. This section also

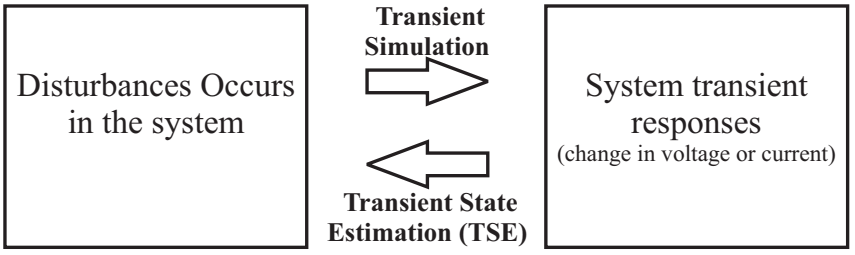

Figure 3.1: Fundamental concept of TSE.

looks at the observability criteria in state estimation. Eventually, the summary of the proposed algorithm is drawn in section 3.5.

3.1 TSE FRAMEWORK

Figure 3.2 shows the framework of TSE. The overall approach is using the network topology and system parameters to derive a mathematical model of the whole system. This model describes the behaviour of the system in a transient state situation. Then compares it with the actual time domain measurements from the system. This is to conclude which transient state is most likely to produce the observed system transient behaviour.

Transient variations in TSE necessitate a time domain solution for the system as well as a dynamic formulation to represent the system components. Therefore a dynamic model of the system is required. Based on the network topology and component parameters, this model is formulated using Numerical Integrator Substitution (NIS). This procedure is explained in section 3.2. Initially, the dynamic modelling is addressed using fundamental electrical circuit lumped elements such as resistor, inductor and capacitor. Then it will be extended to basic power system components such as generators, transformers, transmission lines and loads.

It should be noted that the generated model is valid as long as network configuration and component parameters remain unchanged. In traditional state estimation, the topology of the network is processed by gathering the status of circuit breakers and switches in the substations, which in turn can be used to configure the on-line diagram of the system. Also various network parameters, such as transmission line model parameters, tap changing transformer parameters, shunt capacitor or reactor parameter can be estimated via measurement redundancy [Abur and Exposito 2004]. It is assumed the same processing procedure works for TSE unless there is a reason that it differs.

The proposed method requires the same time step for all the measurements across the network under study. Besides, all measurements should be synchronised together at the same time point. Then, partial synchronized voltage and current measurements are taken from the network and used as inputs for the transient state estimator unit to estimate the current and voltage values at unmonitored locations for the same time point.

Obtaining adequate and reasonably synchronized measurements used to be the main barrier for implementing PQSE and particularly TSE. However,with the growing concern regarding power quality, utilities have been installing PQ monitors that give voltage and current measurements and transmit this information along with GPS timing data to a central location. Moreover, the need to modernize the grid to enable it to meet the needs of the future has led to the Smart Grid concept as a pathway of increasing the smartness of the electrical grid. Part of this

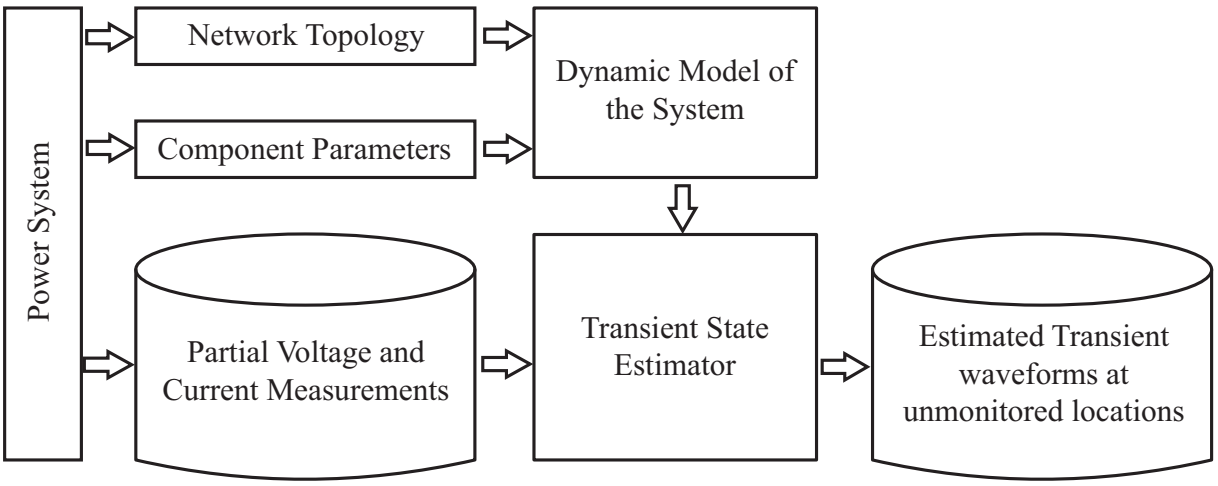

Figure 3.2: The framework of TSE.

involves advances in metering infrastructure which will make a large amount of data including TSE requirements available in the future.

3.2 DYNAMIC MODEL

To show the transient nature of the system, a dynamic model of the system is required. Dommel's EMTP approach (or NIS) combines the method of characteristics for transmission lines and the trapezoidal rule for discretisation of the system elements.

The best model which can realistically describe the physical behavior of the component is a function of time frame of interest and acceptable representation of each component for all frequency ranges is not practically possible. Therefore, from a modelling point of view, it is more appropriate to define the associated time frame with the transient study.

As the proposed TSE is going to be verified against transient events such as voltage dips/sags later in this work, the power system components are modelled according to Table VI (Modelling guidelines for voltage dip studies) from [C4.102 Feb. 2009]. However as this method evolves advanced models suitable for wide range of frequency and time frames, it must be taken into account and tested more thoroughly.

The relevant system components modelled here in this work are as follows:

- Transmission lines are modelled by a three-phase PI model with coupled elements.
- Transformers are modelled by three ideal single-phase transformers represented by a mutual inductance coupling between windings. Connection matrices are used to derive the nodal equation based on coil configuration (e.g., Delta/star-g, Star/star-g, etc).

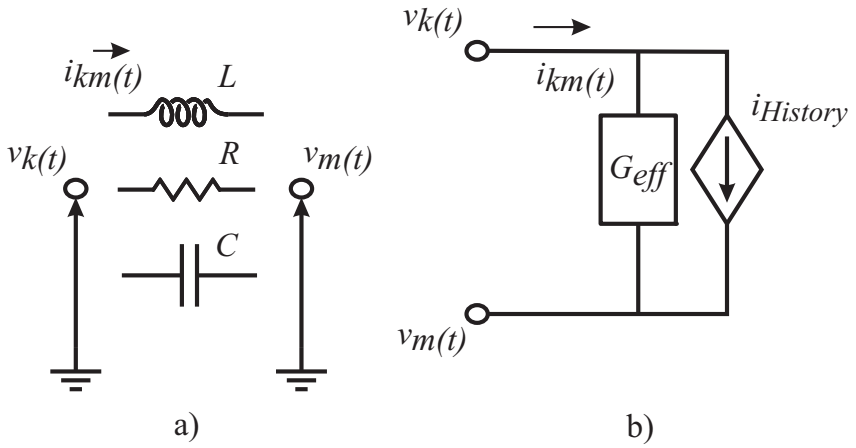

Figure 3.3: a) Basic electrical circuit elements, b) Equivalent circuit diagram

- The real and reactive power components of the static loads are modelled by their equivalent resistances and inductances, respectively.

- Generators can be modelled by three constant voltage sources and their resistance behind the transient reactance.

Starting with a fundamental electrical circuit element, the next sections describe how NIS formulation is employed to model power system components, which in turn is used to build up the TSE problem.

3.2.1 R, L and C model

Figure 3.3(a) shows the fundamental electrical circuit lumped elements, connected between two nodes k and m. The resistor is the simplest element and the current flowing through the resistor can be expressed as:

$$i_{km}(t) = \frac{1}{R}\{v_k(t) - v_m(t)\} \tag{3.1}$$

The transient behaviour of an inductor can be presented by a differential equation in time domain as:

$$v_L(t) = v_k(t) - v_m(t) = L\frac{di_{km}(t)}{dt} \tag{3.2}$$

Rearranging equation 3.2 in integral form gives:

$$i_{km}(t) = i_{km}(t - \Delta t) + \int_{t-\Delta t}^{t} (v_k - v_m)dt \tag{3.3}$$

Applying trapezoidal rule (equation 2.11) results in:

$$\begin{aligned} i_{km}(t) &= i_{km}(t-\Delta t) + \tfrac{\Delta t}{2L}\{(v_k - v_m)_t - (v_k - v_m)_{t-\Delta t}\} \\ &= \underbrace{i_{km}(t-\Delta t) + \frac{\Delta t}{2L}\{v_k(t-\Delta t) - v_m(t-\Delta t)\}}_{History\ Term} + \underbrace{\frac{\Delta t}{2L}\{v_k(t) - v_m(t)\}}_{Instantaneous\ Term} \end{aligned} \tag{3.4}$$

As shown in the last equation, the inductor can be expressed as a Norton equivalent circuit displayed in 3.3(b) or equivalently:

$$i_{km}(t) = i_{History} + G_{eff}\{v_k(t) - v_m(t)\} \tag{3.5}$$

where $G_{eff} = \Delta t/2L$.

Similarly for a capacitor, the transient behaviour can be presented by a differential equation in time domain as:

$$i_{km}(t) = C\frac{d(v_k(t) - v_m(t))}{dt} \tag{3.6}$$

Rearranging this in integral form gives:

$$v_{km}(t) = v_k(t) - v_m(t) = (v_k - v_m)_{t-\Delta t} + \frac{1}{C}\int_{t-\Delta t}^{t} i_{km}dt \tag{3.7}$$

Applying trapezoidal rule (equation 2.11) results in:

$$v_{km}(t) = v_k(t-\Delta t) - v_m(t-\Delta t) + \frac{\Delta t}{2C}\{i_{km}(t) + i_{km}(t-\Delta t)\} \tag{3.8}$$

Hence the current in the capacitor is calculated by:

$$i_{km}(t) = \underbrace{-i_{km}(t-\Delta t) - \frac{2C}{\Delta t}\{v_k(t-\Delta t) - v_m(t-\Delta t)\}}_{History\ Term} + \underbrace{\frac{2C}{\Delta t}\{v_k(t) - v_m(t)\}}_{Instantaneous\ Term} \tag{3.9}$$

Once again, as shown in the last equation the capacitor can be expressed as a Norton equivalent circuit illustrated in 3.3(b) or equivalently:

$$i_{km}(t) = i_{History} + G_{eff}\{v_k(t) - v_m(t)\} \tag{3.10}$$

where $G_{eff} = 2C/\Delta t$.

Table 3.1 summarizes the conductance (instantaneous term) relating the current contribution to the voltage at the present time (G_{eff}) and the current source (history term) which is the contribution to current from the previously computed values for fundamental circuit elements.

The power system components can be simply described as a set of interconnected RLC branches. Considering phase to ground voltages (hereafter called nodal voltages) as variables, the nodal

Table 3.1: Equivalent circuit diagram components.

Element	Instantaneous Term G_{eff}	History Term $I_{History}$
Resistor	$1/R$	–
Inductor	$\Delta t/2L$	$i_{km}(t-\Delta t) + G_{eff}\{v_k(t-\Delta t) - v_m(t-\Delta t)\}$
Capacitor	$2C/\Delta t$	$-i_{km}(t-\Delta t) - G_{eff}\{v_k(t-\Delta t) - v_m(t-\Delta t)\}$

solution is applied to formulate the dynamic model of each system component as well as the entire network. It leads to a coherent nodal system of equations representing single or multiple phase systems in the form of:

$$[G].\ \vec{v}(t) = \vec{i}_s(t) - \vec{I}_{History} \tag{3.11}$$

where:
$[G]$ is the conductance matrix,
$v(t)$ is the vector of nodal voltages,
$i_s(t)$ is the vector of external current sources and
$I_{History}$ is the vector of current sources representing previously computed values.

As long as the network topology and the component parameters remain unchanged, elements of $[G]$ are only dependent on the selected time step. For this reason, by introducing a constant time step, the entries of the matrix $[G]$ are constant at all time points.

3.2.2 Transmission line model

PI section models are often used to represent transmission lines where the transmission line elements are assumed to be lumped parameters. In distribution systems the transmission line lengths are typically short enough to allow the use of a nominal PI model. Those that are not can be implemented using multiple sections.

Figure 3.4 shows a single phase PI model transmission line consisting of one RL branch representing series resistance and inductance as well as two capacitors on either end representing the transmission line capacitance. Regarding series connection of R and L, it is more efficient to treat the series connection of R and L as a combined element, thereby less number of nodes and hence nodal equations for each time step need to be calculated. This reduction can be simply applied using basic circuit analysis. Figure 3.5 shows this branch reduction.

Let's assume v_L represents the voltage across the inductor. The history term for inductor as previously discussed is:

$$I_{L\ History}(t-\Delta t) = i_L(t-\Delta t) + \frac{\Delta t}{2L} v_L(t-\Delta t) \tag{3.12}$$

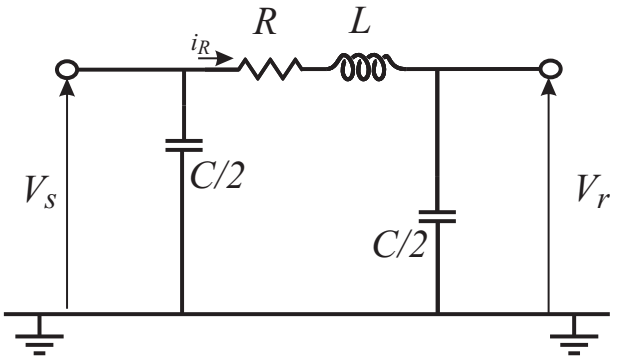

Figure 3.4: Single-phase PI model transmission line.

The voltage across the inductor can be related to the branch voltage ($v_{sr} = v_s - v_r$) as:

$$v_L(t - \Delta t) = v_{sr}(t - \Delta t) - i_R(t - \Delta t)R \tag{3.13}$$

Substituting equation 3.13 into equation 3.12 gives:

$$I_{L\ History} = \frac{\Delta t}{2L}\ v_{sr}(t - \Delta t) - \frac{\Delta t}{2L}\ i_R(t - \Delta t)R + i_L(t - \Delta t) \tag{3.14}$$

Since $i_L = i_R$,

$$I_{L\ History} = (1 - \frac{\Delta t R}{2L})\ i(t - \Delta t) + \frac{\Delta t}{2L}\ v_{sr}(t - \Delta t) \tag{3.15}$$

The value of the current source in the Norton equivalent circuit for the complete RL branch is simply calculated from the current that goes through the short circuited terminal. The short-circuit circuit consists of a current source feeding into two parallel resistors (R and $2L/\Delta t$), with the current in R being the terminal current. The equation for this is:

$$I_{short-circuit} = \frac{(2L/\Delta t)I_{L\ History}}{R + 2L/\Delta t} \tag{3.16}$$

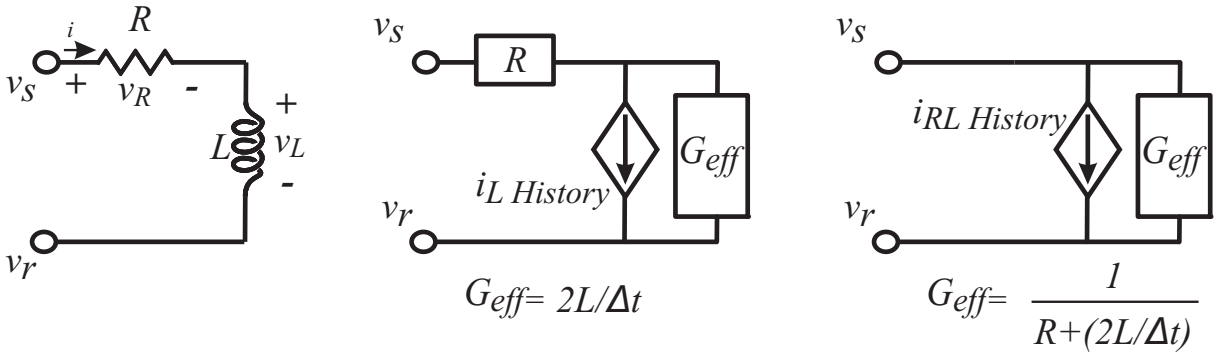

Figure 3.5: Reduction of RL branch.

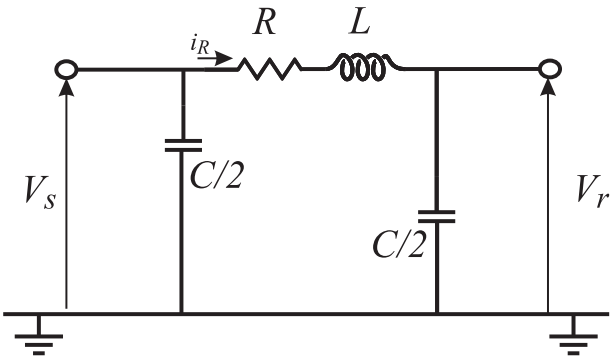

Figure 3.6: PI Transmission Line Norton circuit equivalent.

Substituting $I_{L\ History}$ from 3.15 into 3.16 and rearranging the short circuit current yields:

$$I_{short-circuit} = \frac{1 - \frac{\Delta tR}{2L}}{1 + \frac{\Delta tR}{2L}}\ i(t - \Delta t) + \frac{\frac{\Delta t}{2L}}{1 + \frac{\Delta tR}{2L}}\ v_{sr}(t - \Delta t) \tag{3.17}$$

The instantaneous current term is obtained from the current that flows due to an applied voltage to the terminals (current source open circuited):

$$\frac{1}{R + 2L/\Delta t}\ v_{sr}(t) = \frac{\Delta t/2L}{1 + \Delta tR/2L}\ v_{sr}(t) \tag{3.18}$$

Hence the complete difference equation expressed in terms of RL branch voltage is obtained by adding equations 3.17 and 3.18, which gives:

$$i(t) = \frac{1 - \frac{\Delta tR}{2L}}{1 + \frac{\Delta tR}{2L}}\ i(t - \Delta t) + \frac{\frac{\Delta t}{2L}}{1 + \frac{\Delta tR}{2L}}\ \{v_{sr}(t - \Delta t) + v_{sr}(t)\} \tag{3.19}$$

Equation 3.19 is in general a form of equation 3.11:

$$i_{RL\ history} = \frac{1 - \frac{\Delta tR}{2L}}{1 + \frac{\Delta tR}{2L}}\ i(t - \Delta t) + \frac{\frac{\Delta t}{2L}}{1 + \frac{\Delta tR}{2L}}\ v_{sr}(t - \Delta t) \tag{3.20}$$

or equivalently,

$$i_{RL\ history} = \frac{(2L/\Delta t) - R}{(2L/\Delta t) + R}\ i(t - \Delta t) + \frac{1}{(2L/\Delta t) + R}\ v_{sr}(t - \Delta t) \tag{3.21}$$

where the conductance value is:

$$G_{RL} = \frac{\frac{\Delta tR}{2L}}{1 + \frac{\Delta tR}{2L}} = \frac{1}{(2L/\Delta t) + R} \tag{3.22}$$

Hence, the Norton equivalent for a single-phase transmission line is shown in figure 3.6 and based

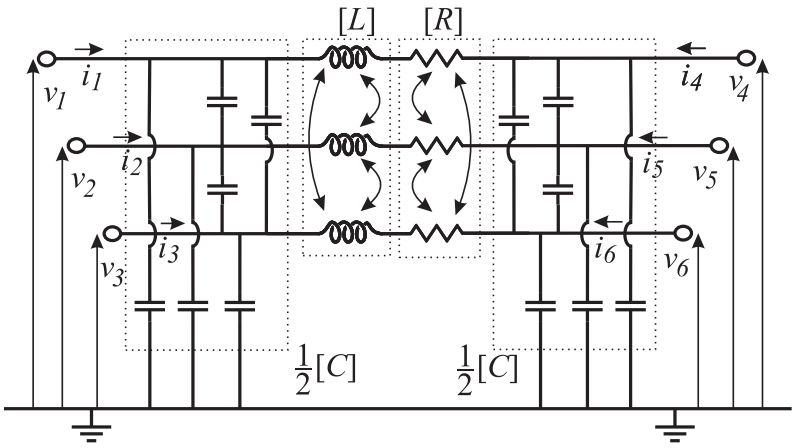

Figure 3.7: Three-phase PI model transmission line with coupled elements

on the given current direction it can be expressed as follows:

$$\begin{bmatrix} G_{RL}+G_C & -G_{RL} \\ -G_{RL} & G_{RL}+G_C \end{bmatrix} \times \begin{bmatrix} V_s(t) \\ V_r(t) \end{bmatrix} = \begin{bmatrix} i_{sr}(t) \\ i_{rs}(t) \end{bmatrix} - \begin{bmatrix} I_{Chistory}+I_{RLhistory} \\ I_{Chistory}-I_{RLhistory} \end{bmatrix} \tag{3.23}$$

The developed model above for a single-phase transmission line can be extended to a three-phase transmission line model with mutual coupling between phases (see figure 3.7).

In order to represent the mutual coupling between phases, the matrix format of the line lumped parameters are employed. This can be accommodated by using the available symmetrical components data. Therefore, the only difference between single-phase and three-phase transmission line models is that the conductance scalar parameters in equation 3.23 are replaced by the appropriate 3×3 matrices. Considering a general case of impedance matrix $[Z]$ for an ideally transposed transmission line this matrix can be described in equation 3.24. The diagonal elements are the self impedances and the off-diagonal elements are the mutual impedances.

$$Z = \begin{bmatrix} Z_{Self} & Z_{Mutual} & Z_{Mutual} \\ Z_{Mutual} & Z_{Self} & Z_{Mutual} \\ Z_{Mutual} & Z_{Mutual} & Z_{Self} \end{bmatrix} \tag{3.24}$$

where:

$$Z_{Self} = \frac{Z^{+Seq}+2Z^{0Seq}}{3} \qquad and \qquad Z_{Mutual} = \frac{Z^{0Seq}-Z^{+Seq}}{3}$$

When forming the nodal conductance matrix to derive a matrix equation in the form of equation 3.11 for a three-phase transmission line, $[G_{RL}]$ associated with the series lumped parameters will be added to two diagonal blocks corresponding to the relevant nodes and subtracted from two off-diagonal blocks. The $[G_C]$ associated with the shunt capacitance will only be added to the

two diagonal blocks. The values for series parameters are calculated according to equation 3.22 with R and L being replaced with matrices using symmetrical component data as indicated in equation 3.24. Considering the notation of the nodal voltage and current as well as the current direction given in figure 3.7, a three-phase transmission line based on NIS formulation can be expressed as:

$$\begin{array}{c|cc|cc|cc} & 1 & 2 & 3 & 4 & 5 & 6 \\ 1 & & & & & & \\ 2 & & [G_{RL}]+[G_C] & & & -[G_{RL}] & \\ 3 & & & & & & \\ \hline 4 & & & & & & \\ 5 & & -[G_{RL}] & & & [G_{RL}]+[G_C] & \\ 6 & & & & & & \end{array} \cdot \begin{bmatrix} v_1(t) \\ v_2(t) \\ v_3(t) \\ v_4(t) \\ v_5(t) \\ v_6(t) \end{bmatrix} = \begin{bmatrix} i_1(t) \\ i_2(t) \\ i_3(t) \\ i_4(t) \\ i_5(t) \\ i_6(t) \end{bmatrix} - \begin{bmatrix} I_{1\ History} \\ I_{2\ History} \\ I_{3\ History} \\ I_{4\ History} \\ I_{5\ History} \\ I_{6\ History} \end{bmatrix} \tag{3.25}$$

3.2.3 Transformer model

Three-phase transformers are modelled by three ideal single-phase transformers represented by two mutually coupled coils. Later on, connection matrices are used to derive the nodal equation for the three-phase transformer based on the transformer coil configuration (e.g., Delta/Star, Star/Star, etc).

Figure 3.8 shows an ideal transformer represented by a leakage inductance and a ratio changer.

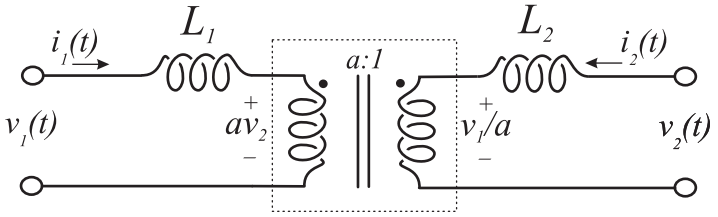

Figure 3.8: Ideal transformer

Having a as turns ratio and considering the current flowing direction as shown in figure 3.8, the relationship between the current and voltage at either side of the transformer can be expressed as equation 3.26 which is simply derived from a short circuit test conducted on the secondary, with a voltage source applied to the primary side:

$$\frac{d}{dt}\begin{bmatrix} i_1(t) \\ i_2(t) \end{bmatrix} = \frac{1}{L}\begin{bmatrix} 1 & -a \\ -a & a^2 \end{bmatrix} \times \begin{bmatrix} v_1(t) \\ v_2(t) \end{bmatrix} \tag{3.26}$$

where $L = L_1 + a^2 L_2$, is the leakage inductance between primary and secondary windings of the transformer as measured from the primary side. To model the transient behaviour of the

transformer using NIS formulation, the trapezoidal rule is applied to each row of equation 3.26, which results in two equations below:

$$\frac{d}{dt}i_1(t) = \frac{1}{L}\{v_1(t) - av_2(t)\} \tag{3.27}$$

$$\frac{d}{dt}i_2(t) = \frac{1}{L/a^2}\{v_2(t) - \frac{1}{a}v_1(t)\} \tag{3.28}$$

For the first equation:

$$\begin{aligned} i_1(t) &= i_1(t-\Delta t) + \tfrac{1}{L}\textstyle\int_{t-\Delta t}^{t}\{v_1(t) - av_2(t)\}dt \\ i_1(t) &= i_1(t-\Delta t) + \tfrac{\Delta t}{2L}\{v_1(t) - av_2(t) + v_1(t-\Delta t) - av_2(t-\Delta t)\} \\ i_1(t) &= \underbrace{i_1(t-\Delta t) + \frac{\Delta t}{2L}\{v_1(t-\Delta t) - av_2(t-\Delta t)\}}_{History\ Term} + \underbrace{\frac{\Delta t}{2L}\{v_1(t) - av_2(t)\}}_{Instantaneous\ Term} \end{aligned}$$

Similarly, for the second equation:

$$i_2(t) = \underbrace{i_2(t-\Delta t) + \frac{\Delta t}{2L}\{-av_1(t-\Delta t) + a^2v_2(t-\Delta t)\}}_{History\ Term} + \underbrace{\frac{\Delta t}{2L}\{-av_1(t) + a^2v_2(t)\}}_{Instantaneous\ Term}$$

Which are in the form of equation 3.11. Rearranging the equations above, gives the equation 3.29 in a matrix format.

$$\underbrace{\frac{\Delta t}{2L}\begin{bmatrix} 1 & -a \\ -a & a^2 \end{bmatrix}}_{G_{Tr}} \times \begin{bmatrix} v_1(t) \\ v_2(t) \end{bmatrix} = \begin{bmatrix} i_1(t) \\ i_2(t) \end{bmatrix} - \begin{bmatrix} I_{1History} \\ I_{2History} \end{bmatrix} \tag{3.29}$$

where history terms are:

$$\begin{bmatrix} I_{1History} \\ I_{2History} \end{bmatrix} = \begin{bmatrix} i_1(t-\Delta t) \\ i_2(t-\Delta t) \end{bmatrix} + \frac{\Delta t}{2L}\begin{bmatrix} 1 & -a \\ -a & a^2 \end{bmatrix} \times \begin{bmatrix} v_1(t-\Delta t) \\ v_2(t-\Delta t) \end{bmatrix} \tag{3.30}$$

The above mentioned approach can be extended to model a three-phase transformer by considering the transformer configuration. First, regardless of the transformer configuration, a three-phase transformer can be represented by the matrix equation 3.31. The *winding* notation are referred to the internal winding of the transformer represented by $v_1, i_1, etc.$ as shown in figure 3.9.

$$\Big[G_{winding}\Big] \cdot \vec{v}_{winding}(t) = \vec{i}_{winding}(t) - \vec{I}_{History_{winding}} \tag{3.31}$$

Figure 3.9 shows a three-phase delta/star transformer grounded in the star winding. V_x and I_x are used to indicate nodal voltage and currents while v_x and i_x indicate winding voltage and

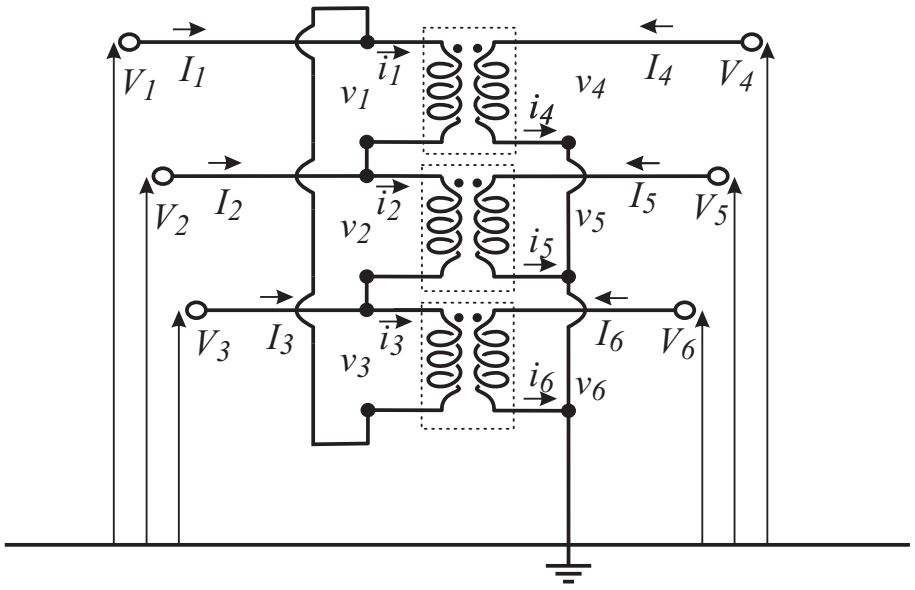

Figure 3.9: Three-phase delta/star connected transformer

current. For example, windings number 1 and 4 specify primary and secondary windings of the single-phase transformer for phase A, respectively. In order to clarify this better, the matrix equation below shows how the corresponding entries for windings number 1 and 4 in equation 3.31 must be replaced considering the values mentioned in equation 3.29 and 3.30:

$$\begin{pmatrix} G_{Tr}(1,1) & \dots & \dots & G_{Tr}(1,2) & \dots & \dots \\ \dots & \dots & \dots & \dots & \dots & \dots \\ \dots & \dots & \dots & \dots & \dots & \dots \\ G_{Tr}(2,1) & \dots & \dots & G_{Tr}(2,2) & \dots & \dots \\ \dots & \dots & \dots & \dots & \dots & \dots \\ \dots & \dots & \dots & \dots & \dots & \dots \end{pmatrix} \cdot \begin{pmatrix} v_1 \\ v_2 \\ v_3 \\ v_4 \\ v_5 \\ v_6 \end{pmatrix} = \begin{pmatrix} i_1 \\ i_2 \\ i_3 \\ i_4 \\ i_5 \\ i_6 \end{pmatrix} - \begin{pmatrix} I_{1History} \\ I_{2History} \\ I_{3History} \\ I_{4History} \\ I_{5History} \\ I_{6History} \end{pmatrix}$$

The transformer configuration is accommodated by considering the relationship between the winding currents and voltages and the nodal currents and voltages. Therefore, equation 3.31 is interfaced with the rest of the network by transforming winding to nodal quantities. This is performed by means of a connection matrix. Considering the notation and the direction given in figure 3.9 for a three-phase delta/star-g transformer, the relationship between node quantities and winding quantities with all nodal voltages being with respect to the reference earth, can be defined as follows:

$$\vec{v}_{winding} = \Big[C\Big] \cdot \vec{V}_{Node} \tag{3.32}$$

$$\vec{I}_{Node} = \Big[C\Big]^T \cdot \vec{i}_{winding} \tag{3.33}$$

where $[C]$, connection matrix, for a delta/star-g configuration is:

$$\Big[C\Big] = \begin{bmatrix} 1 & -1 & 0 & 0 & 0 & 0 \\ 0 & 1 & -1 & 0 & 0 & 0 \\ -1 & 0 & 1 & 0 & 0 & 0 \\ 0 & 0 & 0 & 1 & 0 & 0 \\ 0 & 0 & 0 & 0 & 1 & 0 \\ 0 & 0 & 0 & 0 & 0 & 1 \end{bmatrix} \tag{3.34}$$

Substituting the winding parameters with nodal parameters in equation 3.31, using equations 3.32 and 3.34, yields:

$$\Big[G_{winding}\Big] \cdot \Big[C\Big] \cdot \vec{V}_{Node} = \Big[C\Big]^{T^{-1}} \{\vec{I}_{Node}(t) - \vec{I}_{History_{Node}}\} \tag{3.35}$$

Multiplying both sides by $[C]^T$ gives:

$$\Big[C\Big]^{T} \cdot \Big[G_{winding}\Big] \cdot \Big[C\Big] \cdot \vec{V}_{Node} = \vec{I}_{Node}(t) - \vec{I}_{History_{Node}} \tag{3.36}$$

The term $[C]^T \cdot [G_{winding}] \cdot [C]$ is the nodal conductance matrix for a three-phase transformer and it is added to the appropriate entries of the system nodal conductance matrix.

3.2.4 Load model

Static loads are considered here as the load model. They express the active and reactive powers as a function of busbar voltage at any instant of time. For static loads the real and reactive power components are modelled by their equivalent resistance and inductance, respectively. This can be shown as a parallel R-L circuit as depicted in figure 3.10. Based on this figure and the R and L model explained in section 3.2.1, the associated matrix equation can be expressed in equation 3.37. The relevant values are simply selected from the values given in table 3.1.

$$\begin{bmatrix} \frac{1}{R_1} + \frac{\Delta t}{2L_1} & 0 & 0 \\ 0 & \frac{1}{R_2} + \frac{\Delta t}{2L_2} & 0 \\ 0 & 0 & \frac{1}{R_2} + \frac{\Delta t}{2L_2} \end{bmatrix} \cdot \begin{bmatrix} V_1(t) \\ V_2(t) \\ V_3(t) \end{bmatrix} = \begin{bmatrix} I_1(t) \\ I_2(t) \\ I_3(t) \end{bmatrix} - \begin{bmatrix} I_{1History} \\ I_{2History} \\ I_{3History} \end{bmatrix} \tag{3.37}$$

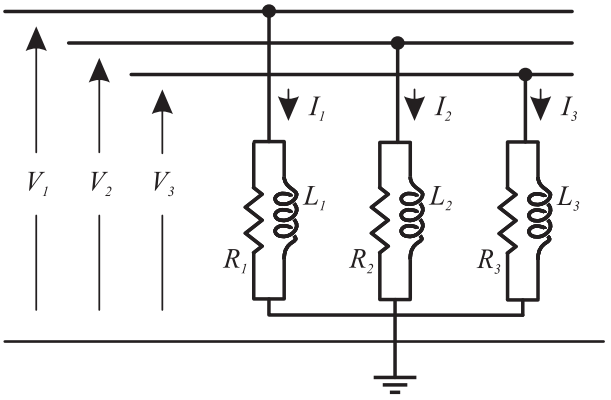

Figure 3.10: Three-phase delta/star connected transformer

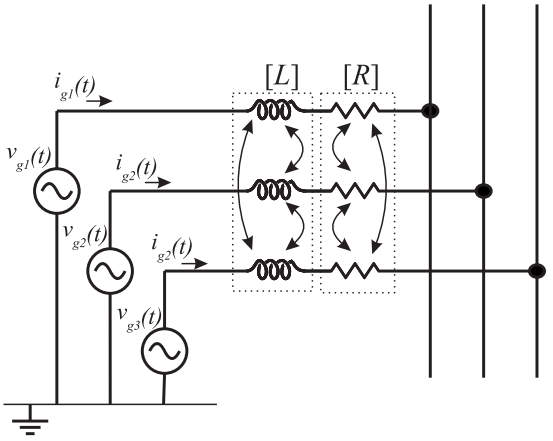

Figure 3.11: Generator RL equivalent model

3.2.5 Generator model

Generators are modelled by series RL branches as shown in figure 3.11. If RL series branch are mutually coupled, then it can be treated the same as the RL series branches for transmission lines mentioned in section 3.2.2. Otherwise, as a simple R and L they can be modelled as explained in section 3.2.1.

3.3 TSE CONSTRUCTION

The general form of the state estimation problem was explained in section 2 and repeated here (equation 2.1) in order to improve the readability. The task of this section is to show how the

entries must be selected in order to form this equation for TSE.

$$\underbrace{\begin{bmatrix} z_1 \\ z_2 \\ \vdots \\ z_m \end{bmatrix}}_{Z} = \underbrace{\begin{bmatrix} h_{1,1} & h_{1,2} & \cdots & h_{1,n} \\ h_{2,1} & h_{2,2} & \cdots & h_{2,n} \\ \vdots & \vdots & \ddots & \vdots \\ u_{m,1} & u_{m,2} & \cdots & h_{m,n} \end{bmatrix}}_{H} \cdot \underbrace{\begin{bmatrix} x_1 \\ x_2 \\ \vdots \\ x_m \end{bmatrix}}_{X} + \underbrace{\begin{bmatrix} \varepsilon_1 \\ \varepsilon_2 \\ \vdots \\ \varepsilon_m \end{bmatrix}}_{\varepsilon} \tag{3.38}$$

where z is a (m×1) vector of measured (known) quantities and x is a (n×1) vector of state variables (unknown quantities) for which the equation must be solved. $[H]$ is a (m×n) measurement function relating the known quantities to state variables and ε is the vector of measurement errors.

In a TSE problem, the z entries are selected from nodal voltages as well as branch and also load currents. In other words, these quantities are chosen from the network as measured quantities. Therefore, each measurement adds one row to the TSE problem in the form of equation 2.1. For example, having m number of measurements results in a $m \times 1$ matrix representing the $[z]$ matrix. The state variables or the matrix x entries in TSE are nodal voltages. The reason behind this selection is due to the fact that once the nodal voltages are known, other dependent variables such as branch currents, etc. can be calculated accordingly.

To construct the measurements matrix [H], each measurement point results in one equation that adds a corresponding row from the dynamic model. In other words, each z entry is associated with a row in [H] which is selected from a corresponding dynamic model explained in the previous section. This procedure is described based on measurement type as follows:

Measuring nodal Voltage: When a node voltage is measured the corresponding row in the [H] matrix will comprise of all zeros except at the position corresponding to the node that was measured (where the entry will be one). Similarly, when a voltage is measured across two nodes, the corresponding row in the [H] will comprise of all zeros except the positions corresponding to either end (where the entries will be 1 and -1 accordingly).

Measuring branch current: When a branch current is measured a row will be added to [H] consisting of all zeros except at the locations associated with the sending and receiving end nodes, which will contain the appropriate conductance entries from the [G] matrix.

To illustrate how the relevant entries in [H] must be selected, the following cases are considered for an arbitrary measurement number "r" for the fundamental electrical circuit elements shown in figure 3.3. (The dynamic model formulation was previously explained in section 3.2.1)

Table 3.2: Measurement equation construction.

Measurement Type	Measurement Vector Entry $[z]$	Measurement Matrix $[H]$	State Variables $[x]$
Nodal voltage to ground	$v_k(t)$	$[1 \quad \cdots \quad 0]$	$[v_k(t) \ \cdots \ v_m(t)]^T$
Voltage across element	$v_k(t) - v_m(t)$	$[1 \quad \cdots -1]$	
Branch current	$i_{km}(t) - I_{History}$	$[G_{eff} \ \cdots \ -G_{eff}]$	

For instantaneous nodal voltage (v_k) measurement:

$$\begin{aligned} z_r(t) &= v_k(t) \\ H_{r,k} &= 1.0 \end{aligned} \tag{3.39}$$

For instantaneous voltage measurement across R, L or C between nodes k and m:

$$\begin{aligned} z_r(t) &= v_k(t) - v_m(t) \\ H_{r,k} &= 1.0 \\ H_{k,m} &= -1.0 \end{aligned} \tag{3.40}$$

For instantaneous current measurement through R, L or C from sending node m to receiving node k:

$$\begin{aligned} z_r(t) &= i_{measured}(t) - I_{History} \\ H_{r,k} &= G_{eff} \\ H_{k,m} &= -G_{eff} \end{aligned} \tag{3.41}$$

This procedure has been summarized in table 3.2 for the fundamental electrical circuit elements shown in figure 3.3 and the relevant values defined in table 3.1.

Given the fact that all system components are modelled by integrating R, L and C elements, the above mentioned approach can be simply extended to be used for a three phase system component as well. As an example, lets consider the three-phase transmission line shown in figure 3.7 and the relevant equations given in section 3.2.2. Assuming that the branch current measurement leaving node 3 (i_C) and the nodal voltage number 2 (V_2) are the selected measurement

points, the following transient state estimation problem is constructed as:

$$\begin{bmatrix} \vdots \\ i_C(t) - I_{3History} \\ V_2 \\ \vdots \end{bmatrix} = \begin{bmatrix} \vdots & \vdots & \cdots & \vdots \\ G_{TL}(3,1) & G_{TL}(3,2) & \cdots & G_{TL}(3,6) \\ 0 & 1 & \cdots & 0 \\ \vdots & \vdots & \cdots & \vdots \end{bmatrix} \cdot \begin{bmatrix} V_1(t) \\ V_2(t) \\ V_3(t) \\ V_4(t) \\ V_5(t) \\ V_6(t) \end{bmatrix} \tag{3.42}$$

The left hand side of the equation above is known for time point t; $i_C(t)$ is measured and $I_{3History}$ is known from the previous time step. The entries of the [G] matrix is already known from the mathematical model which has been developed for transmission lines in form of equation 3.11. This process is continued for every single measurement points within the network. Once enough measurements are collected and the TSE problem is derived, it must be solved for the state variables (nodal voltages) which is the subject of the next section.

3.4 SOLUTION OF MEASUREMENT EQUATION

In the previous section we saw how the transient state estimation problem (equation 2.1) is constructed as a linear system of equations. To solve the constructed state estimation problem, the methods available depend on the rank of the [H] matrix. This determines whether the system is under-determined or over-determined. It also helps to verify whether the state variables are observable, non observable or just partially observable.

When the number of unknown quantities (n) is greater than the number of equations (m) (i.e. $n < m$) the system is called under-determined. In the case where the number of unknown state variables is equal or less than the number of equations, the system is said to be completely determined or over-determined, respectively. In traditional state estimation there is an abundant number of measurement devices (revenue meters) and it results in an over-determined system of equations. However, estimation equation in PQSE and particularly TSE, is generally under-determined due to the cost of PQ monitoring devices and also the different ownership of different part of the system.

A system is said to be observable if the complete state of the system can be determined using measurements. In other words, the derived system of equations for TSE is observable if all the state variables (x) can be determined from the measurement information (z). In some cases the system under study is not observable, however some of the state variables can still be determined. In this case the system is partially observable.

The set of linear equations constructed in the previous section is a function of time. For this

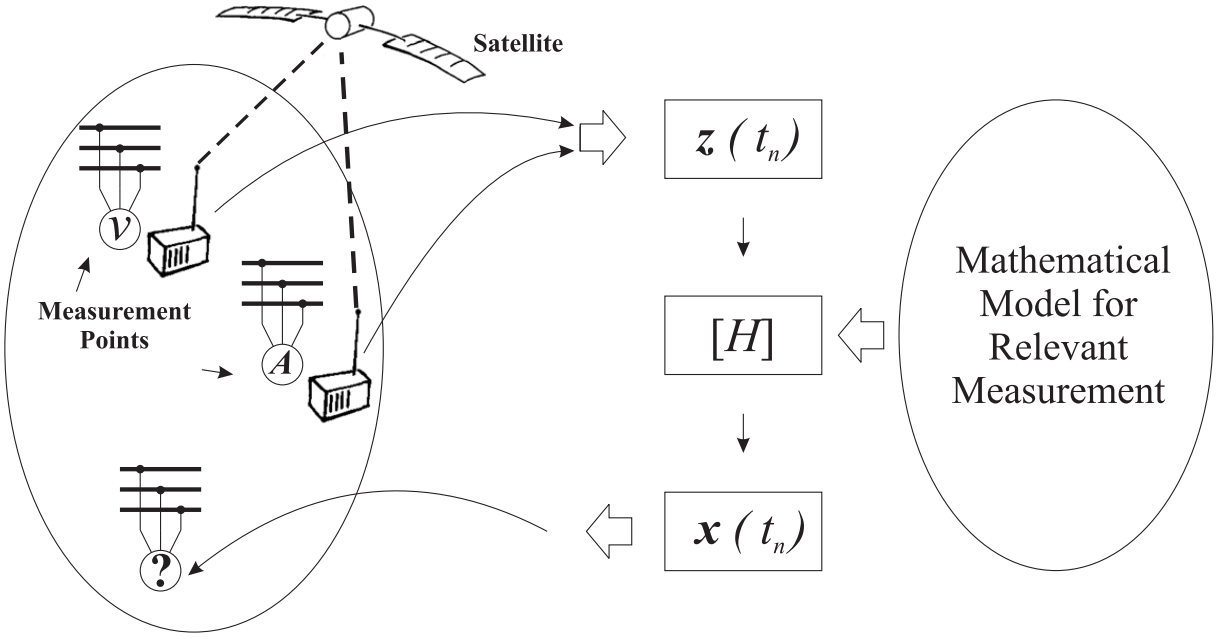

Figure 3.12: TSE Solution.

reason, the period in which the system is under study is divided into time steps with a fixed time interval. Then the TSE problem as shown in equation 3.43 must be solved at each time point. It also should be noted that by assuming the fixed time step, H matrix obtained from G matrix remains constant at all the time points:

$$\vec{z}(t_n) = [H] \; . \; \vec{x}(t_n) \tag{3.43}$$

where:
$z(t_n)$: depends on the selected measurement, is a vector of measured currents or voltages at the time t_n.
$x(t_n)$: is a vector of the nodal voltages at the same time t_n which equation must be solved for.
$[H]$: is the measurement matrix which is relating vector $z(t_n)$ to $x(t_n)$ according to the conductance matrix describing the dynamic model of the system (equation 3.11).

Figure 3.12 shows the basic concept of TSE in which the measurements are read in at the time t_n and the state variables are estimated for the same time t_n (the error vector ε is ignored from equation 2.1). In other words, at each time step synchronised measurement values are read in and the matrix equation above is solved for the unmonitored nodal voltage values at the same time point. For the very first initial condition, $t_n = 1$, the system initial currents and voltages could be set. Power flow results for a steady state situation could be used for initialization or they could be set as zero and TSE could quickly settle in and track the system.

Once the state variables (nodal voltages) and dependent variables (such as branch currents) are calculated, these values are saved to be used as previous history term for the next time step. In

selecting the time step, consideration must be given to the time constants of the network and phenomena as well as the travelling time of the transmission lines if travelling wave transmission line mode is used.

Singular Value Decomposition (SVD) is the method of choice to solve the TSE problem in this work over a normal equation approach due to its robustness and ability to cope with under-determined systems [Press 2007]. SVD also provides observability analysis as a by product. These will be outlined in further details in the next subsections:

3.4.1 SVD

The SVD method is usually used for solving matrices that are either singular or close to singular. Under this situation the normal equation approach fails to provide matrix inverse and hence reliable results. However, compared to the normal equation approach, computational requirements to perform SVD is much higher.

The SVD method is based on the linear algebra theorem saying that any M×N matrix H can be rewritten as:

$$[H]_{m\times n} = \underbrace{\begin{pmatrix} u_{1,1} & u_{1,2} & \cdots & u_{1,m} \\ u_{2,1} & u_{2,2} & \cdots & u_{2,m} \\ \vdots & \vdots & \ddots & \vdots \\ u_{m,1} & u_{m,2} & \cdots & u_{m,m} \end{pmatrix}}_{[\,U\,]} \cdot \underbrace{\begin{pmatrix} s_1 & & & \\ & s_2 & & \\ & & \ddots & \\ & & & s_n \end{pmatrix}}_{[\,S\,]} \cdot \underbrace{\begin{pmatrix} v_{1,1} & v_{1,2} & \cdots & v_{1,n} \\ u_{2,1} & u_{2,2} & \cdots & v_{2,n} \\ \vdots & \vdots & \ddots & \vdots \\ v_{n,1} & v_{n,2} & \cdots & v_{n,n} \end{pmatrix}^T}_{[\,V\,]^T} \tag{3.44}$$

where U (m×m) and V^T (n×n) are orthogonal matrices and S (m×n) is a diagonal matrix with the entries of singular values of H. These factored forms can be calculated through eigenvalue analysis. SS^T is an eigenvalue diagonal matrix. $[U]$ is the eigenvector matrix of HH^T and its columns whose same numbered elements of singular values which are non-zero are an orthonormal set of basis vectors that span the range of matrix H. $[V]$ is the eigenvector matrix of H^TH and its columns whose same numbered elements of singular values which are zero are an orthonormal set of basis vectors that span the null space of matrix H.

As mentioned earlier, the TSE problem is an under-determined equation ($m < n$), hence the measurement matrix H can be expressed as:

$$[H]_{m\times n} = \begin{pmatrix} \\ U \\ \\ \end{pmatrix} \cdot \begin{pmatrix} s_1 & & & \\ & s_2 & & \\ & & \ddots & \\ & & & s_n \end{pmatrix} \cdot \begin{pmatrix} v_{1,1} & v_{1,2} & \cdots & v_{1,n} \\ u_{2,1} & u_{2,2} & \cdots & v_{2,n} \\ \vdots & \vdots & \ddots & \vdots \\ v_{n,1} & v_{n,2} & \cdots & v_{n,n} \end{pmatrix} \tag{3.45}$$

In this case, singular values of [S] for $j = m+1, \cdots, n$ and the corresponding columns of [U] will all be zero. The inverse of measurement matrix, $[H]$ (m×n), can be represented as:

$$\Big[H\Big]^{-1} = \Big[V\Big] \cdot \Big[diag\ (1/s_j)\Big]^{-1} \cdot \Big[U\Big]^{T} \tag{3.46}$$

Then the solution of TSE for time t_n can be calculated as follows:

$$\vec{x}(t_n) = \Big[V\Big] \cdot \Big[diag\ (1/s_j)\Big]^{-1} \cdot \Big[U\Big]^{T} \cdot \vec{z}(t_n) \tag{3.47}$$

If some of the s_j's $j = 1, 2, \cdots, n$ are zero or near zero, then the measurement matrix is singular. In this case, a zero is placed in the diagonal element of $[S]^{-1}$ (instead of $[1/s]$). Equation 3.46 with the singular $1/s_j$'s replaced with zero, is called the pseudo-inverse of $[H]$.

Two scenarios are possible depending on whether or not $\vec{x}$ relies in the range of $[H]$. If it does then the singular set of equations 3.43 have more than one solution, since any vector in the null space can be added to x and gives another valid solution. However, equation 3.47 is able to produce the one shortest length among many.

If $\vec{z}$ is not in the range of $[H]$, then the set of equations 3.43 has no solution. In such a case, equation 3.47 can still be used to construct a "solution" vector x. This vector x, will not exactly solve the estimation problem, but among all possible vectors x, it finds:

$$\vec{x} \ \ which\ minimizes \ \ r \equiv |H\ .\ x - z| \tag{3.48}$$

where r is called the residual of the solution.

3.4.2 Observability Criteria

A normal equation approach can be applied only when the system is fully observable and hence an inverse of matrix H exists. It requires that prior Observability Analysis (OA) is performed to ensure the system observability. However, SVD is able to give reliable answers for some state variables even when the system is partially observable. Moreover, inspection of the singular values and component matrices also gives important information on observability.

Basically, SVD is able to produce an infinite number of solutions that satisfies the TSE equation, expressed by:

$$\left[x\right] = \left[x_p\right] + \sum_{i=0}^{N} k_i \left[x_{ni}\right] \tag{3.49}$$

where $[x_p]$ is the particular solution, k_i is a constant and $[x_{ni}]$ is the null space vector. The number of null space vectors N, is the number of zero w_j's in matrix $[W]$ equal to zero or equivalently $(n - rank(H))$.

We already saw the columns of $[V]$ whose same numbered elements of singular values of zero are an orthonormal set of basis vectors that span the null space of matrix H. These columns can define the observability by inspecting the position of the zero inputs. If all the $i-th$ entries from all orthonormal sets of basis vectors are zero then adding any combination of the null space to a particular solution will not change the solution of the $i-th$ state variable (nodal voltage). For this reason, the nodal voltage is among the observable state variables (the busbar is observable). Otherwise, since the nodal voltages corresponding to the non-zero entries cannot be uniquely defined they are classified among the unobservable state variables (the busbar is unobservable). Therefore, SVD provides OA as a by-product by means of inspecting the null space vectors before or during the transient state estimation.

This can simply be done through MATLAB command $[U, S, V] = svd(H)$ which returns three factored matrices U,S,V representing [H]. In order to explain this procedure, let's assume $m = n - 3$ (keep in mind that TSE is usually an under-determined system). $[S]$ and $[V]$ will be in the form of:

$$
S_{m\times n} = \begin{array}{c} \\ 1^{St} \\ \vdots \\ i^{th} \\ \vdots \\ m^{th} \\ \vdots \\ \\ \vdots \\ \\ n^{th} \end{array}
\begin{pmatrix}
s_1 & & & & & & & & \\
& \ddots & & & & & & & \\
& & s_i & & & & & 0 & \\
& & & \ddots & & & & & \\
& & & & s_m & & & & \\
& & & & & \underbrace{s_{m+1,n-2}}_{0} & & & \\
& & & & & & \underbrace{s_{m+2,n-1}}_{0} & & \\
& & 0 & & & & & \underbrace{s_{m+3,n}}_{0} &
\end{pmatrix}
$$

$$
V_{n\times n} = \begin{array}{c} \\ 1^{St} \\ \vdots \\ i^{th} \\ \vdots \\ m^{th} \\ \vdots \\ \vdots \\ n^{th} \end{array}
\begin{pmatrix}
1 & & & \cdots & & n-2 & n-1 & n \\
v_{1,1} & \cdots & & & & & & \\
\vdots & \ddots & \vdots & & \vdots & \vdots & \vdots & \vdots \\
v_{i,1} & \cdots & v_{i,i} & \cdots & v_{i,m} & v_{i,n-2} & v_{i,n-1} & v_{i,n} \\
\vdots & & \vdots & \ddots & \vdots & \vdots & \vdots & \vdots \\
 & & & & v_{m,m} & & & \\
 & & & & & v_{m+1,n-2} & & \\
 & & & & & & v_{m+2,n-1} & \\
 & & & & & & & v_{m+3,n}
\end{pmatrix}
$$

The singular values of matrix $[S]$ are sorted in ascending order and for the elements $n-2, n-1$ and n are zero. In this case, inspecting the same numbered columns in $[V]$ defines a set of basis nullspace vectors as well as the system observability. For example, i^{th} state variable is observable if and only if all the entries of $[v_{i,n-2} \quad v_{i,n-1} \quad v_{i,n}]$ are zero.

3.5 IMPLEMENTATION SUMMARY

The proposed transient state estimation has been implemented in MATLAB and applied to a distribution test system (results will be outlined in the next chapter).

Figure 3.13 summarizes the implementation algorithm of the proposed transient state estimator. Here is the description of each block step by step:

Step 1, The equations representing the dynamics of each system component such as transformers, transmission lines, etc. are developed in a form suitable for including in equation 3.11 (This has been explained in section 3.2).

Step 2, Individual equations are interfaced with the rest of the network to form a system dynamic model.

Step 3, The measurements type and location are selected arbitrary. All the measurements should be synchronized together at the same time point to estimate the value for the nodal voltage of interest at the same time point. Hence if the measurement data is captured with different sample rates then resampling (interpolation is required) to get data at the same time points is required. In a similar vein, unsynchronised data can be used so long as the data is time-stamped as then resampling can be used.

Step 4, Selection in the previous step is followed by using corresponding rows from the dynamic model to create the measurement equation $[H]$. (This has been explained in section 3.3.)

Step 5, If it is the first step then initial current and voltages are read in. Although power flow results could be used for initialization in this work they are set to zero and TSE quickly settles in and tracks the system.

Step 6, If it is not the first step, the history terms are read in or in case the required values are among observable variables, it could be calculated from the previous time step values.

Step 7, Pseudo-inverse of the measurement matrix [H] is calculated and the derived TSE problem is solved for the nodal voltages ($\vec{x}$). This is simply performed by calling the MATLAB command $pinv(h)$.

Step 8, From the obtained nodal voltages, the dependent variables such as branch currents, etc. are calculated.

Step 9, The calculated voltages and currents are used to update the history terms for the next time step. The implemented time step (Δt) is 50 μs in this work.

Step 10, The new measurement samples are used in equation 2.1 and solved for the state vector x for the next time step ($t + 50\mu s$).

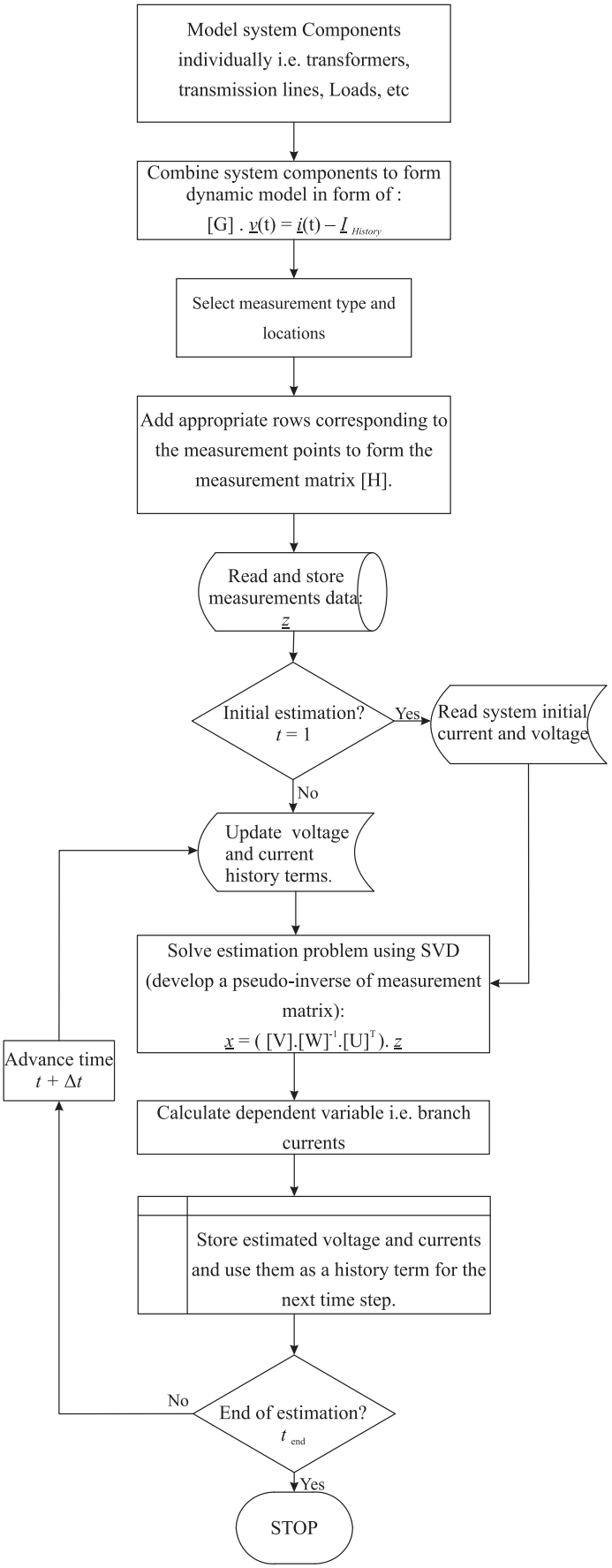

Figure 3.13: Transient state estimator flowchart.

Chapter 4

SIMULATION AND TEST RESULTS

The proposed TSE method was outlined in the previous chapter. This chapter applies this method to a distribution test system in order to verify the accuracy of the TSE performance in different cases.

4.1 TEST SYSTEM

The distribution test system used in this work is shown in figure 4.1. This is an 11 kV distribution network taken from the Killinchy area, a rural area in South Canterbury supplying a major milk treatment factory in the South Island of New Zealand. The system consists of 16 busbars and a ring of 11 kV overhead lines and the lateral outgoing feeders. Due to the lack of field measurements, PSCAD/EMTDC simulation software will be used to generate the field data for

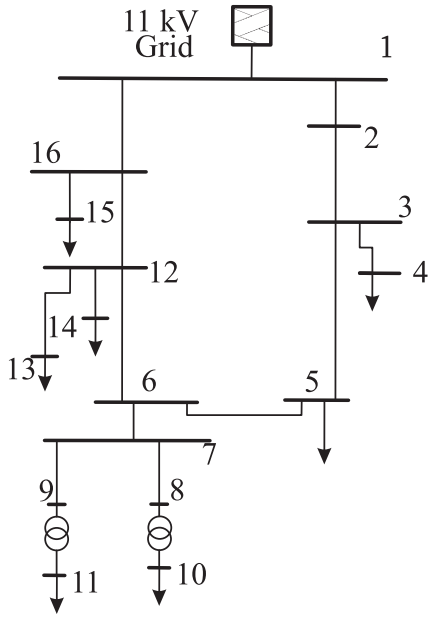

Figure 4.1: Distribution Test System.

the test system. Then the required time domain voltage and current measurements are taken and fed to the transient state estimator. The taken measurements which are the output of PSCAD/EMTDC simulation software are hereafter called actual measurements.

4.2 VERIFICATION METHOD

In the preceding discussions, TSE was introduced as a valuable tool to identify the cause of an occurred transient in power systems. To demonstrate this, figure 4.2 shows the general approach has been considered to verify the effectiveness of the proposed TSE method in order to identify the source of transient change in system parameters such as voltage or current.

With the knowledge of the type and the location of occurred event in the test system, the system and the transient event is simulated in a time domain. Then, the assigned current and voltage measurements by estimator are selected and their values at time t_n forms the matrix $[z(t_n)]$ which in turn is going to be used for the estimation block ($[z] = [H].[x]$). All the voltage and current results which are not assigned by the estimator are replaced as actual values.

On the other hand, based on the selected type and location of measurements the corresponding rows (as discussed in section 3.3) forms the measurement matrix $[H]$. The constructed transient estimator solves the estimation equation for unmonitored nodal voltages. Eventually, the estimated values are inspected to identify the possible reasons for the simulated event. The obtained waveforms are then compared with the actual waveforms (simulated in software) to validate the TSE accuracy.

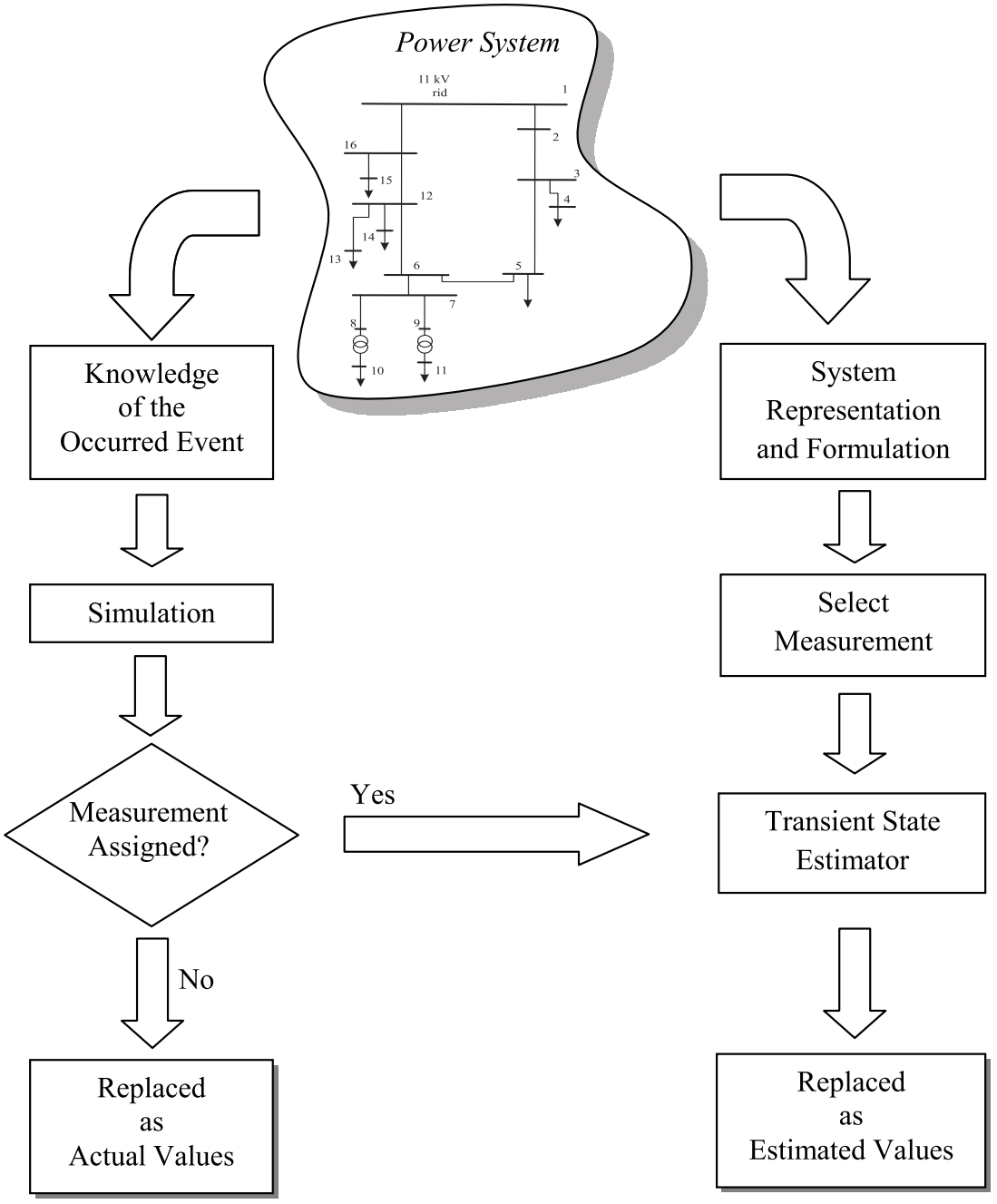

Figure 4.2: TSE Verification.

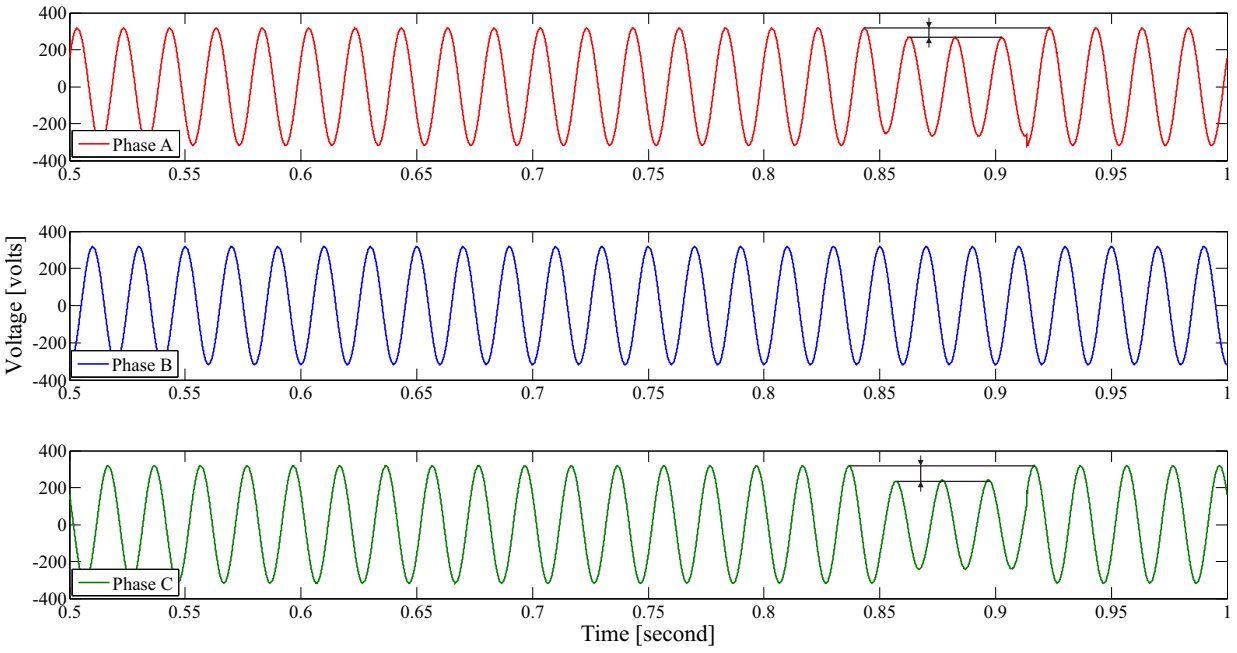

Figure 4.3: Voltage sag recorded at busbar 11.

4.2.1 Event Simulation

Voltage sags are common events in power systems caused by network faults and large load sudden connections. This power quality issue can affect a wide range of electrical equipment in the form of malfunctions, interruptions or losses and is of particular concern to industry. TSE is demonstrated here to identify the source of the occurred voltage sag within the network. In order to generate the measurement field data, different types of short circuit faults under different situations (causing voltage sags) are simulated at the busbars which are not monitored. Then TSE algorithm is performed to estimate the voltage waveform at these busbars. Inspection of the estimated waveform is expected to reveal the information of interest. The results are compared to the actual values and will be discussed in the following subsections.

A single-phase to ground short circuit at busbar No.5 is simulated using PSCAD/EMTDC to begin with. The impedance of the fault is 0.01 ohm. The fault occurs at $t = 0.85$ second and lasts for 0.0635 second, the fault will be cleared afterward. No measurements on or near this busbar is located. This simulation shows an approximately 70% retained voltage on phases A and C recorded at busbar 11 (figure 4.3). Then the selected voltage and current measurements shown in figure 4.4 are considered as TSE inputs and will be used to form the z matrix in equation 3.43.

The 11 kV grid is modelled as a Thevenin equivalent. The power system components have been simulated according to the Table VI (Modelling guidelines for voltage dip studies) from [C4.102 Feb.

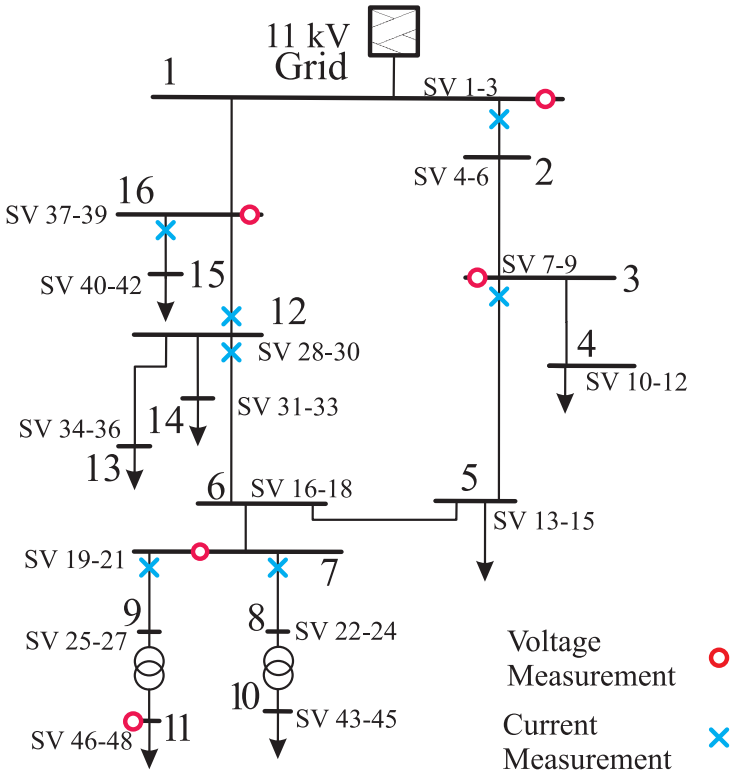

Figure 4.4: Measurement placement and node numbers.

2009].

A time step of 50 μ seconds is reasonably standard for this type of fault transient simulation as it captures the frequencies of interest. So the transient simulation is run using a 50 μ seconds time step for the models thereby creating a TSE algorithm that assumes the same sampling time.

4.2.2 Measurements

The measurement placement is indicated by cross and circle symbols in figure 4.4. The cross symbols represent time domain three-phase line current measurements and the circle symbols represent time domain three-phase voltage measurements in reference to earth (nodal voltages).

Figure 4.4 also shows the state variables (node numbers) representing each busbar. The node numbers are not in a particular order. Table 4.1 determines how the busbars are related to the node numbers.

It should be noted that the number of measurements is 36 compared to 48 unknown state variables (number of equations is less than the number of unknown state variables). Hence the

Table 4.1: Busbars and node numbers.

Busbar	Node Numbers	Busbar	Node Numbers
1	1,2,3	*9*	25,26,27
2	4,5,6	*10*	43,44,45
3	7,8,9	*11*	46,47,48
4	10,11,12	*12*	28,29,30
5	13,14,15	*13*	34,35,36
6	16,17,18	*14*	31,32,33
7	19,20,21	*15*	40,41,42
8	22,23,24	*16*	37,38,39

estimation problem is an under-determined linear system of equations.

Based on the type and location of the selected measurements in figure 4.4, the corresponding rows and columns in the measurement matrix, [H] are constructed using the system component modelling discussed in Chapter 4.

4.2.3 Solution

Having the [z] entries at time t_n from PSCAD/EMTDC simulation results and the [H] matrix constructed here, SVD is used to solve the transient state estimate equation for the state variables for time t_n as follows:

$$\vec{x}(t_n) = \underbrace{\Big[V\Big] \cdot \Big[diag\ (1/s_j)\Big]^{-1} \cdot \Big[U\Big]^{T}}_{[H]\ pseudo-inverse} \cdot \vec{z}(t_n)$$

Pseudo-inverse of the [H] matrix is simply performed by calling the MATLAB command $pinv(h)$.

4.3 SYSTEM OBSERVABILITY

SVD serves as as valuable tool for solution of estimation equation as well as observability analysis. Previously, in section 3.4.2, observability analysis using SVD was discussed. A numerical example of observability analysis on the 11kV test system is discussed here.

The [H] matrix constructed in the previous section can be rewritten as:

$$[H]_{36\times 48} = \underbrace{\begin{pmatrix} u_{1,1} & u_{1,2} & \cdots & u_{1,36} \\ u_{2,1} & u_{2,2} & \cdots & u_{2,36} \\ \vdots & \vdots & \ddots & \vdots \\ u_{36,1} & u_{36,2} & \cdots & u_{36,36} \end{pmatrix}}_{[\,U\,]} \cdot \underbrace{\begin{pmatrix} s_1 & & & \\ & s_2 & & \\ & & \ddots & \\ & & & s_{48} \end{pmatrix}}_{[\,S\,]} \cdot \underbrace{\begin{pmatrix} v_{1,1} & v_{1,2} & \cdots & v_{1,48} \\ u_{2,1} & u_{2,2} & \cdots & v_{2,48} \\ \vdots & \vdots & \ddots & \vdots \\ v_{48,1} & v_{48,2} & \cdots & v_{48,48} \end{pmatrix}^T}_{[\,V\,]^T}$$

The test system observability is illustrated by inspection of the relevant factored matrices ($[S]$ and $[V]$). Calling the MATLAB command $[U, S, V] = svd(H)$ returns three factored matrices U,S,V representing the [H] matrix. Tables 4.2 and 4.3show the value of the entries of the interest.

Table 4.2 shows the diagonal entries (s_j) of $[S]$ which are not zero (s_j's $j = 37, 38, ..., 48$ are zero). The off-diagonal entries of the matrix $[S]$ are zero. The corresponding columns of $[V]$ whose s_j's ($j = 37, 38, ..., 48$) are equal to zero are shown in table 4.3. Basically, the i^{th} (i represents node number) state variable is observable if and only if all the entries of $[v_{i,37} \ \cdots \ \mathrm{v}_{i,48}]$ are zero.

The first column in table 4.3 shows the unmonitored busbars 2, 4, 5 and 16 (nodes 4, 5, 6, 10, 11, 12, 13, 14, 15, 40, 41, 42) as well as the corresponding entries of $[V]$. Inspection of the position of the zeros defines the observability. For example, busbar 5 (node 13, 14 and 15) is observable due to the fact that all corresponding entries for rows 13, 14 and 15 are zero, hence adding any combination of the null-space vectors to a particular solution does not change the solution for this busbar. In contrast, busbar 4 is unobservable as adding the null-space vectors to the particular solution results in another solution for this busbar.

Table 4.2: Non-zero diagonal entries (s_j) of $[S]$.

j	s_j	j	s_j	j	s_j	j	s_j
1	1.018813	*10*	1.000059	*19*	0.131758	*28*	0.023100
2	1.018813	*11*	1.000014	*20*	0.093643	*29*	0.010891
3	1.004718	*12*	1.000003	*21*	0.093643	*30*	0.010891
4	1.004718	*13*	1.000000	*22*	0.029337	*31*	0.010299
5	1.000816	*14*	1.000000	*23*	0.027848	*32*	0.010299
6	1.000358	*15*	1.000000	*24*	0.026323	*33*	0.005315
7	1.000322	*16*	0.139138	*25*	0.025396	*34*	0.004737
8	1.000322	*17*	0.139138	*26*	0.025396	*35*	0.002729
9	1.000059	*18*	0.131758	*27*	0.023100	*36*	0.002155

Based on the conducted observability analysis on the 11kV test system, the observable nodes (and the corresponding busbars) are shown in figure 4.5.

Table 4.3: Columns of $[V]$ whose corresponding s_j values are equal to zero.

Node Number	37	38	39	40	41	42	43	44	45	46	47	48
4	0.00	0.00	0.00	0.00	0.00	0.00	0.00	0.00	0.00	0.00	0.00	0.00
5	0.00	0.00	0.00	0.00	0.00	0.00	0.00	0.00	0.00	0.00	0.00	0.00
6	0.00	0.00	0.00	0.00	0.00	0.00	0.00	0.00	0.00	0.00	0.00	0.00
10	0.28	-0.28	0.05	-0.65	0.45	0.43	0.00	0.00	0.00	-0.01	-0.05	-0.02
11	0.58	0.54	0.58	0.03	-0.01	-0.01	0.00	0.00	0.00	0.03	0.08	0.00
12	0.17	-0.43	0.08	0.18	-0.00	-0.02	0.00	0.00	0.00	0.31	0.80	-0.01
13	0.00	0.00	0.00	0.00	0.00	0.00	0.00	0.00	0.00	0.00	0.00	0.00
14	0.00	0.00	0.00	0.00	0.00	0.00	0.00	0.00	0.00	0.00	0.00	0.00
15	0.00	0.00	0.00	0.00	0.00	0.00	0.00	0.00	0.00	0.00	0.00	0.00
40	0.00	0.00	0.00	0.00	0.00	0.00	0.00	0.00	0.00	0.00	0.00	0.00
41	0.00	0.00	0.00	0.00	0.00	0.00	0.00	0.00	0.00	0.00	0.00	0.00
42	0.00	0.00	0.00	0.00	0.00	0.00	0.00	0.00	0.00	0.00	0.00	0.00

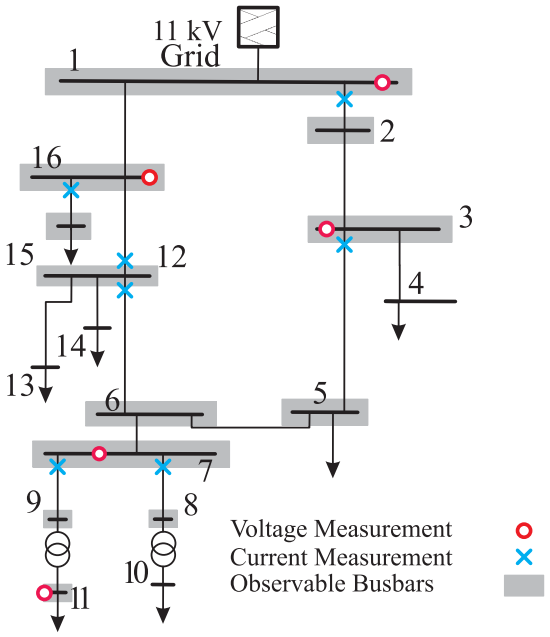

Figure 4.5: Observable busbars.

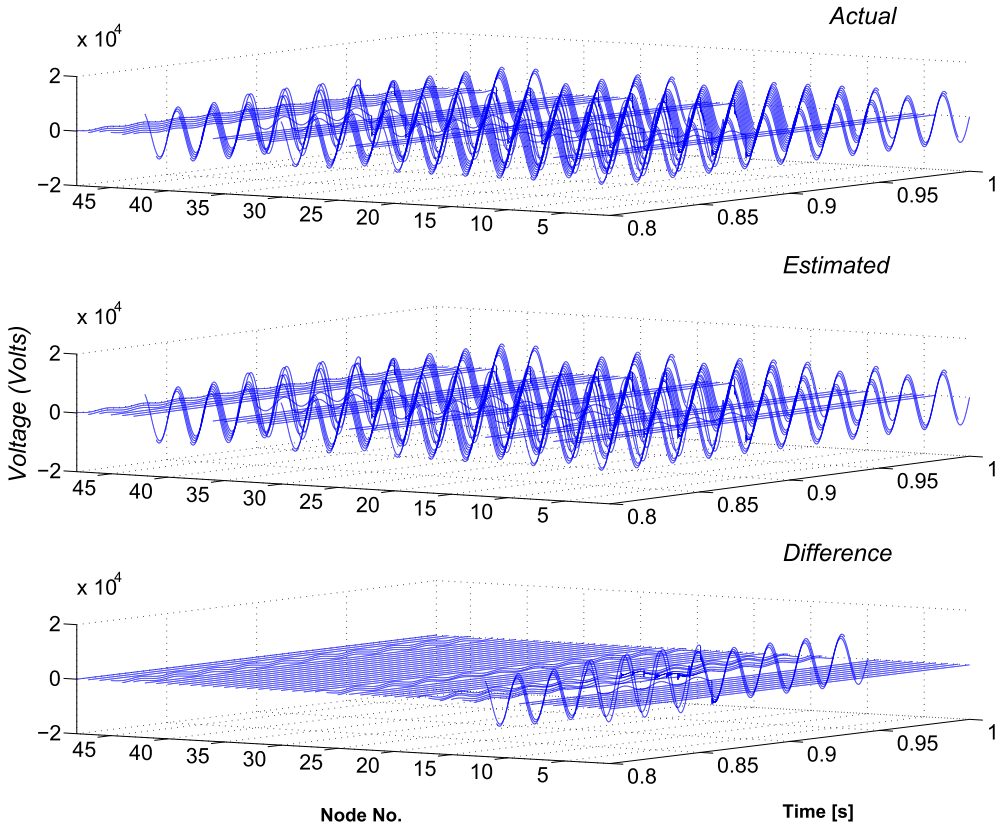

Figure 4.6: 3D illustration of the TSE results

Figure 4.6 illustrates a comparison between measured and estimated voltages at unmonitored nodes as a 3-D plot, to give an overview of the accuracy of the estimation of the whole system. It includes all nodes, both observable and unobservable. The unobservable nodes (10, 11 and 12 which are part of busbar 4 as a three-phase representation) are clearly evident by the error between the estimated and actual results and the observability analysis indicates these nodes are not observable.

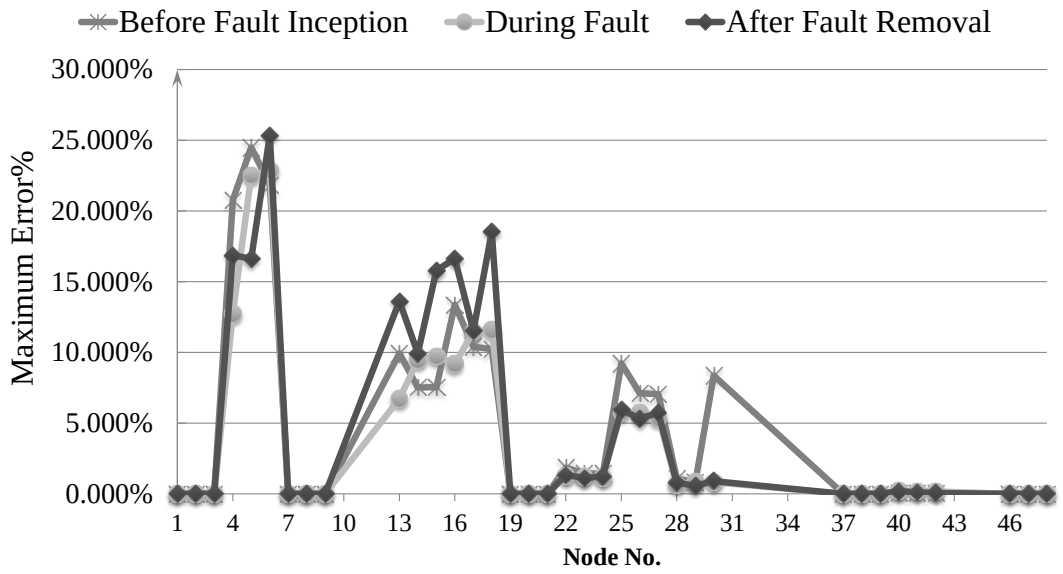

Figure 4.7: Maximum percentage error in the voltage for the observable nodes (for the case shown in figure 4.6)

Figure 4.7 depicts the estimation error for the observable nodes before the fault inception, during the fault and after the fault removal. The error values are expressed as a percentage and are calculated according to equation 4.1:

$$Error\% = 100 \times | \frac{v_{actual}(t) - v_{estimated}(t)}{Maximum(v_{estimated})} | \tag{4.1}$$

where $v_{estimated}(t)$ and $v_{actual}(t)$, which are time functions, are the estimated voltage values obtained from the TSE algorithm and the actual values as generated by the simulation software respectively. $Maximum(v_{estimated})$ is the maximum estimated voltage for the healthy phases. $Maximum(v_{estimated})$ is used to normalize rather than $v_{estimated}$ to avoid dividing by zero at zero-crossings.

4.4 SIMULATION RESULTS

According to the verfication method (section 4.2), an event (subsection 4.2.1) is simulated and the measurements placed at the specified locations (subsection 4.2.2) are taken to be used for inspection and identifying the source of voltage sag which was recorded at busbar 11 (figure 4.3).

Figures 4.8 - 4.11 show the three-phase actual and estimated voltages at the unmonitored busbars. These observable busbars are assumed to be susceptible for initiating the voltage dip/sag at busbar 11. Therefore, investigation of their characteristic behaviour should reveal useful information. For each busbar the actual and estimated results are plotted as solid and dotted lines, respectively. However, they are indistinguishable due to the similarity.

The oscillations around the estimated voltage phases B and C in figure 4.8 are due to the well-known numerical error in the Trapezoidal rule. Chatter removal is disabled in the PSCAD/EMTDC. Therefor, this isolation is to be expected as a chatter removal algorithm has not yet been implemented in TSE. The numerical error as a result of employing the Trapezoidal rule is discussed later in section 4.4.6.

Now that the state variables (nodal voltages) are known, other dependent variables (such as branch currents) in the system can be calculated. The accuracy of the state variables will indicate the accuracy of all other derived quantities. Figures 4.12 and 4.13 show the three-phase actual and estimated branch currents.

Inspection of the plotted voltages verifies that a single-phase short circuit on Phase A at busbar No. 5 occurred. The short circuited phase displayed in the estimated voltage waveform can be identified as the source of voltage sag at busbar No. 11.

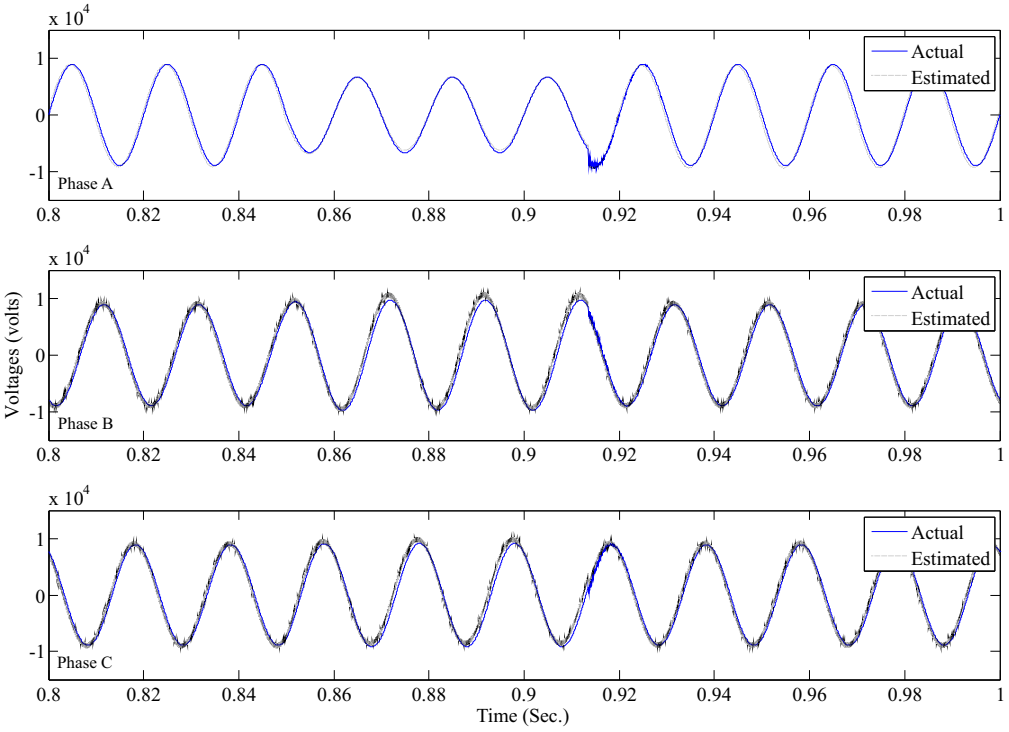

Figure 4.8: Three-phase actual and estimated voltage at busbar No.2

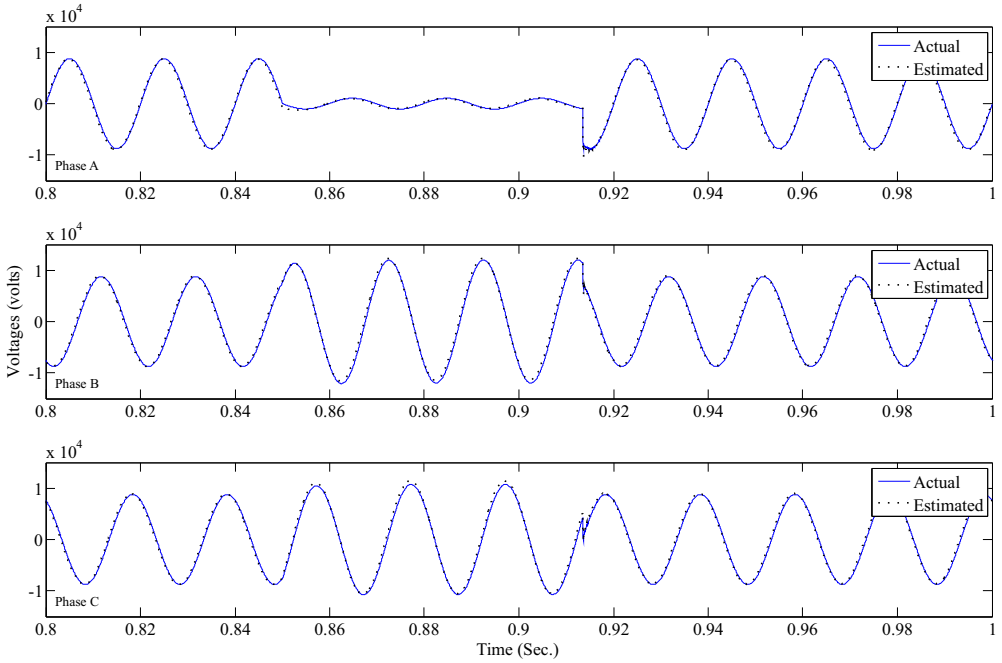

Figure 4.9: Three-phase actual and estimated voltage at busbar No.6

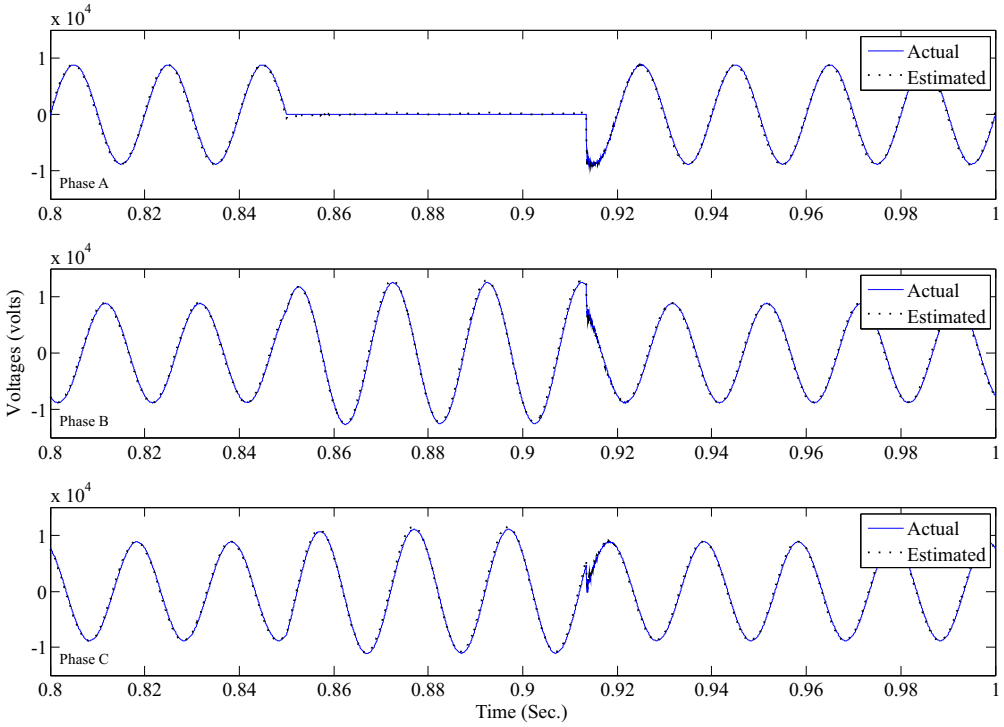

Figure 4.10: Three-phase actual and estimated voltage (Volts) at busbar No.5

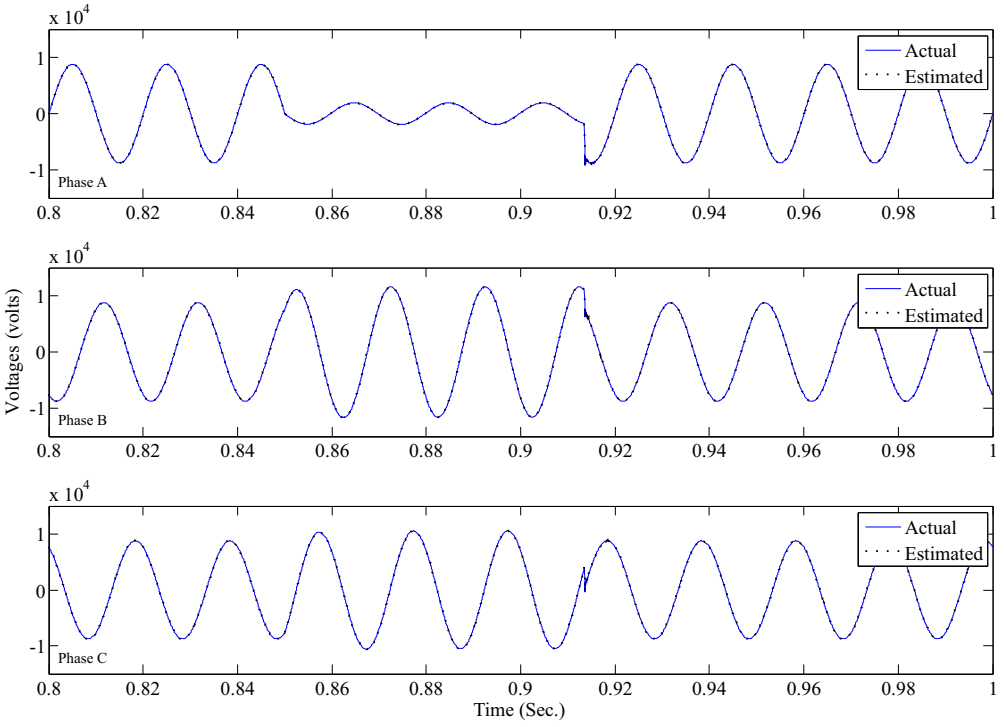

Figure 4.11: Three-phase actual and estimated voltage (Volts) at busbar No.15

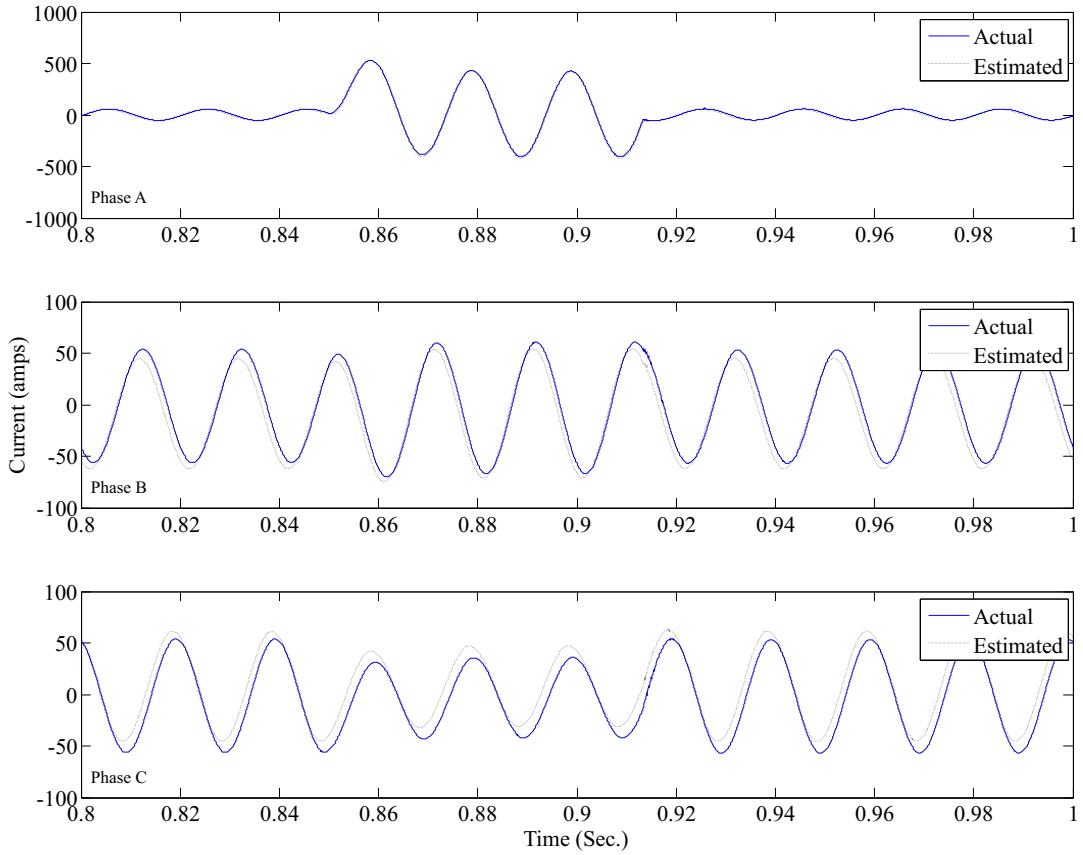

Figure 4.12: Three-phase actual and estimated line currents from bus 6 to bus 5

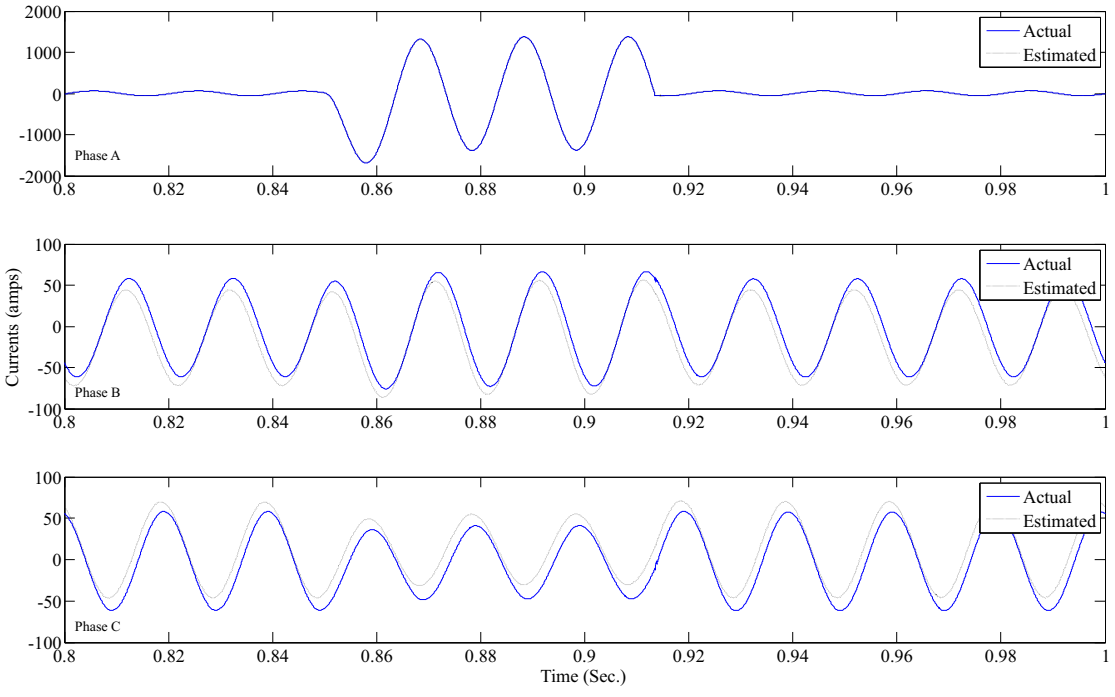

Figure 4.13: Three-phase actual and estimated line currents from bus 2 to bus 3

4.4.1 TSE with measurement noise

In practice, all measured signals are corrupted by a random variation called measurement noise. Measurement noise is classified as a source of bad data in state estimation and adversely affects the accuracy of the estimated quantity. In order to demonstrate the robustness of the proposed TSE method, measurement noise was added to the measurement points.

The normal distribution is so commonly encountered in order to describe the measurement noise as follows:

$$Measurement\ noise = \bar{x} \pm \sigma_{\bar{x}} \tag{4.2}$$

where:

$\bar{x}$ is the mean

$\sigma_{\bar{x}}$ is the standard deviation from the mean

For this purpose, the MATLAB random number generator that generates a normal distribution (randn) is called. The mean value is set to zero and the standard deviation is set to 5%.

It should be noted that measurement noise is applied to each measurement point individually for each time step. In other words, each measured value at time t_n is separately multiplied by a random number selected between $[-0.05\ , +0.05]$, added to 1 and will be replaced in the relevant entries of the matrix $[z]$. Equation 4.3 below shows how the relevant entry from the $[z]$ matrix is replaced with the corresponding nodal voltage measurement associated with measurement noise. Figure 4.14 shows the distribution of measurement noise generated for a measurement point in MATLAB.

$$z_{t_n} = (Node\ voltage\ at\ _{t=t_n}) \times \underbrace{\{1 + 0.05 \times randn()\}}_{Measurement\ Noise} \tag{4.3}$$

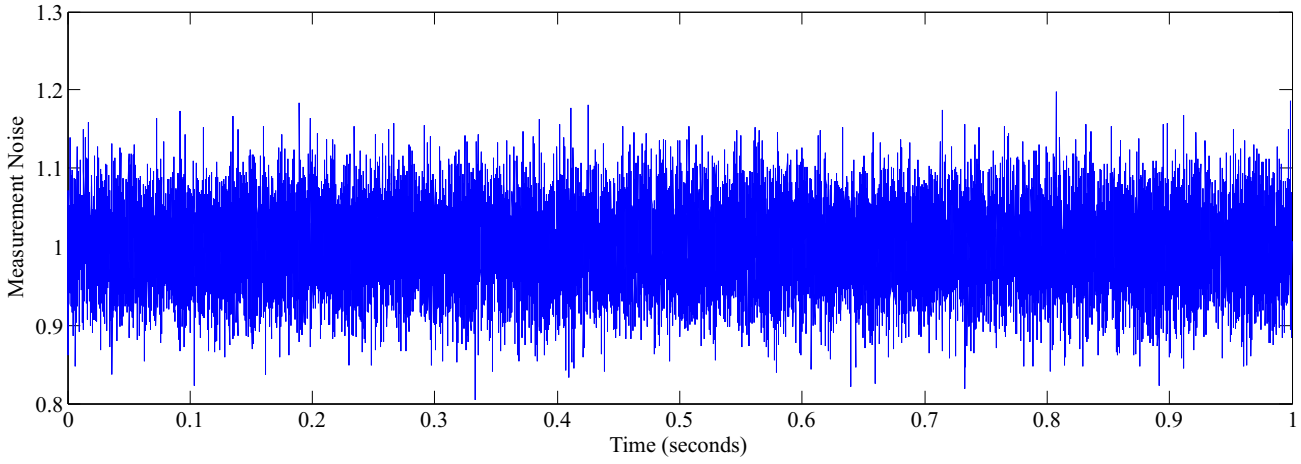

Figure 4.14: Measurement noise distribution.

Figures 4.15 and 4.16 show the actual and estimated voltages as well as estimation error at busbar No. 5 when 5% normally distributed measurement noise is applied to all the measurements separately.

Figure 4.17 illustrates the maximum percentage voltage error at the identified faulted busbar before the fault inception, during the fault and after fault removal. It clearly proves that the developed TSE is able to make good estimates, even in the presence of measurement noise.

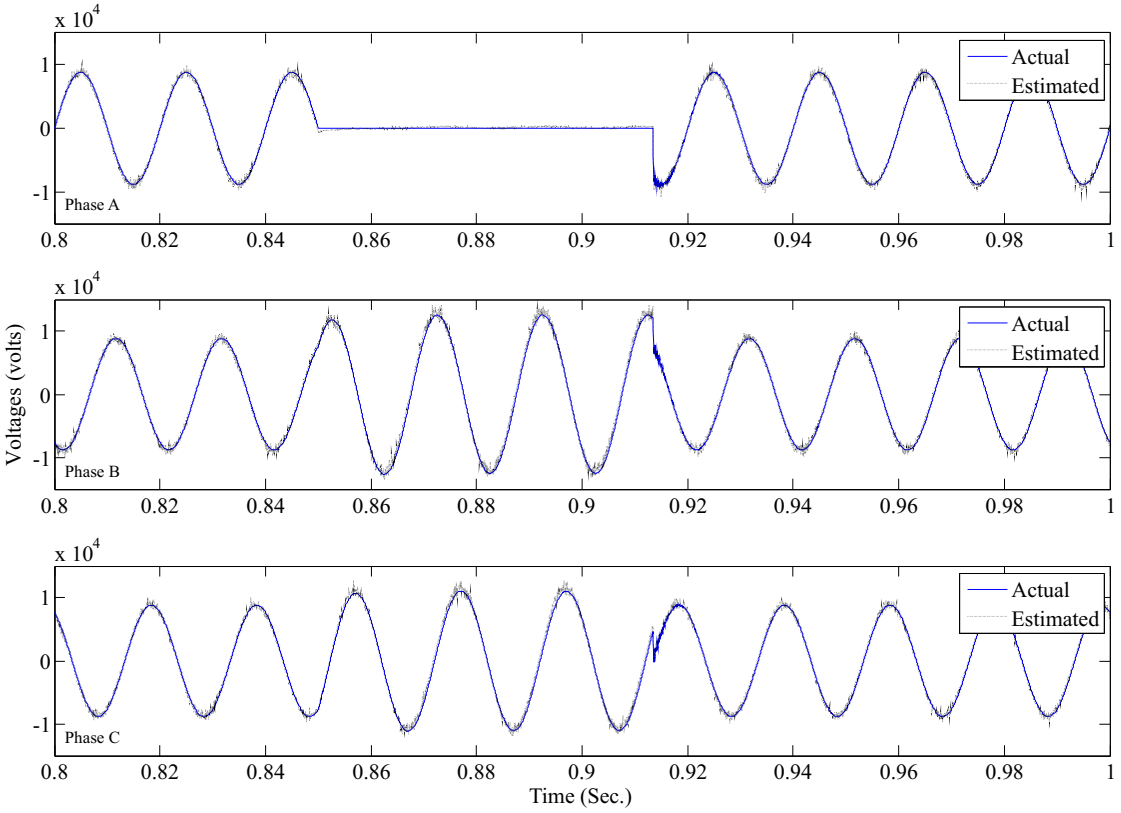

Figure 4.15: Three-phase actual and estimated voltage (Volts) at busbar No.5 in presence of 5% measurement noise.

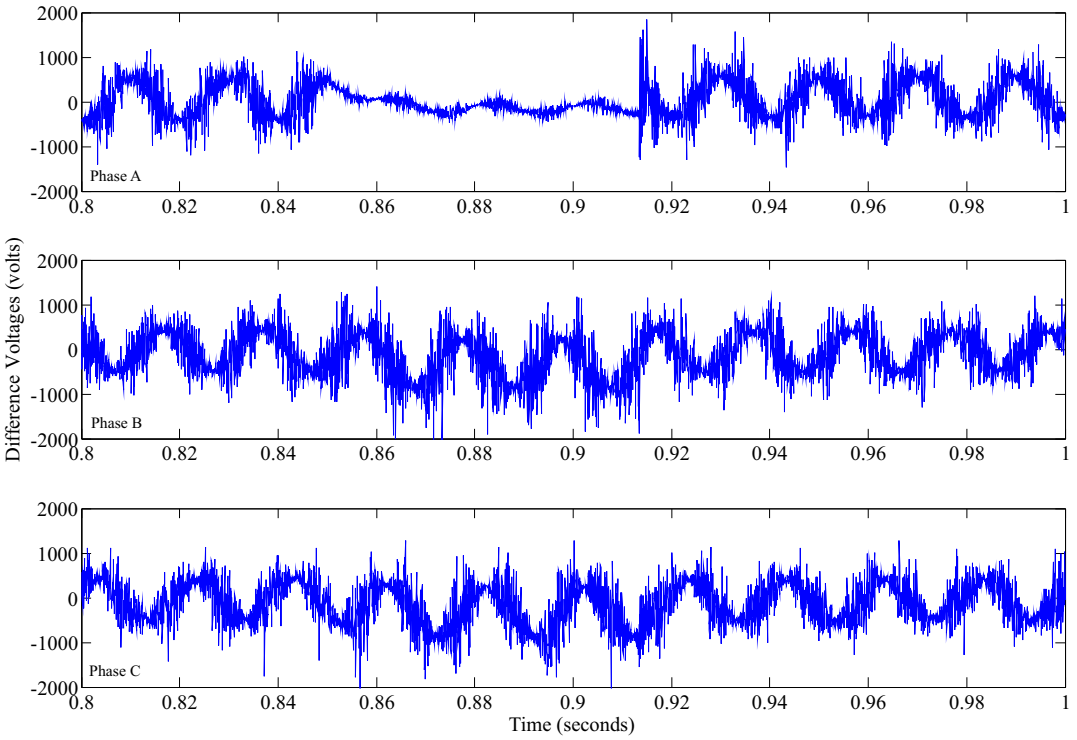

Figure 4.16: Difference between measured and estimated voltages (Volts) at busbar No.5 in presence of 5% measurement noise.

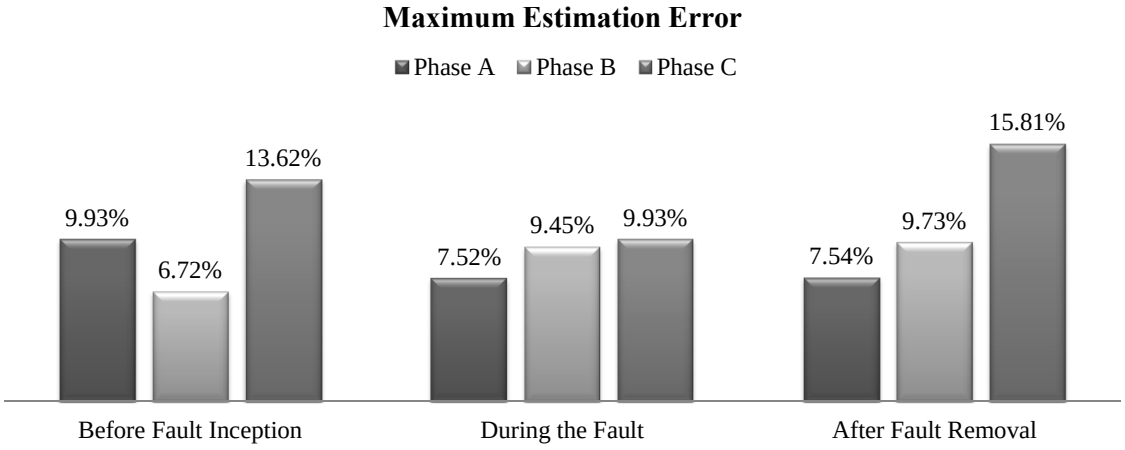

Figure 4.17: Maximum voltage percentage error at busbar No. 5.

4.4.2 Presence of background harmonics

One feature of rural networks is the background harmonic distortion level due to the widespread use of VSD driven irrigation pumps. To make the example more realistic and verify the algorithm in the presence of harmonics, this distortion has been simulated by adding voltage harmonics to the voltage source based on the field measurements made at a rural substation at 11 kV. The values are shown in table 4.4.

Table 4.4: Background Harmonic Voltages

Odd Harmonics		Even Harmonics	
h	V_h	h	V_h
3	0.1%	*2*	0.07%
5	5.2%	*4*	0.06%
7	2%	*6*	0.02%
9	0.06%	*8*	0.014%
11	0.18%	*10*	0.015%
13	0.18%		
15	0.02%		
17	0.9%		
19	0.14%		
21	0.03%		
23	0.09%		
25	0.09%		

For this purpose, a MATLAB based EMT simulation program was developed. This allowed the easy introduction of background harmonics to the system. First the MATLAB based EMT program was benchmarked against PSCAD/EMTDC to ensure it gave the correct answers. Figure 4.18 shows a representative plot for three busbars showing the match achieved as they are indistinguishable.

The verification method previously discussed in section 4.2 was applied once again, this time in the presence of the harmonic distortions using MATLAB based EMT results taken as measurements. The observable busbars which are not monitored assumed to be susceptible for the cause of voltage sag occurred at bus 11. The results are shown in figures 4.19, 4.20 and 4.21. They display a comparison between the TSE estimate of the busbar voltage against the actual waveform generated by the MATLAB simulation, for susceptible and unmonitored busbars 2, 5, and 15 respectively.

The actual and estimated results are plotted as solid and dotted lines, respectively. They are almost indistinguishable due to their similarity.

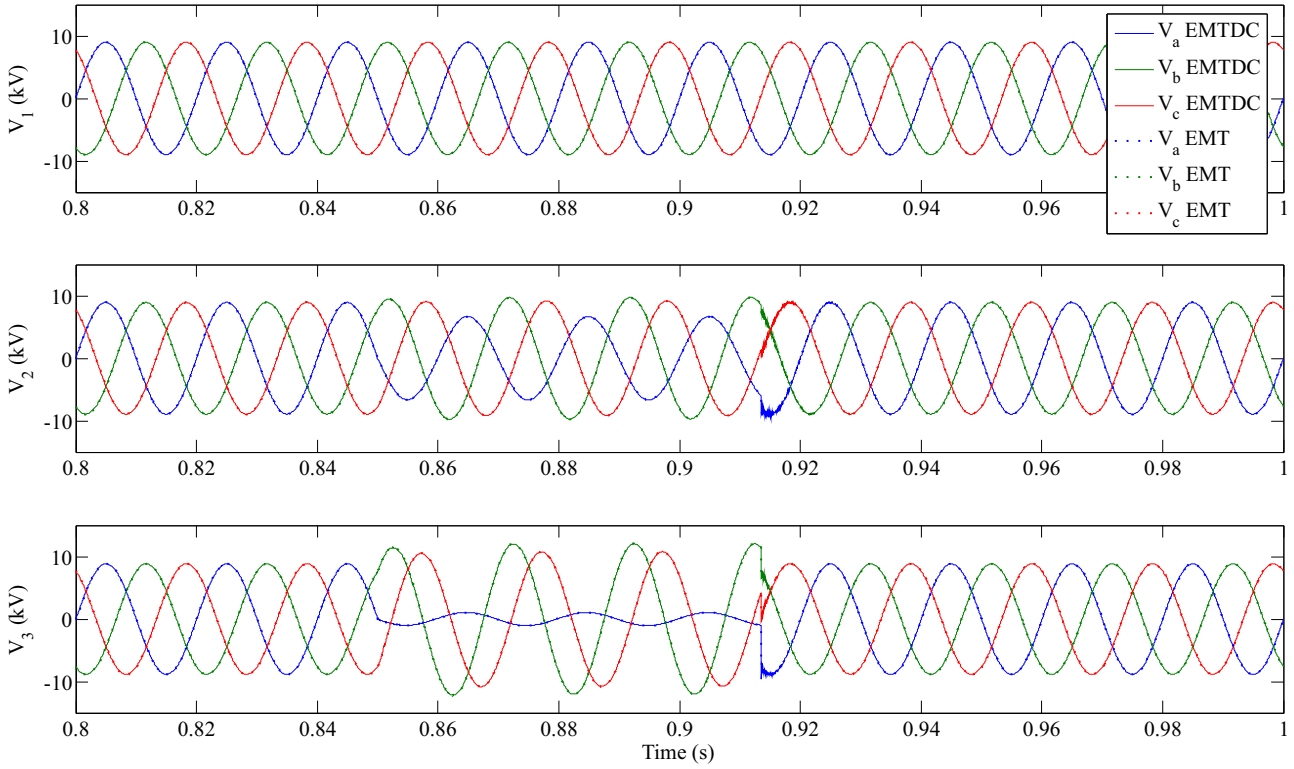

Figure 4.18: Comparison of PSCAD/EMTDC & EMT (MATLAB)

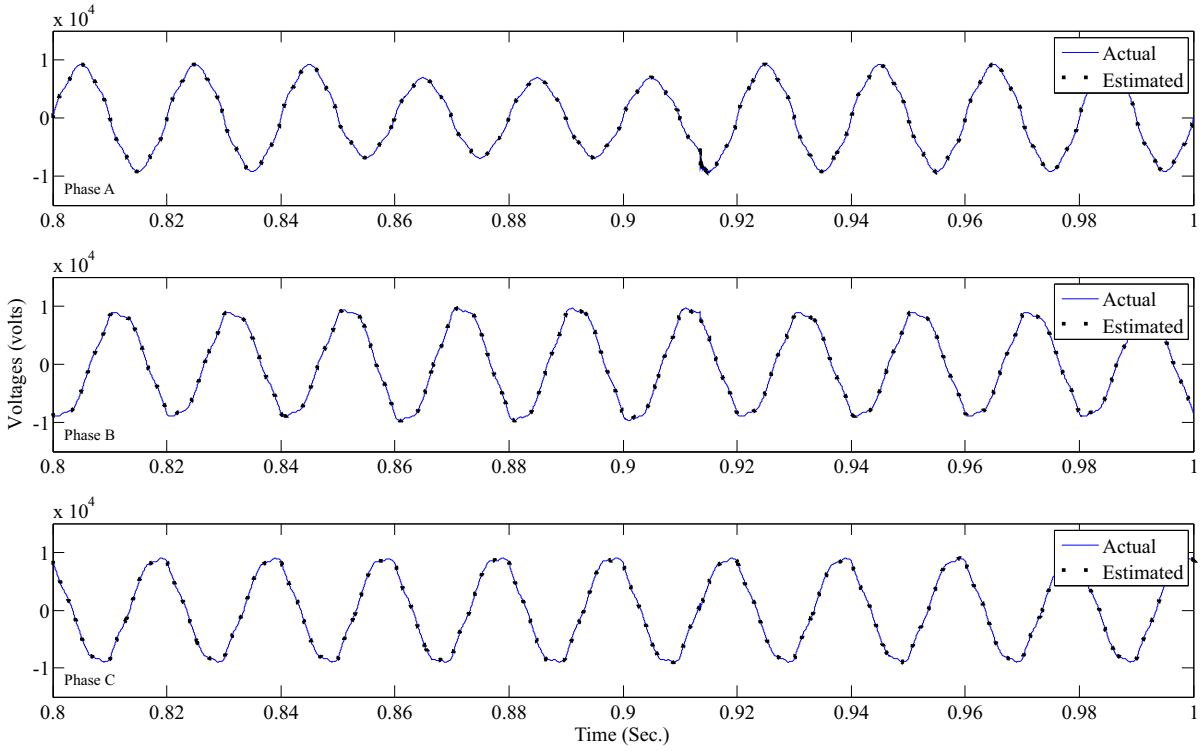

Figure 4.19: Three-phase actual and estimated voltage at busbar No.2

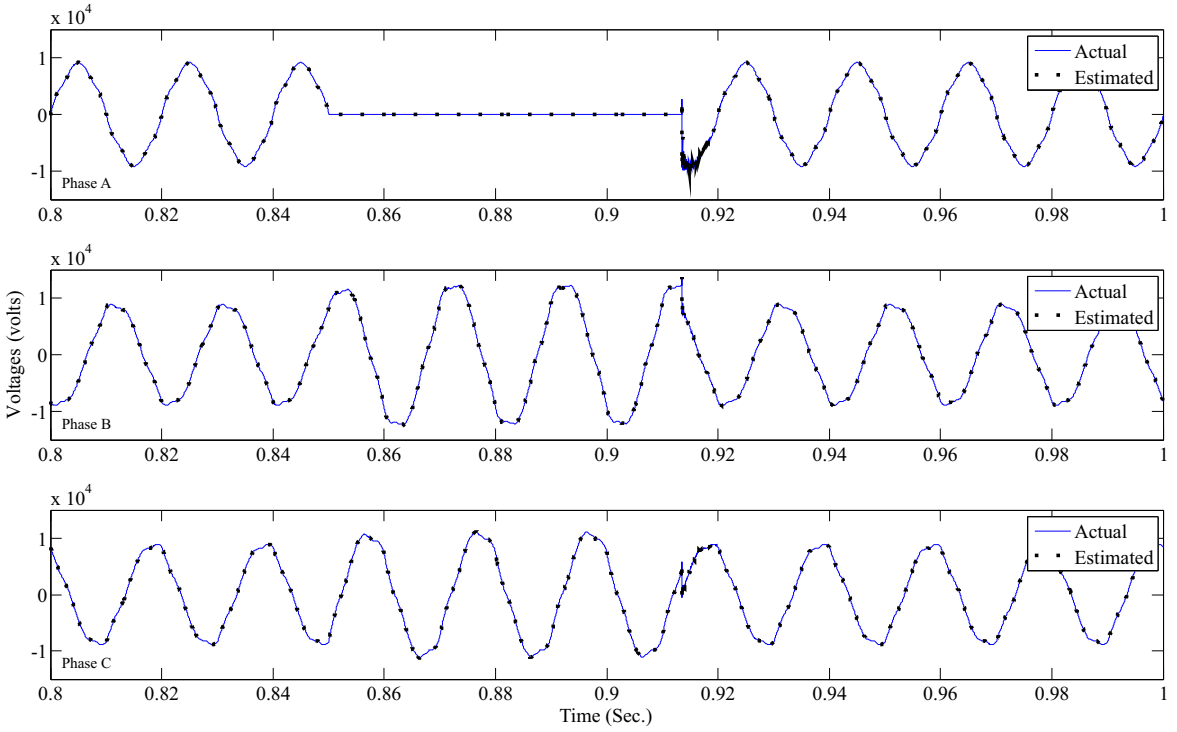

Figure 4.20: Three-phase actual and estimated voltage at busbar No.5

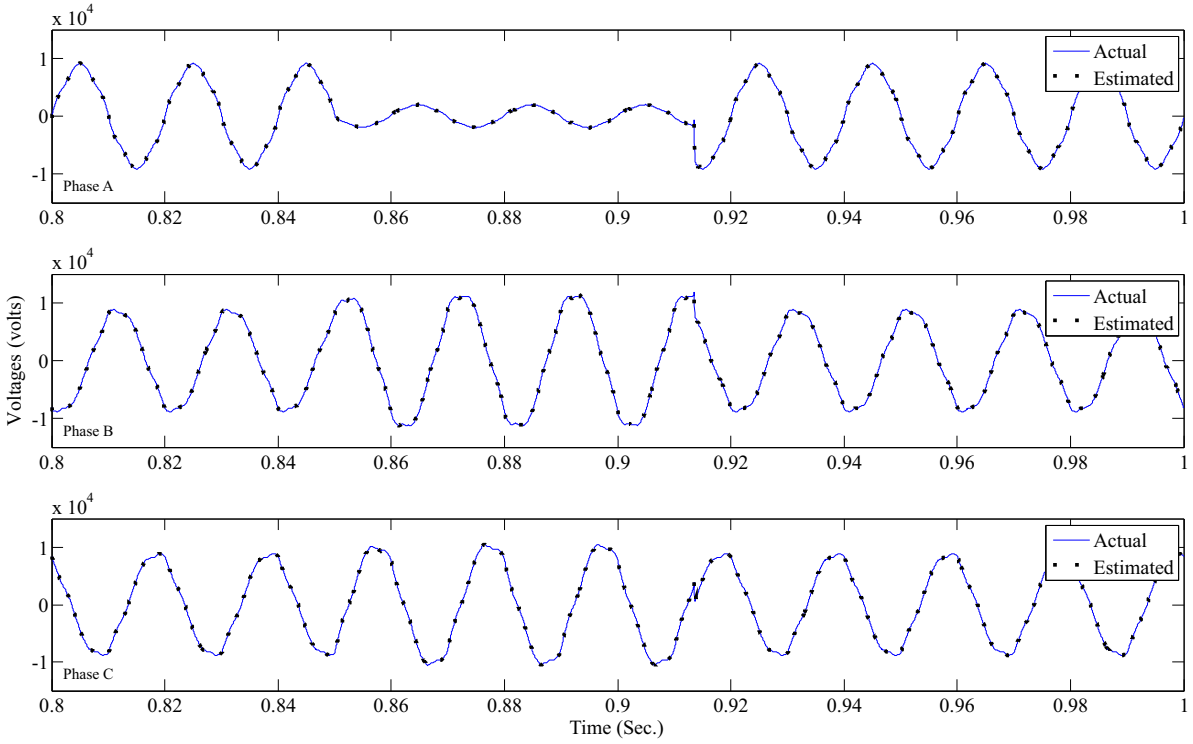

Figure 4.21: Three-phase actual and estimated voltage at busbar No.15

4.4.3 TSE with background harmonics and measurement noise:

In this section, the performance of the proposed TSE is verified against background harmonics and measurement noise at the same time. Figures 4.22 and 4.23 below show the estimated and actual voltage waveforms as well as the difference at busbar 5 in the presence of the harmonics background and 5% normally distributed measurement noise.

The graphs show good estimation results and the capability of the proposed TSE to identify the single-phase short circuit on Phase A at busbar number 5 as the cause of the disturbance even in the presence of harmonics distortion and measurement noise.

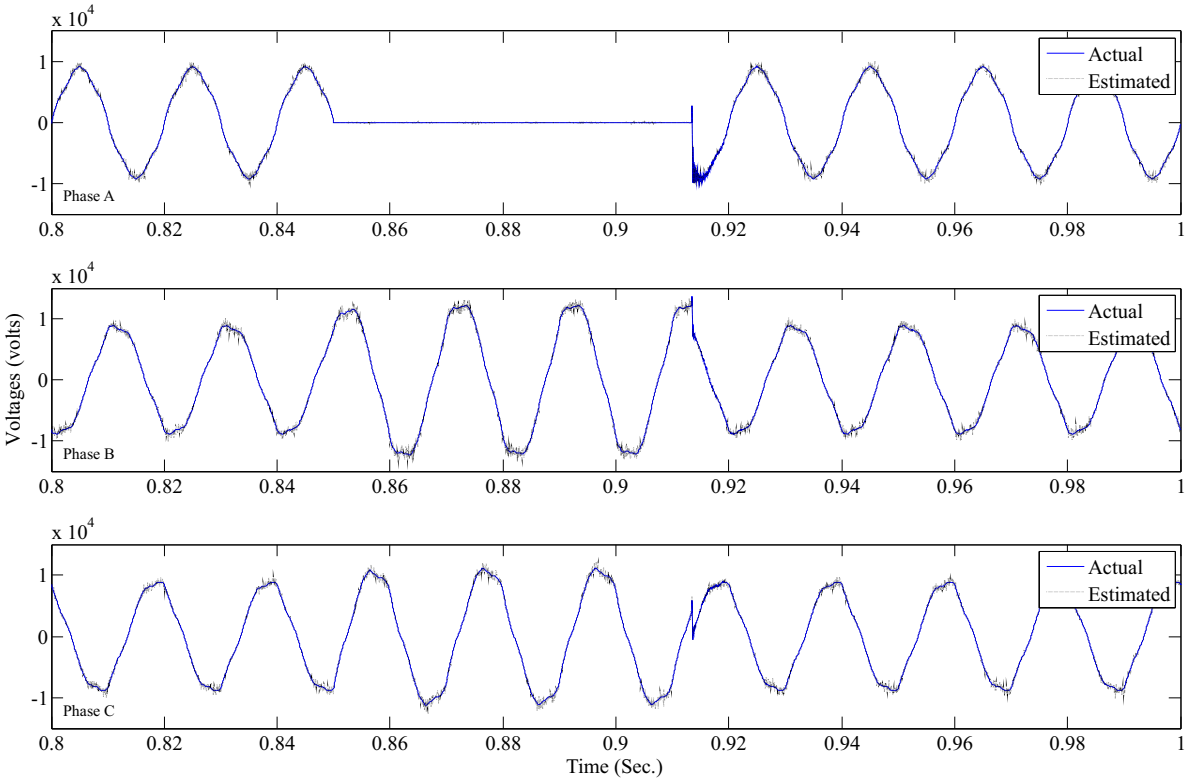

Figure 4.22: Three-phase actual and estimated voltage at busbar 5 in presence of ±5% measurement noise.

4.4.4 Multiple faults

TSE can be used to determine the location or source of transients in a power system. This can be performed by inspection of nodal mismatch voltage within the observable part of the network. Figure 4.24 shows this procedure. Since an unexpected fault event is not in the network model, the difference between the estimated state variables and calculated state variables will lead to a voltage mismatch which can be used to identify the fault/disturbance type and location.

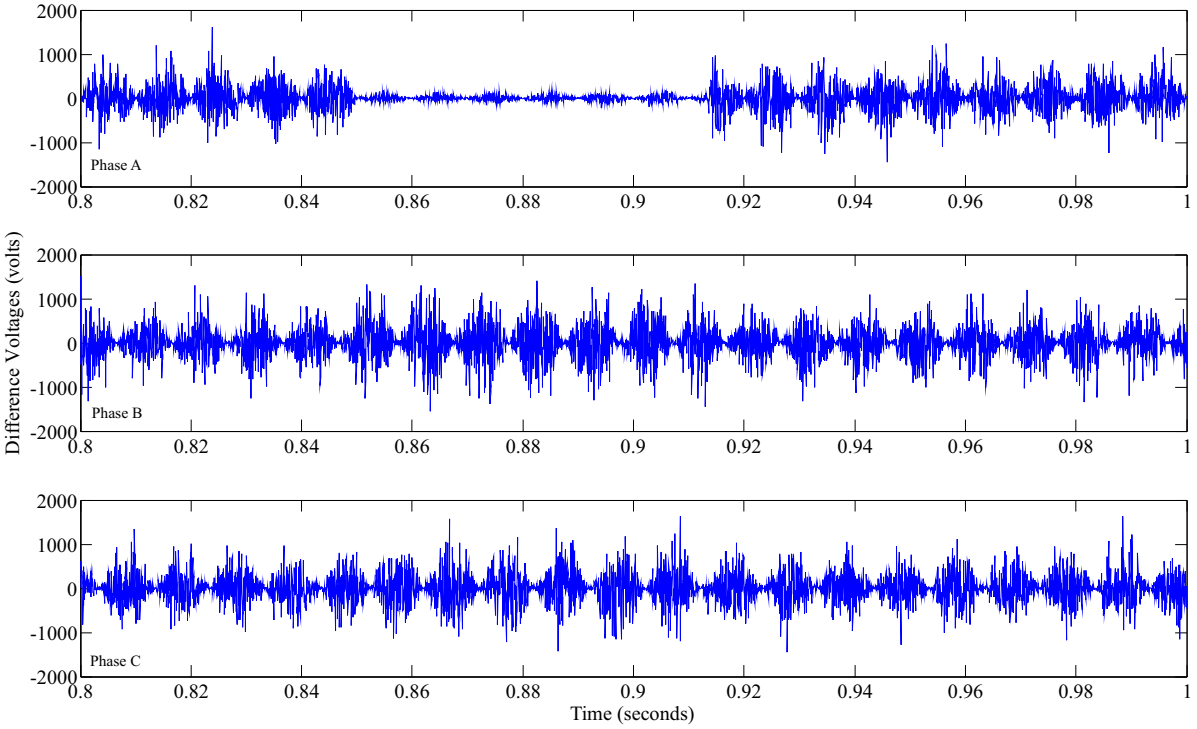

Figure 4.23: Difference between measured and estimated voltages at busbar 5 in presence of ±5% measurement noise.

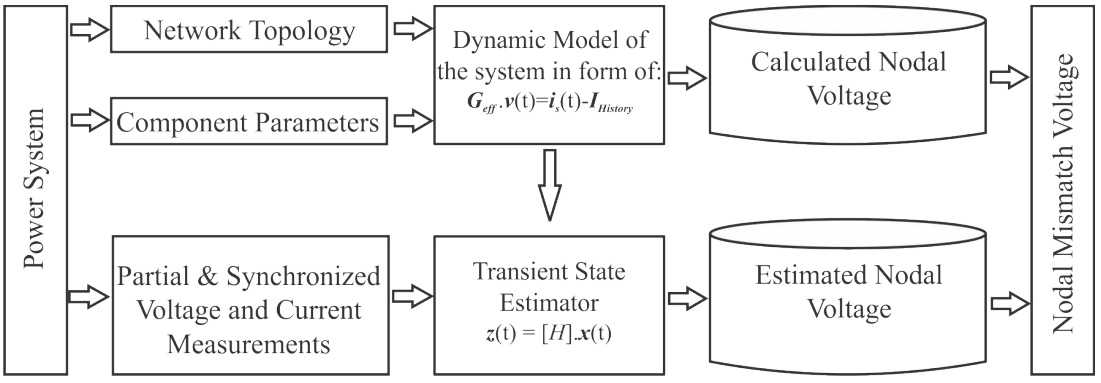

Figure 4.24: Nodal mismatch voltage calculation

Given the fact that TSE provides time domain estimation, it can be used to assess voltage dip/sag as well as identifying different causes of voltage sag via inspection of the estimated voltage waveform by signal processing techniques [Bollen *et al.* 2007]. However, here it is assumed that the cause of voltage sag is fault current. The verification method previously discussed in section 4.2 was applied once again this time in case there is multiple faults in the test system. This could simulate the case which is likely to happen in storm related events.

For this purpose, two single-phase short circuits at busbars No. 5 and No.15 are simulated. This could simulate the case which is likely to happen in storm related events. There are no

measurements on or near these busbars. A three-phase voltage measuring at busbar 11 displays an approximately 70% retained voltage on Phases A and B.

As said previously, the TSE simulation can be used to determine the location or source of transients in a power system. Figure 4.25 shows the maximum nodal mismatch voltage values for observable nodes over the time period which the system is under study. It depicts the maximum difference between the simulations of TSE, with and without the disturbance. It can be observed from figure 4.25 that the node with the largest change in voltage are nodes 13 and 41 indicating that these nodes are most likely the source of the transient recorded at busbar 11 (these nodes representing Phase A from busbar 5 and Phase B from busbar 15).

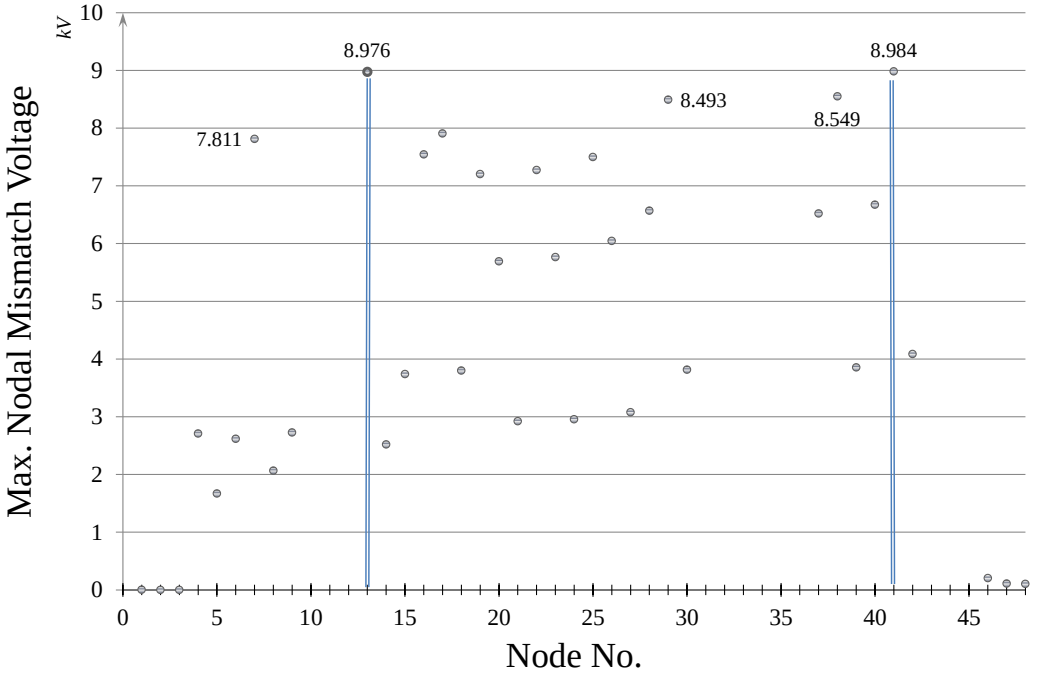

Figure 4.25: Maximum nodal mismatch voltage values for observable nodes.

Figures 4.26 - 4.29 show the three-phase actual and estimated voltages for the suspicious location (busbars No. 5 and 15) as well as the difference between actual and estimated voltages. The actual and estimated results are plotted as solid and dotted lines, respectively. However, they are indistinguishable due to the similarity. Inspecting the waveform also confirms that the voltage sag occurred owing to single-phase short circuits at Phases A and B from busbars 5 and 15, respectively.

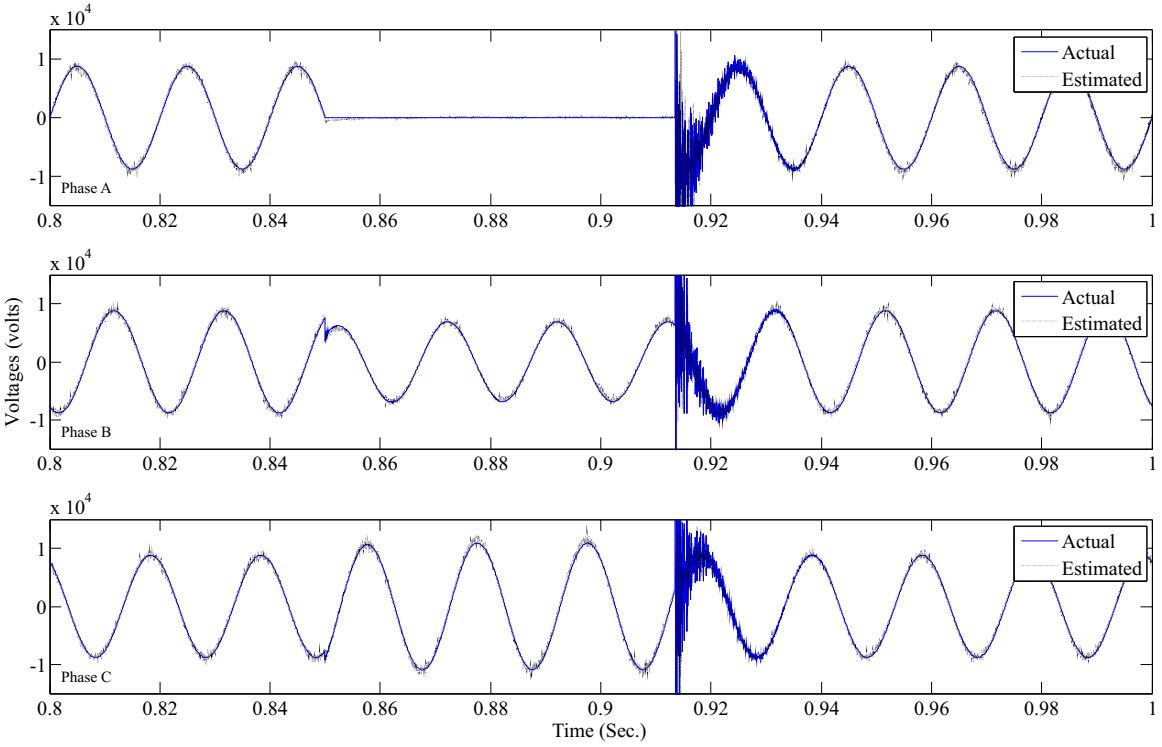

Figure 4.26: Three-phase actual and estimated voltage at busbar No.5 in presence of 5% measurement noise.

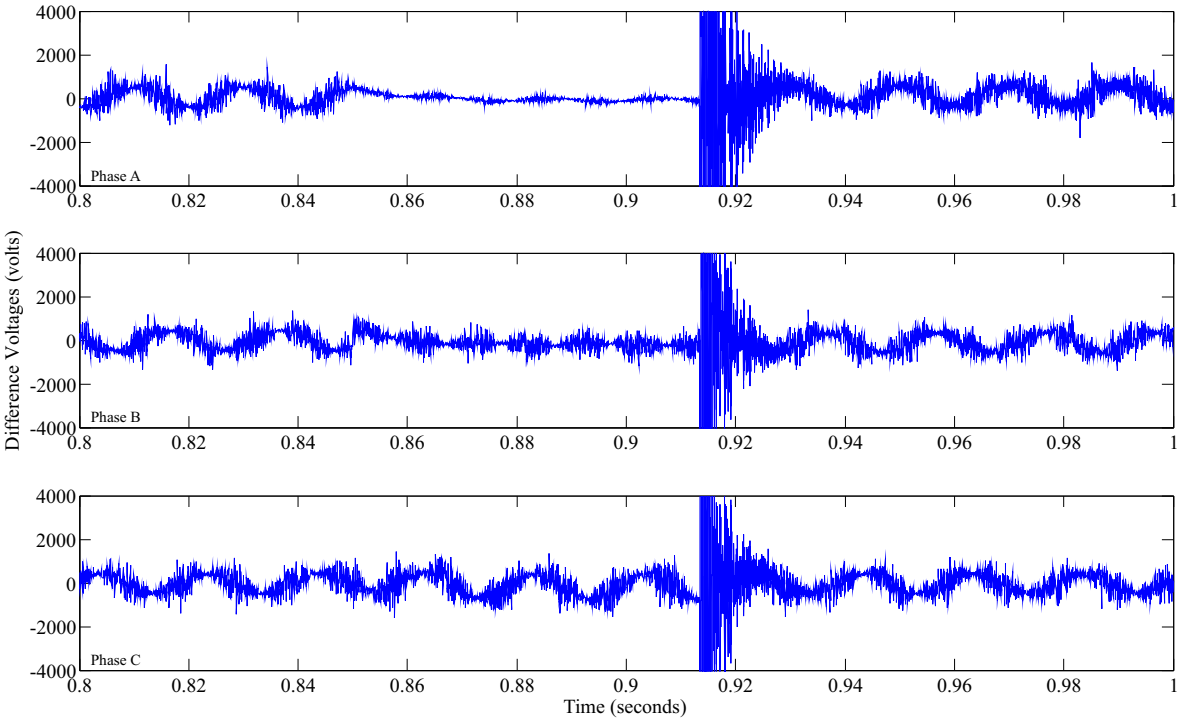

Figure 4.27: Difference between actual and estimated voltages at busbar No. 5 in presence of 5% measurement noise.

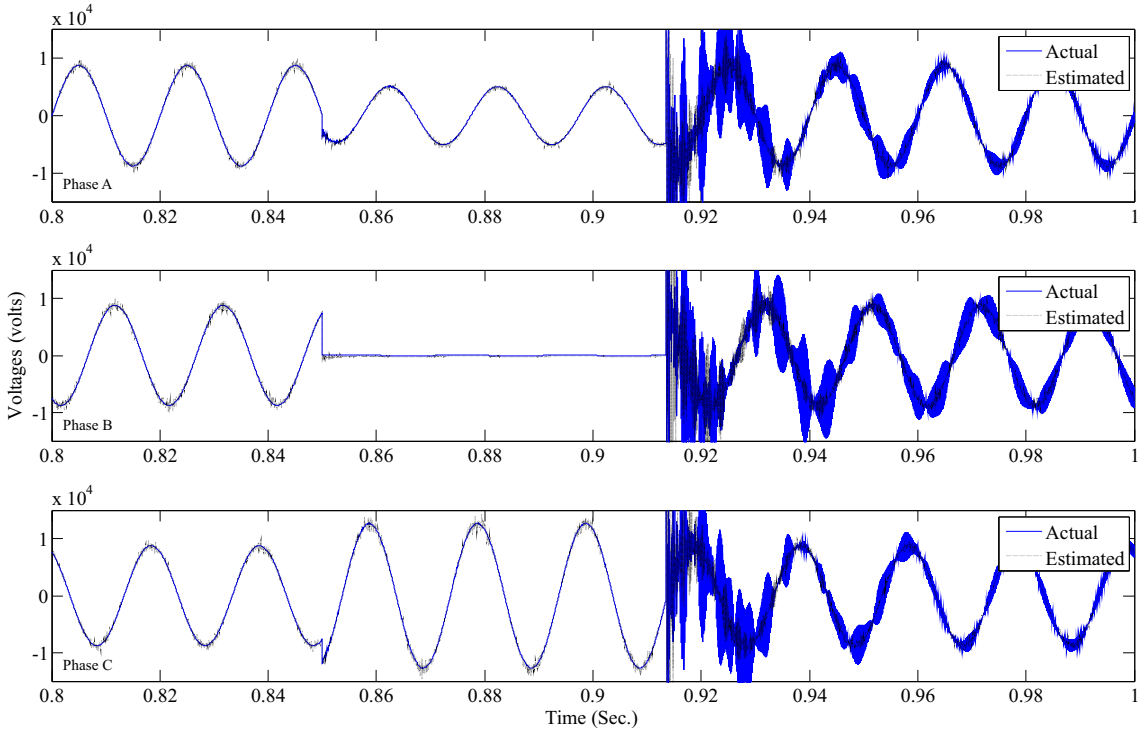

Figure 4.28: Three-phase actual and estimated voltage at busbar No.15 in presence of 5% measurement noise.

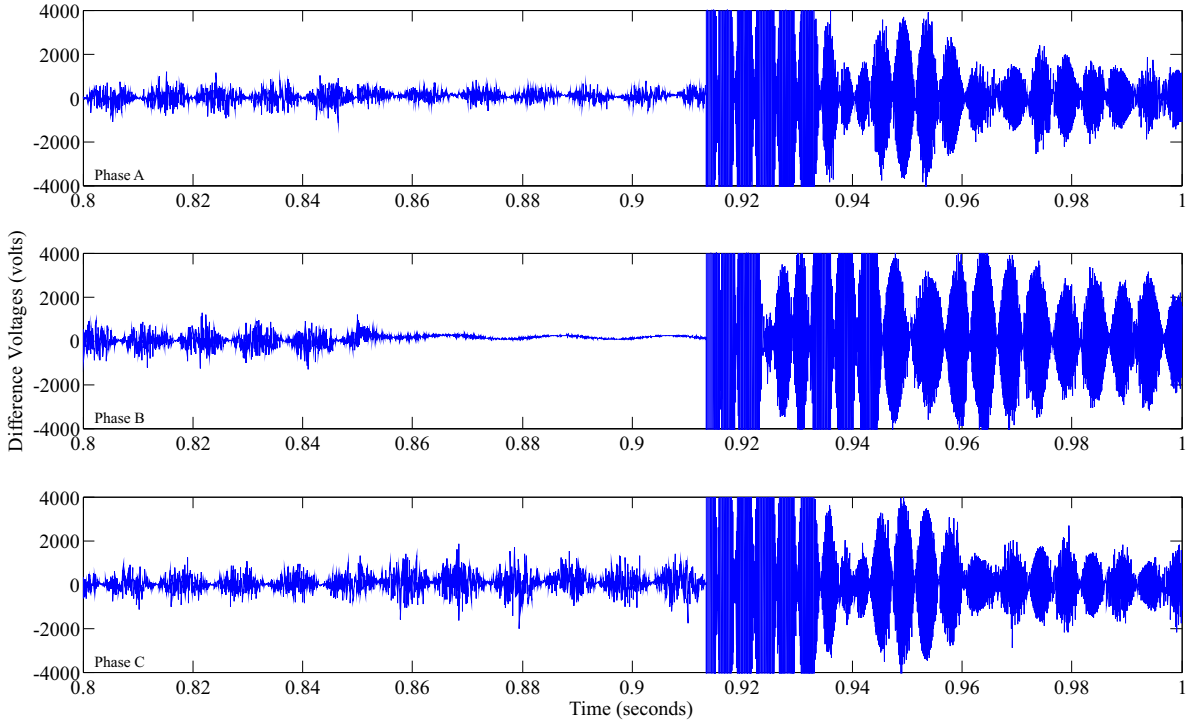

Figure 4.29: Difference between actual and estimated voltages at busbar No.15 in presence of 5% measurement noise.

4.4.5 Different fault types

To show the robustness of the proposed TSE the following verifications have been performed using DIgSILENT's PowerFactory in order to reproduce more realistic conditions under which the TSE works. This time the simulated test system uses a frequency dependent transmission line model with the frequency which the parameters of the lumped PI-models of the state estimator have been calculated. So, the proposed TSE still uses the lumped PI-models while the actual measurements are taken from simulated network with frequency dependant line models (5% measurement noise is added). Different types of short circuits were simulated including:

- Single-phase-to-ground
- Phase-to-phase
- Phase-to-phase-to-ground
- Three-phase-to-ground

The proposed TSE was tested for its performance with different fault types and the results are summarized in Table 4.5. The results for three unmonitored busbars, which were randomly selected are shown. The percentage error was calculated according to 4.1 for the three periods (before fault inception, during the fault and after fault removal).

Figures 4.30 - 4.32 show the three-phase actual and estimated voltages at these observable busbars. The error values of table 4.5 are somewhat deceiving as the maximum error is one point and not indicative of the overall error at the other time points. For example the highest error, 30.97%, was on Phase A at busbar 6 during the fault. Figure 4.32 shows the comparison, which is good with only one high error point and the rest typically have a maximum error of approximately 8%. This system is only partially observable, moreover noise is included in the measurements which exasperate the estimation problem. As can be seen the estimated results oscillate around the actual value during the fault period. This is mainly due to the difference in the transmission line representation (although other errors contribute slightly) and will be resolved if a travelling wave transmission line model was used in the TSE.

As is the case for any transient study judicious selection of component models is needed to ensure fidelity of the results. A simplified representation is adequate for most of the components; however some components will have more of an influence on the waveforms at a given point and hence require more detailed modeling in order to faithfully reproduce the response at this point. This test case has shown the discrepancy expected when a simple transmission line model is used and the actual system is more complex (represented by a full travelling wave model).

The results verify that proposed TSE algorithm is sufficiently accurate for identifying the location of disturbances as well as the voltages and currents at observable busbars and branches,

even with a simple transmission line model. This was true for all the different types of faults tested even though the system is under-determined and measurement noise is included.

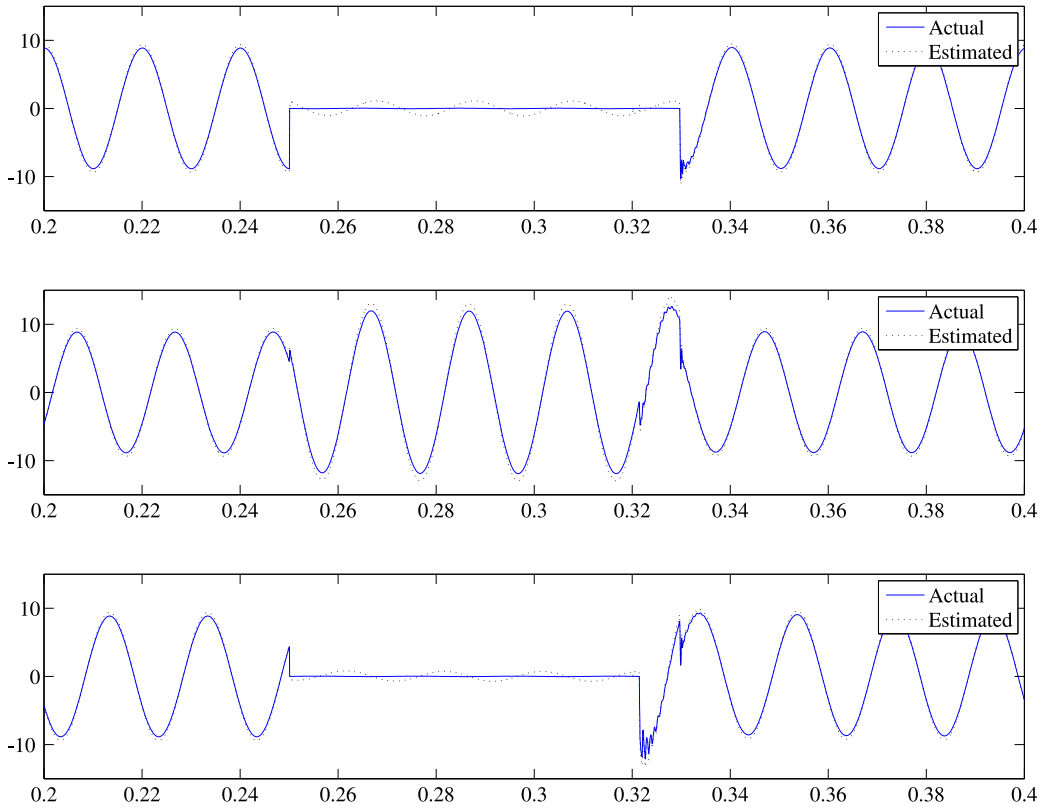

Figure 4.30: Two-phase-to-ground short circuit actual and estimated voltage (kV) at busbar No.5

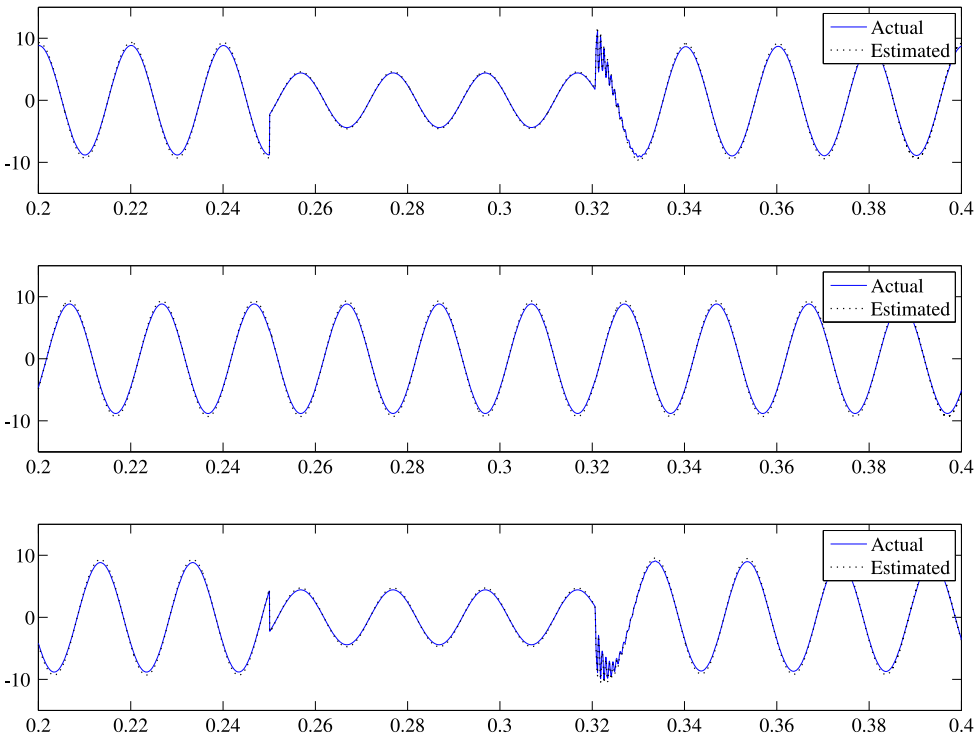

Figure 4.31: Two-phase short circuit actual and estimated voltage (kV) at busbar No.16

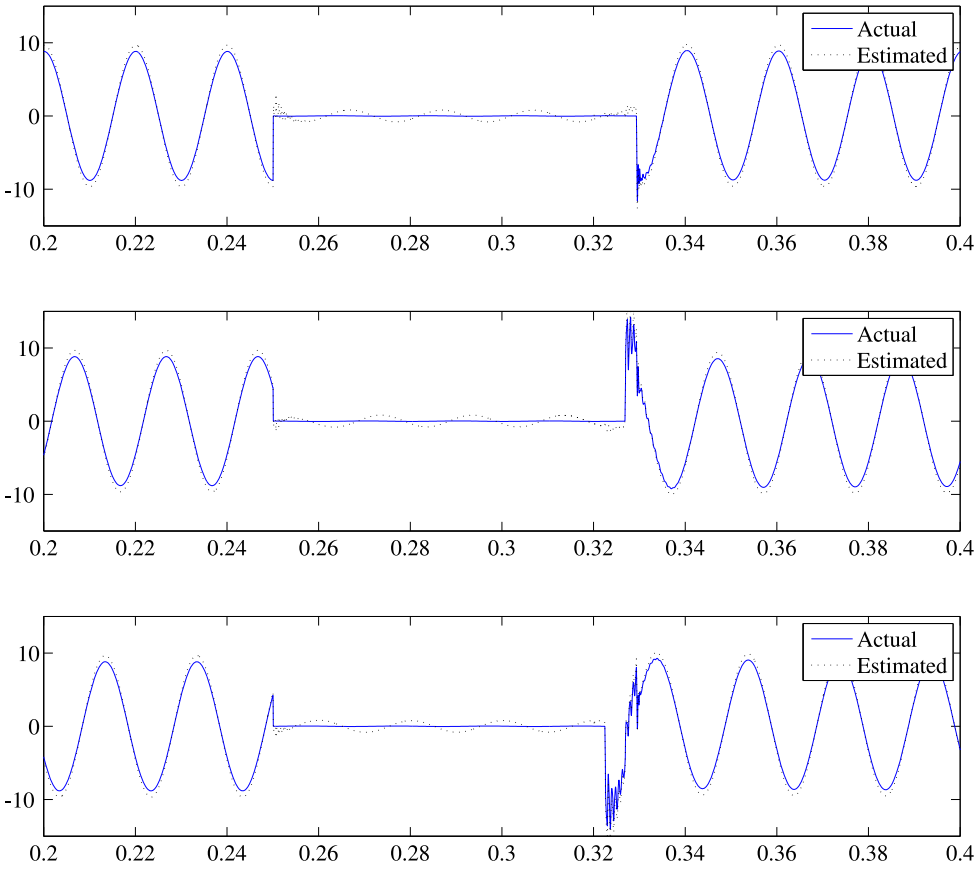

Figure 4.32: Three-phase to ground short circuit actual and estimated voltage (kV) at busbar No.6

Table 4.5: Different type of fault and percentage error

Bus No.	Fault Type	Maximum Error (%) Before Fault			During Fault			After Fault		
		Phase A	Phase B	Phase C	Phase A	Phase B	Phase C	Phase A	Phase B	Phase C
5	L-G	5.49%	5.44%	5.44%	11.78%	14.42%	14.37%	10.37%	13.70%	10.37%
	L-L	5.49%	5.44%	5.44%	7.40%	5.44%	10.31%	5.77%	5.44%	6.88%
	L-L-G	5.49%	5.44%	5.44%	11.61%	11.64%	13.20%	11.09%	14.07%	12.52%
	3-Ph-G	5.49%	5.44%	5.44%	10.55%	10.09%	10.06%	10.28%	16.36%	14.22%
6	L-G	8.86%	8.75%	8.75%	18.95%	24.35%	24.18%	12.37%	18.71%	15.11%
	L-L	8.86%	8.75%	8.75%	22.05%	8.75%	25.27%	8.83%	8.75%	10.21%
	L-L-G	8.86%	8.75%	8.75%	25.72%	16.59%	21.58%	12.38%	19.13%	15.12%
	3-Ph-G	8.86%	8.75%	8.75%	30.97%	14.26%	16.34%	14.58%	19.82%	18.11%
16	L-G	5.23%	5.16%	5.16%	5.15%	7.70%	7.77%	6.55%	7.67%	6.83%
	L-L	5.23%	5.16%	5.16%	6.98%	5.16%	6.10%	5.33%	5.16%	6.08%
	L-L-G	5.23%	5.16%	5.16%	5.15%	7.32%	9.00%	6.74%	8.04%	7.81%
	3-Ph-G	5.23%	5.16%	5.16%	5.15%	2.68%	2.49%	6.82%	9.91%	9.72%

4.4.6 Numerical error associated with the Trapezoidal rule

It was discussed that the difference equations are developed to transform the differential equations representing the power system at discrete time points. Dommel's method was used as an example of the NIS method which uses the Trapezoidal rule (see section 2.6). The Trapezoidal rule contains a truncation error which normally shows itself as isolation in the waveforms when the time step is large compared to the time constant of the system which is the topic of this section.

The test study case and data which were used for this purpose are obtained from 60 Hz IEEE 14 busbar test system. Figure 4.33 shows the test system and the measurement placement. State variable numbers or equivalent node numbers corresponding to each bus are indicated as "SV". 36 measurement points were considered including 12 voltage nodes and 24 line currents. Due to the fact that the test system consists of 42 state variables or nodes (14bus × 3phase), unobservable buses are expected. The SVD approach (inspection of the S,U and V matrices) shows that all the busbars are observable except for busbar number 1 which is unobservable.

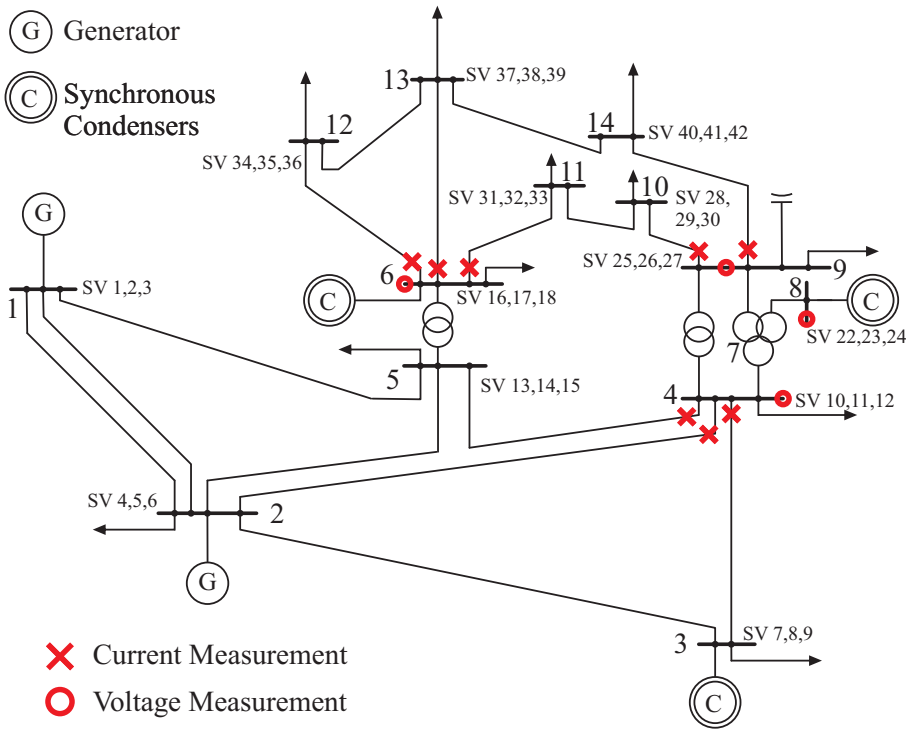

Figure 4.33: IEEE 14 busbar test system and the measurement placement

The approach is similar to what was explained in section 4.2. The system components were modelled as per section 3.2. In order to replace the line current measurements in the z matrix and based on equation 3.5 for inductor:

$$i_{km}(t) = i_{History}(t) + G_{eff}\{v_k(t) - v_m(t)\} \tag{4.4}$$

where $G_{eff} = \Delta t/2L$.

Also the history term can be calculated as follows:

$$i_{History}(t) = i_{km}(t - \Delta t) + G_{eff}\{v_k(t - \Delta t) - v_m(t - \Delta t)\} \tag{4.5}$$

From equation 4.4 for the time $(t - \Delta t)$,

$$i_{km}(t - \Delta t) = i_{History}(t - \Delta t) + G_{eff}\{v_k(t - \Delta t) - v_m(t - \Delta t)\} \tag{4.6}$$

Rearranging the equation above, gives:

$$G_{eff}\{v_k(t - \Delta t) - v_m(t - \Delta t)\} = i_{km}(t - \Delta t) - i_{History}(t - \Delta t) \tag{4.7}$$

and finally, Substituting equation 4.7 into equation 4.5 yields to:

$$\begin{aligned} i_{History}(t) &= i_{km}(t - \Delta t) + i_{km}(t - \Delta t) - i_{History}(t - \Delta t) \\ &= 2i_{km}(t - \Delta t) - i_{History}(t - \Delta t) \end{aligned} \tag{4.8}$$

Hence the inductor history term can be calculated using purely the current and previous history term. Although equations 4.5 and 4.8 are mathematically equivalent, equation 4.5 is slightly more efficient. On the other hand, based on equation 3.16, the history term for a RL branch is calculated as follows:

$$i_{RL-History}(t) = \frac{(2L/\Delta t)}{R + 2L/\Delta t}\{2i_{km}(t - \Delta t) - i_{RL-History}(t - \Delta t)\} \tag{4.9}$$

The test system was modelled in PSCAD/EMTDC with a single-phase short circuit event simulated at busbar No. 13 and the indicated measurements were taken and fed to the TSE algorithm. A 50 μs time-step was used for the PSCAD/EMTDC simulation and hence the component models used for developing the TSE also used a 50 μs time step.

Figure 4.34 shows the estimated and actual voltage waveforms at the busbar number 13 and figure 4.35 shows the error between estimated and actual values. An oscillation is evident around the true value during fault, although of small magnitude and will not affect the ability to identify the source of the transient disturbance. As TSE uses the Trapezoidal rule to discretise the differential equations to form difference equations, the same numerical issues already encountered with simulation with abrupt changes are to be expected.

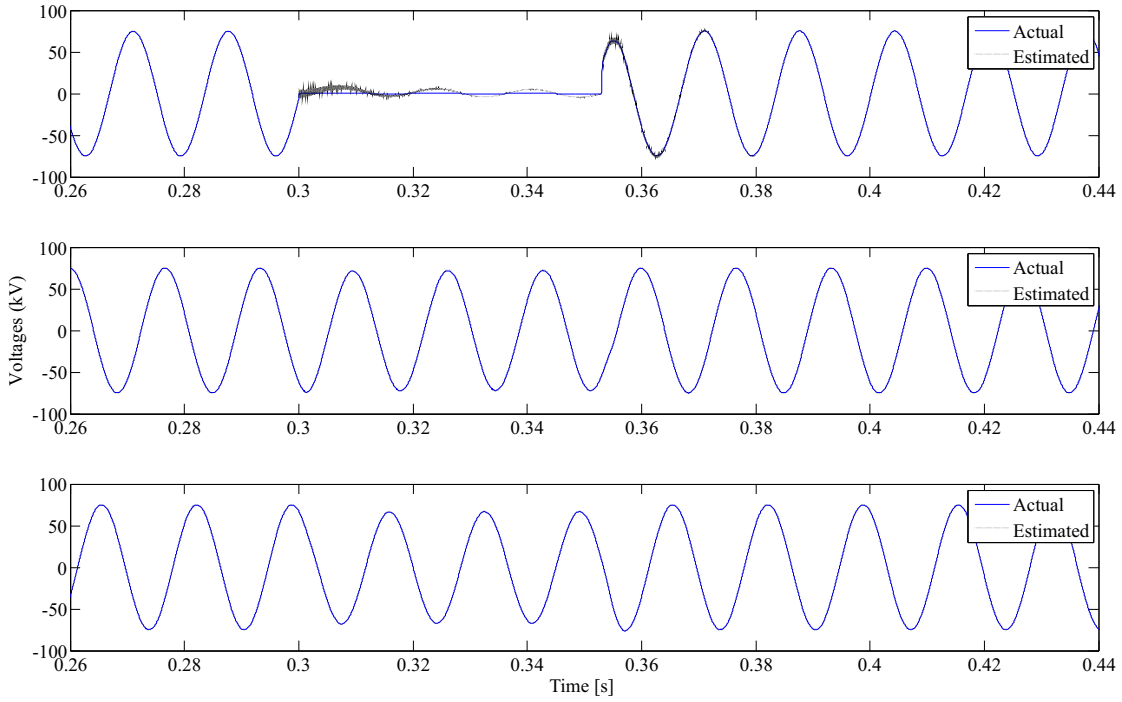

Figure 4.34: Estimated and actual voltage at busbar 13 (Trapezoidal Integrator)

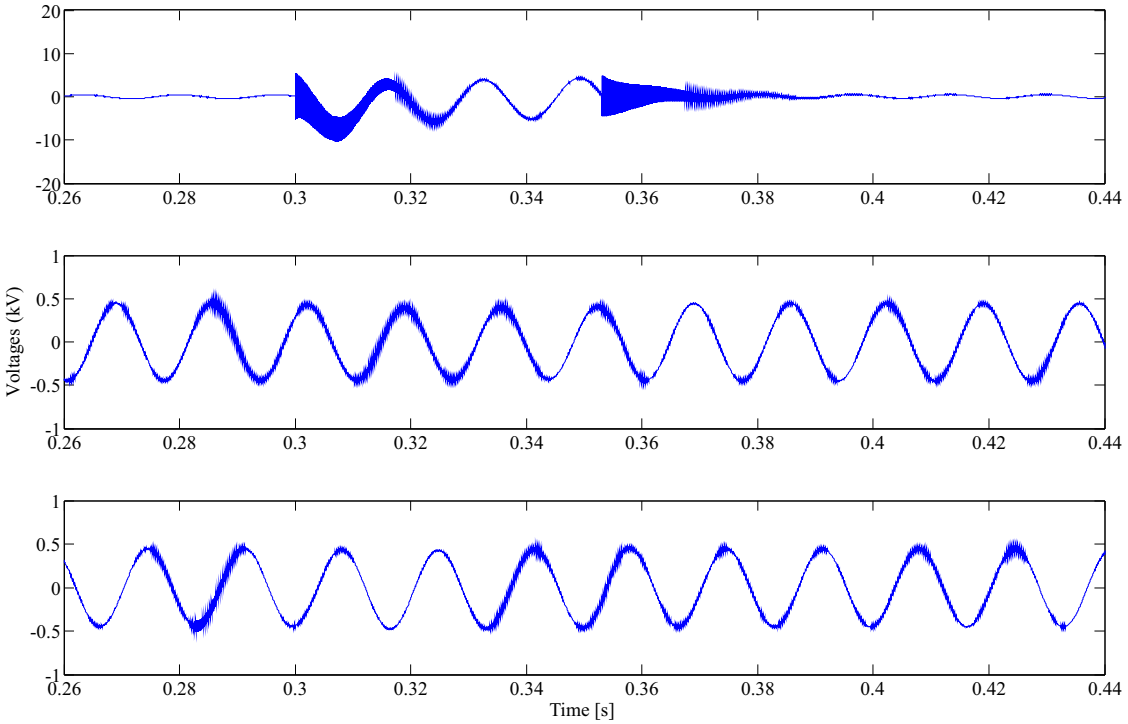

Figure 4.35: Error in busbar 13 voltage estimate (Trapezoidal Integrator)

To verify that this oscillation is due to the well documented numerical error that occurs with the Trapezoidal rule a rectangular integrator (that is the backward Euler method) was substituted in instead of the Trapezoidal rule. The NIS and the different examples are well explained in [Watson and Arrillaga 2002]. However for completeness of this section, figure 4.36 briefly shows a comparison between different types and table 4.6 shows the Norton components for an inductor that results from using each integrator method.

Name	Forward rectangular (forward Euler)	Backward rectangular (backward Euler)	Trapezoidal
Waveform	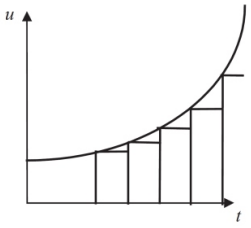	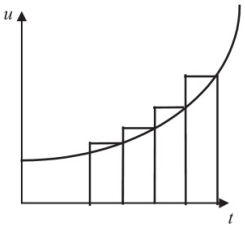	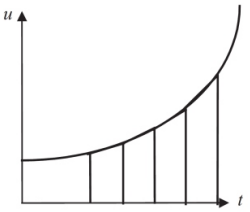
Integrator	$y_k = y_{k-1} + \Delta t f_{k-1}$	$y_k = y_{k-1} + \Delta t f_k$	$y_k = y_{k-1} + \frac{\Delta t}{2}(f_k + f_{k-1})$
Differentiator	$\dot{y}_k = \frac{y_{k+1} - y_k}{\Delta t}$	$\dot{y}_k = \frac{y_k - y_{k-1}}{\Delta t}$	$\dot{y}_k = \frac{2}{\Delta t}(y_k - y_{k-1}) - \dot{y}_{k-1}$

Figure 4.36: Different numerical integrator characteristic

Table 4.6: Norton components for different integration formula

Integration method	R_{eff}	$I_{History}$
Trapezoidal	$2L/\Delta t$	$i_{n-1} + (t/2L)v_{n-1}$
Backward Euler	$L/\Delta t$	i_{n-1}

The same IEEE 14 busbar system is used. Figures 4.37 and 4.38 display the comparison and error respectively, for busbar 13 using this new discretization for the TSE. These figures do not show this oscillation and give extremely good results. There is no tendency for numerical oscillations as would be expected for the backward Euler method.

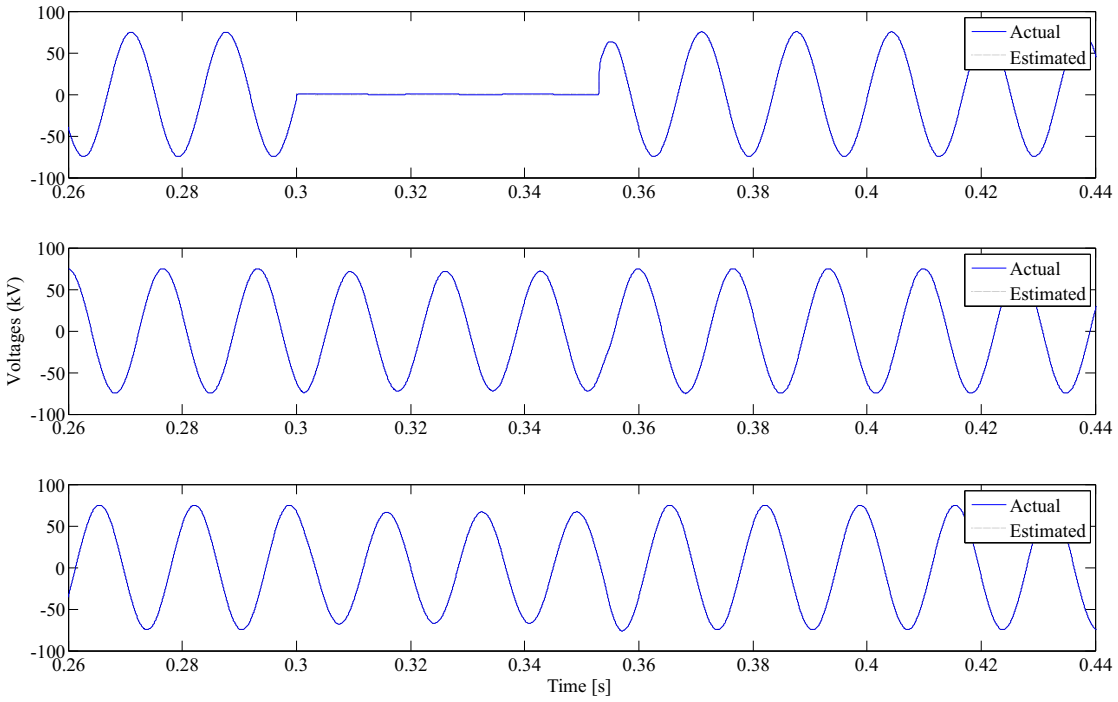

Figure 4.37: Estimated and actual voltage at busbar 13 (backward Euler Integrator)

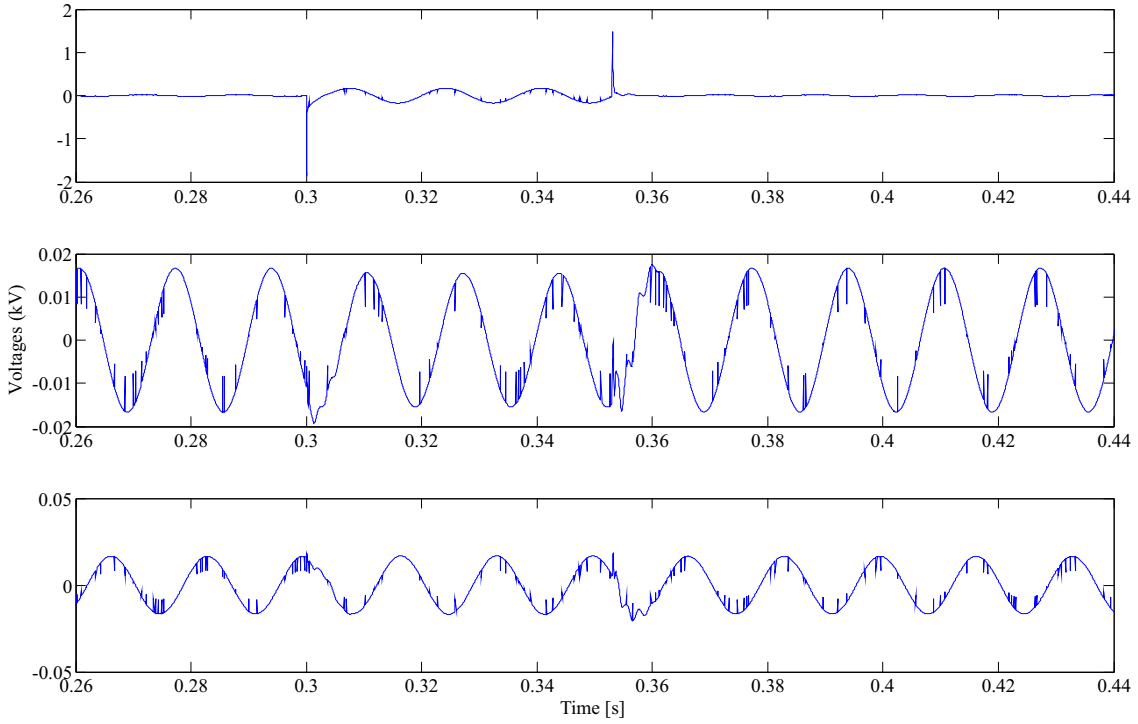

Figure 4.38: Error in busbar 13 voltage estimate (backward Euler Integrator)

Another more robust and accurate technique alternative to NIS is the root-matching method. This method is extremely robust and accurate with no tendency for numerical oscillations. The details of the root-matching technique are very well explained in [Watson and Arrillaga 2002] but for the sake of completeness it is briefly introduced here.

Root-matching technique was originally developed for matching the position of the poles and zeros of the difference equation for the differential equation it represents.

The application of Dommel's method to represent a series RL branch was previously discussed and it was shown in equation 3.19:

$$i(t) = \underbrace{\frac{1 - \frac{\Delta t R}{2L}}{1 + \frac{\Delta t R}{2L}}}_{1^{st}\ term}\ i(t - \Delta t) + \underbrace{\frac{\frac{\Delta t}{2L}}{1 + \frac{\Delta t R}{2L}}}_{2^{nd}\ term}\ \{v_{sr}(t - \Delta t) + v_{sr}(t)\}$$

Close inspection of this equation suggests that the first and second term can be approximated by the exponential form as follows:

$$i(t) = e^{-\Delta t\ R/L}\ i(t - \Delta t) + (1 - e^{-\Delta t\ R/L})\ \{v_{sr}(t - \Delta t) + v_{sr}(t)\}$$

Figure 4.39 shows a comparison in the Norton equivalent of a series RL branch for Dommel's method and exponential form. Applying the root-matching technique to form a new TSE gives the excellent results as shown in figures 4.40 and 4.41.

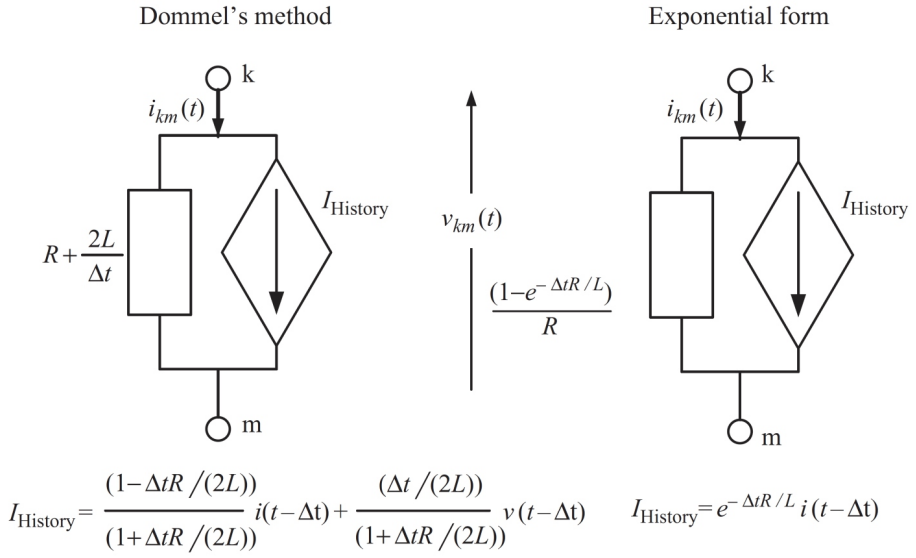

Figure 4.39: Norton equivalent for RL branch

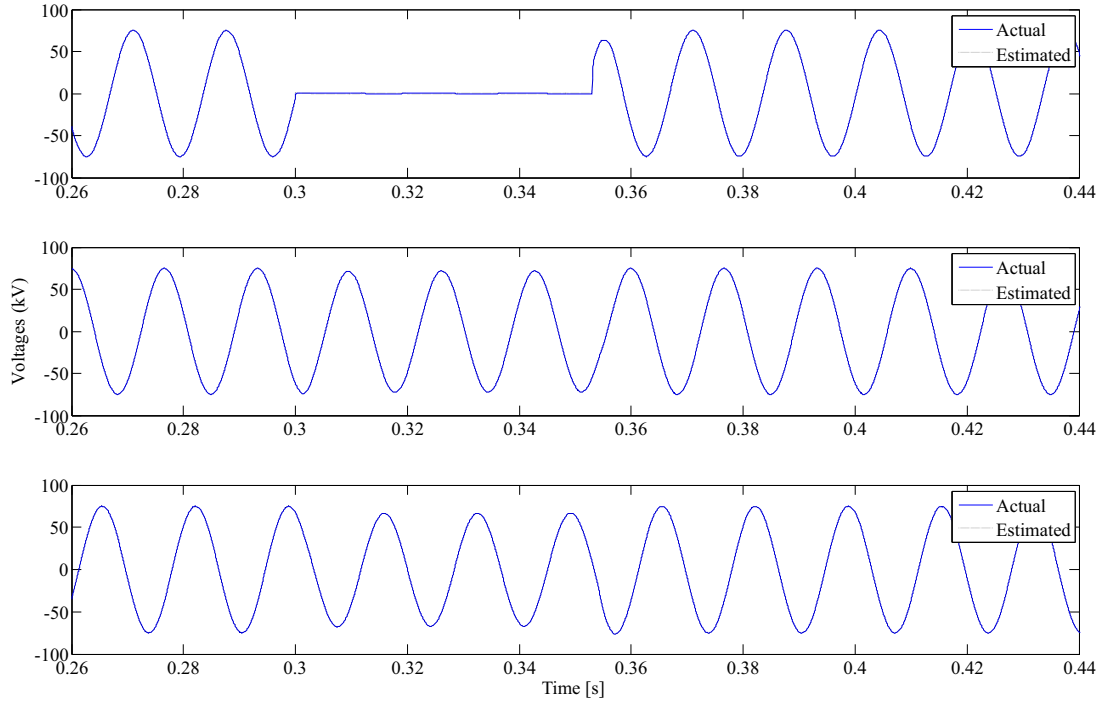

Figure 4.40: Estimated and actual voltage at busbar 13 (root-matching)

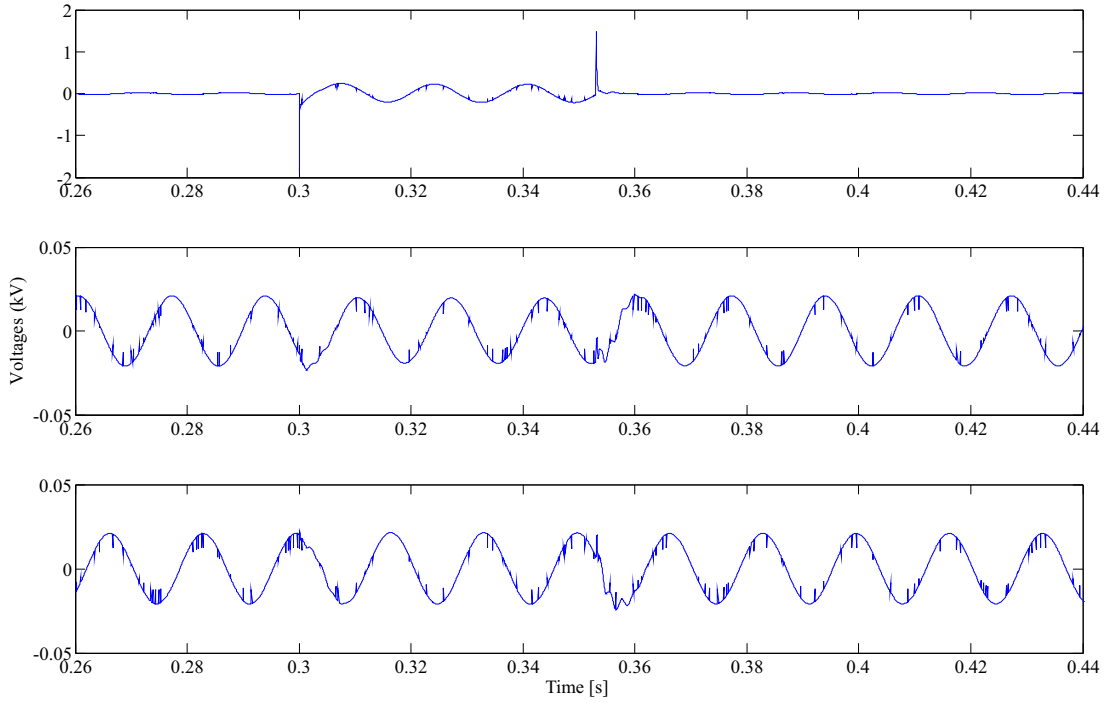

Figure 4.41: Error in busbar 13 voltage estimate (root-matching)

Chapter 5

CONCLUSION AND FUTURE WORK

5.1 CONCLUSIONS

As the electrical network evolves into a Smart Grid, new algorithms are needed to aid distribution system management. PQSE has been proposed as a smart algorithm for power quality management issues in a smart grid environment where a large amount of data are available. The output from a PQSE can be used not only for detecting sources of power quality emissions but has potential also for taking remedial actions. The focus of this work has been on one type of PQSE namely transient state estimation.

A new three-phase TSE based on NIS has been presented and its allocation to a realistic power system was demonstrated. For this purpose, first it was discussed how the dynamic of the system components can be modelled using NIS formulation. Then based on the type and location of the measurements in the system, these models were put together to construct the transient state estimation problem. It was discussed that a TSE problem is an under-determined system of equations as the number of known variables are less than the number of unknown variables. SVD was proposed to solve the TSE problem and it was explained how this could help for observability analysis as a by-product.

The performance of the proposed TSE was verified by implementing the algorithm on a 11 kV distribution test system. The conducted study showed that the TSE algorithm is able to produce good estimation for the observable busbars under different situations such as presence of background harmonics or 5% normally distributed measurement noise. The implemented estimator successfully determined the voltage at observable busbars and currents in observable branches.

It was shown that the inspection of the estimated voltage waveform could be used for diagnostic purposes in the network. For this purpose, a voltage sag/dip caused by different fault types was simulated in PSCAD/EMTDC. Then the selected measurements were taken and fed into TSE for each scenario. The implemented TSE performed very well despite a partially observable test system, measurement noise and the presence of background harmonics.

Oscillations around the true values were observed on some of the estimated voltage waveforms and these were verified to be due to numerical noise inherent in the Trapezoidal rule at sharp discontinuities. In order to verify this, two new TSE's were formed by reformulating using backward Euler integrator and root-matching techniques and the performance of these new TSE's were verified.

Although obtaining adequate measurements is the main barrier to transient state estimation at present, the emergence of smarter power grids and Advanced Metering Infrastructure (AMI) in particular, will alleviate this. These meters can provide large volumes of data to a central location. Once the data is available, the next step is how to obtain useful information from these data. In this situation, smart algorithms such as PQSE can play a significant role in this area.

5.2 FUTURE WORK

Since TSE is in its infancy compared to electromagnetic transient simulation there are many topics worth studying as future work. Some of the topics suggested by the author would be including, but not limited to:

5.2.1 System component modelling

The focus of this work has been on the concept of TSE and the new formulation approach. Therefore, more research is needed to develop each system component model with more detail. In fact these improvements will open the doors for testing a greater range of transient issues within the network. For example, using distributed parameters of transmission lines and their incorporation into TSE will extend its application to the transmission level (where the length of lines necessitate the travelling wave model instead of the PI model).

A similar situation exists wheere the non-linearity of the system components is needed to be taken into account. Modelling a non-linear load could be an example. Another example would be considering the non-linear characteristics of transformers. This will help to extend the TSE application to study a wider range of transient phenomena such as transformer energisation, etc.

5.2.2 Bad data analysis

The ability to treat bad data depends on the number of measurements and number of unknowns. Bad data detection and correction can be performed effectively on over-determined systems as there are redundant measurements. Bad data analysis for an under-determined system by means of inspection of equation residuals will serve as a big step towards the maturity of TSE.

5.2.3 Load identification

Similar to HSE, one feature of TSE could be identifying the nature of the loads connected to the network. In other words, inspection of the transient response for a network with and without the load being modelled could lead to determining the load behaviour and hence load identification.

APPENDIX

The 11kV test system is shown here and the corresponding data is summarized below.

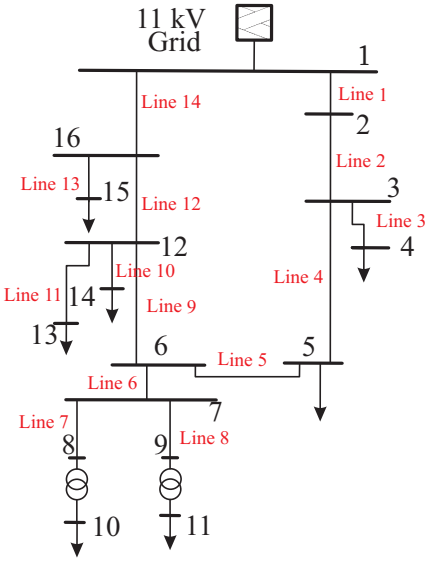

- Transmission line parameters

Line Name	l [km] Length	r [Ohm/km] Resistance	x [Ohm/km] Reactance	c [nF/km] Capacitance	r0 [Ohm/km] Zero seq. resistance	x0 [Ohm/km] Zero seq. reactance	c0 [nF/km] Zero seq. capacitance
1	1.606	0.4803	0.4452	21.0606	0.628	1.787	8.4146
2	1.274	0.986	1.1366	42.1212	2.4632	6.2799	16.8292
3	0.529	2.464	0.81	21.0606	2.76	3.478	8.4146
4	0.87	0.2733	0.3532	10.5303	0.421	1.695	4.2073
5	1.471	0.5466	0.7064	21.0606	0.842	3.39	8.4146
6	0.108	2.734	0.824	10.5303	3.03	3.492	4.2073
7	0.123	3.42	0.652	472.712	4.436	2.39	4.133
8	0.319	4.2566	1.0321	10.5303	5.5431	5.1537	4.2073
9	1.07	0.5466	0.7064	21.0606	0.842	3.39	8.4146
10	0.406	0.446	0.378	10.5303	0.594	1.711	4.2073
11	0.954	1.9006	1.0914	30.7726	2.344	5.109	12.5476
12	0.079	0.5466	0.7064	21.0606	0.842	3.39	8.4146
13	0.083	0.5466	0.7064	21.0606	0.842	3.39	8.4146
14	5.149	0.986	1.1366	42.1212	2.4632	6.2799	16.8292

- Load data

Load number	Bus	Voltage (kV)	Active power (KW)	Reactive power (KVAR)
1	4	11	38.80113	9.72448
2	5	11	23.28	5.83
3	10	0.4	460.76	115.47
4	11	0.4	567.46	142.22
5	14	11	58.2	58.2
6	13	11	77.6	10.94
7	15	11	11.64	2.91

- Transformers

Transformer number	Bus	Voltage (kV)	Bus	Voltage (kV)	Configuration	Impedance ratio (%)
1	8	11	10	0.4	Dyn	5
2	9	11	11	0.4	Dyn	5

REFERENCES

Abur, A. (1990), 'A bad data identification method for linear programming state estimation', *Power Systems, IEEE Transactions on*, Vol. 5, No. 3, pp. 894–901.

Abur, A. and Exposito, A.G. (2004), *Power System State Estimation: Theory and Implementation*, Marcel-Dekker, New York, USA.

Arrillaga, J. and Watson, N. (2001), *Computer modelling of electrical power systems*, Wiley.

Beides, H. and Heydt, G. (1991), 'Dynamic state estimation of power system harmonics using kalman filter methodology', *Power Delivery, IEEE Transactions on*, Vol. 6, No. 4, pp. 1663–1670.

Bellini, A., Filippetti, F., Franceschini, G., Tassoni, C. and Kliman, G. (2001), 'Quantitative evaluation of induction motor broken bars by means of electrical signature analysis', *Industry Applications, IEEE Transactions on*, Vol. 37, No. 5, Sep, pp. 1248–1255.

Bergeron, L. (1961), *Water hammer in hydraulics and wave surges in electricity*, Wiley.

Bin, W., Wilsun, X. and Zhencun, P. (2005), 'Voltage sag state estimation for power distribution systems', *Power Systems, IEEE Transactions on*, Vol. 20, No. 2, pp. 806–812.

Bollen, M. (1996), 'Fast assessment methods for voltage sags in distribution systems', *Industry Applications, IEEE Transactions on*, Vol. 32, No. 6, pp. 1414–1423.

Bollen, M. (1998), 'Method of critical distances for stochastic assessment of voltage sags', *Generation, Transmission and Distribution, IEE Proceedings-*, Vol. 145, No. 1, pp. 70–76.

Bollen, M.H., Gu, I.Y., Axelberg, P.G. and Styvaktakis, E. (2007), 'Classification of underlying causes of power quality disturbances: deterministic versus statistical methods', *EURASIP J. Appl. Signal Process.*, Vol. 2007, No. 1, pp. 172–172.

C4.102, C.T.F. (Feb. 2009), 'Voltage dip evaluation and prediction tools'.

Clements, K. (1990), 'Observability methods and optimal meter placement', *International Journal of Electrical Power & Energy Systems*, Vol. 12, No. 2, pp. 88–93.

Conrad, L. and Bollen, M. (1997), 'Voltage sag coordination for reliable plant operation', *Industry Applications, IEEE Transactions on*, Vol. 33, No. 6, pp. 1459–1464.

Conrad, L., Little, K. and Grigg, C. (1991), 'Predicting and preventing problems associated with remote fault-clearing voltage dips', *Industry Applications, IEEE Transactions on*, Vol. 27, No. 1, pp. 167–172.

David Strong & Associates (June 2009), *Development and implementation of system protection schemes*, Technical Report, Electricity Commission.

Dommel, H. (1969), 'Digital computer solution of electromagnetic transients in single- and multiphase networks', *Ieee Transactions on Power Apparatus and Systems*, Vol. Pa88, No. 4, p. 388.

Du, Z., Arrillaga, J. and Watson, N. (1996), 'Continuous harmonic state estimation of power systems', *Generation, Transmission and Distribution, IEE Proceedings-*, Vol. 143, No. 4, pp. 329–336.

Du, Z., Arrillaga, J., Watson, N. and Chen, S. (1999), 'Identification of harmonic sources of power systems using state estimation', *Generation, Transmission and Distribution, IEE Proceedings-*, Vol. 146, No. 1, pp. 7–12.

El-Hawary, M. (2002), 'Pes news', *Power Engineering Review, IEEE*, Vol. 22, No. 4, pp. 28–28.

Espinosa-Juarez, E. and Hernandez, A. (2007), 'A method for voltage sag state estimation in power systems', *Power Delivery, IEEE Transactions on*, Vol. 22, No. 4, pp. 2517–2526.

Espinosa-Juarez, E., Espinoza-Tinoco, J. and Hernandez, A. (2009), 'Neural networks applied to solve the voltage sag state estimation problem: An approach based on the fault positions concept', In *Electronics, Robotics and Automotive Mechanics Conference, 2009. CERMA '09.*, pp. 88–93.

Faried, S. and Boreshaid, S. (2003), 'Stochastic evaluation of voltage sags in series capacitor compensated radial distribution systems', *Power Delivery, IEEE Transactions on*, Vol. 18, No. 3, pp. 744–750.

Faried, S., Billinton, R. and Boreshaid, S. (2005), 'Stochastic evaluation of voltage sag and unbalance in transmission systems', *Power Delivery, IEEE Transactions on*, Vol. 20, No. 4, pp. 2631–2637.

Gomez, J., Morcos, M., Tourn, D. and Felici, M. (2005), 'A novel methodology to locate originating points of voltage sags in electric power systems', In *Electricity Distribution, 2005. CIRED 2005. 18th International Conference and Exhibition on*, pp. 1–3.

Hamzah, N., Mohamed, A. and Hussain, A. (2004), 'A new approach to locate the voltage sag source using real current component', *Electric Power Systems Research*, Vol. 72, No. 2, pp. 113–123.

Hart, D., Peterson, W., Uy, D., Schneider, J., Novosel, D. and Wright, R. (2000), 'Tapping protective relays for power quality information', *Computer Applications in Power, IEEE*, Vol. 13, No. 1, pp. 45–49.

Heine, P. and Lehtonen, M. (2003), 'Voltage sag distributions caused by power system faults', *Power Systems, IEEE Transactions on*, Vol. 18, No. 4, pp. 1367–1373.

Heydt, G. (1989), 'Identification of harmonic sources by a state estimation technique', *Power Delivery, IEEE Transactions on*, Vol. 4, No. 1, pp. 569–576.

Heydt, G. (1991), *Electric Power Quality*, Stars in a Circle Publications: West LaFayette, Indiana, USA, second ed.

(1995), 'Ieee recommended practice for monitoring electric power quality', *IEEE Std 1159-1995*, p. i.

Juarez, E. and Hernandez, A. (2006), 'An analytical approach for stochastic assessment of balanced and unbalanced voltage sags in large systems', *Power Delivery, IEEE Transactions on*, Vol. 21, No. 3, pp. 1493–1500.

Kanao, N., Yamashita, M., Yanagida, H., Mizukami, M., Hayashi, Y. and Matsuki, J. (2005), 'Power system harmonic analysis using state-estimation method for japanese field data', *Power Delivery, IEEE Transactions on*, Vol. 20, No. 2, pp. 970–977.

Laughman, C., Lee, K., Cox, R., Shaw, S., Leeb, S., Norford, L. and Armstrong, P. (2003), 'Power signature analysis', *Power and Energy Magazine, IEEE*, Vol. 1, No. 2, Mar, pp. 56–63.

Leborgne, R., Karlsson, D. and Daalder, J. (2006), 'Voltage sag source location methods performance under symmetrical and asymmetrical fault conditions', In *Transmission & Distribution Conference and Exposition: Latin America, 2006. TDC '06. IEEE/PES*, pp. 1–6.

Lehn, P., Rittiger, J. and Kulicke, B. (1995), 'Comparison of the atp version of the emtp and the netomac program for simulation of hvdc systems', *Power Delivery, IEEE Transactions on*, Vol. 10, No. 4, pp. 2048–2053.

Li, C., Tayjasanant, T., Xu, W. and Liu, X. (2003), 'Method for voltage-sag-source detection by investigating slope of the system trajectory', *Generation, Transmission and Distribution, IEE Proceedings-*, Vol. 150, No. 3, pp. 367–372.

Lo, K., Zeng, P., Marchand, E. and Pinkerton, A. (1992), 'New bad-data detection and identification technique based on rotation of measurement order for sequential state estimation [for power systems]', *Generation, Transmission and Distribution, IEE Proceedings C*, Vol. 139, No. 5, pp. 387–401.

Long, W., Cotcher, D., Ruiu, D., Adam, P., Lee, S. and Adapa, R. (1990), 'Emtp-a powerful tool for analyzing power system transients', *Computer Applications in Power, IEEE*, Vol. 3, No. 3, pp. 36–41.

Madtharad, C., Premrudeepreechacharn, S. and Watson, N. (2003), 'Power system state estimation using singular value decomposition', *Electric Power Systems Research*, Vol. 67, No. 2, pp. 99–107.

Madtharad, C., Premrudeepreechacharn, S., Watson, N. and Ratchai, S.U. (2005), 'An optimal measurement placement method for power system harmonic state estimation', *Power Delivery, IEEE Transactions on*, Vol. 20, No. 2, pp. 1514–1521.

Marti, J. and Linares, L. (1994), 'Real-time emtp-based transients simulation', *Power Systems, IEEE Transactions on*, Vol. 9, No. 3, pp. 1309–1317.

Matair, S., Watson, N., Wong, K., Pham, V. and Arrillaga, J. (2000), 'Harmonic state estimation: a method for remote harmonic assessment in a deregulated utility network', In *Electric Utility Deregulation and Restructuring and Power Technologies, 2000. Proceedings. DRPT 2000. International Conference on*, pp. 41–46.

Meliopoulos, A., Fan, Z. and Zelingher, S. (1994), 'Power system harmonic state estimation', *Power Delivery, IEEE Transactions on*, Vol. 9, No. 3, pp. 1701–1709.

Monticelli, A. (1999), *State estimation in electric power systems: a generalized approach*, Kluwer Academic Publisher, USA.

Olguin, G., Vuinovich, F. and Bollen, M. (2006), 'An optimal monitoring program for obtaining voltage sag system indexes', *Power Systems, IEEE Transactions on*, Vol. 21, No. 1, pp. 378–384.

Parsons, A., Grady, W., Powers, E. and Soward, J. (2000), 'A direction finder for power quality disturbances based upon disturbance power and energy', *Power Delivery, IEEE Transactions on*, Vol. 15, No. 3, pp. 1081–1086.

Phadke, A., Thorp, J., Nuqui, R. and Zhou, M. (2009), 'Recent developments in state estimation with phasor measurements', In *Power Systems Conference and Exposition, 2009. PSCE '09. IEEE/PES*, pp. 1–7.

Pradhan, A. and Routray, A. (2005), 'Applying distance relay for voltage sag source detection', *Power Delivery, IEEE Transactions on*, Vol. 20, No. 1, pp. 529–531.

Press, W.H. (2007), *Numerical recipes : the art of scientific computing*, Cambridge University Press, Cambridge, UK ; New York, 3rd ed.

Qader, M., Bollen, M. and Allan, R. (1999), 'Stochastic prediction of voltage sags in a large transmission system', *Industry Applications, IEEE Transactions on*, Vol. 35, No. 1, pp. 152–162.

Schweppe, F. (1970), 'Power system static-state estimation, part iii: Implementation', *Power Apparatus and Systems, IEEE Transactions on*, Vol. PAS-89, No. 1, pp. 130–135.

Schweppe, F. and Rom, D. (1970), 'Power system static-state estimation, part ii: Approximate model', *Power Apparatus and Systems, IEEE Transactions on*, Vol. PAS-89, No. 1, pp. 125–130.

Schweppe, F. and Wildes, J. (1970), 'Power system static-state estimation, part i: Exact model', *Power Apparatus and Systems, IEEE Transactions on*, Vol. PAS-89, No. 1, pp. 120–125.

Seon-Ju, A., Dong-Jun, W., Chung, D.Y. and Seung, U.M. (2004), 'Determination of the relative location of voltage sag source according to event cause', In *Power Engineering Society General Meeting, 2004. IEEE*, pp. 620–625 Vol.1.

Shaw, S., Laughman, C., Leeb, S. and Lepard, R. (2000), 'A power quality prediction system', *Industrial Electronics, IEEE Transactions on*, Vol. 47, No. 3, Jun, pp. 511–517.

Shivakumar, N. and Jain, A. (2008), 'A review of power system dynamic state estimation techniques', In *Power System Technology and IEEE Power India Conference, 2008. POWERCON 2008. Joint International Conference on*, pp. 1–6.

Tayjasanant, T., Chun, L. and Xu, W. (2005), 'A resistance sign-based method for voltage sag source detection', *Power Delivery, IEEE Transactions on*, Vol. 20, No. 4, pp. 2544–2551.

Transpower New Zealand, Ltd (December 2008), *Wairakei Ring Investment Proposal, Attachment E Final Long-list and Short-list criteria*, Technical Report.

Transpower New Zealand, Ltd (July 2010), *Grid Upgrade Plan 2009, Instalment 6 Part IX: Bunnythorpe-Haywards Thermal Upgrade (2006) Investment Proposal*, Technical Report.

Transpower New Zealand, Ltd (June 2007), *Connecting and Dispatching New Generation in New Zealand: Overview*, Technical Report.

Wang, J., Chen, S. and Lie, T. (2005), 'System voltage sag performance estimation', *Power Delivery, IEEE Transactions on*, Vol. 20, No. 2, pp. 1738–1747.

Wang, B., Dong, X., Pan, Z., Bo, Z. and Yip, T. (2011), 'Bad data identification for voltage sag state estimation in distribution system with wind farm connections', *Universities' Power Engineering Conference (UPEC), Proceedings of 2011 46th International*, pp. 1–5.

Watson, N. (2010), 'Power quality state estimation', *European Transactions on Electrical Power*, Vol. 20, No. 1, pp. 19–33.

Watson, N. and Arrillaga, J. (2002), *Power systems electromagnetic transients simulation*, Institution of Electrical Engineers, London.

Watson, N. and Yu, K. (2008), 'Transient state estimation', In *Harmonics and Quality of Power, 2008. ICHQP 2008. 13th International Conference on*, pp. 1–6.

Watson, N., Arrillaga, J. and Du, Z. (2000), 'Modified symbolic observability for harmonic state estimation', *Generation, Transmission and Distribution, IEE Proceedings-*, Vol. 147, No. 2, pp. 105–111.

Wu, F.F. (1990), 'Power system state estimation: a survey', *International Journal of Electrical Power & Energy Systems*, Vol. 12, No. 2, pp. 80–87.

Wu, F., Liu, W. and Lun, S. (1988), 'Observability analysis and bad data processing for state estimation with equality constraints', *Power Systems, IEEE Transactions on*, Vol. 3, No. 2, pp. 541–548.

Yamamoto, K., Irwin, G., Nayak, O. and Ametani, A. (1999), 'Combined iteration algorithm for nonlinear elements in electromagnetic transient simulation', In *International Power System Transient (IPST1999)*, Budapest (Hungary).

Yu, K. (2005), *Harmonic state estimation and transient state estimation*, PhD thesis, Electrical and Electronic Engineering Department at University of Canterbury., Christchurch, New Zealand.

Yu, K. and Watson, N. (2004), 'Three-phase harmonic state estimation using svd for partially observable systems', In *Power System Technology, 2004. PowerCon 2004. 2004 International Conference on*, Nov., pp. 29 – 34 Vol.1.

Yu, K. and Watson, N. (2005), 'Identification of fault locations using transient state estimation', In *International Power System Transient (IPST2005)*, Montreal (Canada).

Yu, K. and Watson, N. (2007), 'An approximate method for transient state estimation', *Ieee Transactions on Power Delivery*, Vol. 22, No. 3, pp. 1680–1687.

Yu, K., Watson, N. and Arrillaga, J. (2005), 'Error analysis in static harmonic state estimation: a statistical approach', *Power Delivery, IEEE Transactions on*, Vol. 20, No. 2, pp. 1045–1050.